COMBINED MAGNETIZATION OF MAGNETIC MATERIALS

Thesis presented for the degree of Ph.D.

by

William Drummond Sutherland B.Sc. (Hons.)

February, 1953.

COMBINED MAGNETIZATION OF MAGNETIC MATERIALS

Introductory Note

Electrical machinery and transformers are usually supplied with voltages which are so nearly sinusoidal that the iron cores are magnetized under conditions of sine-flux. In some cases it is also possible to magnetize the core material under sine-current conditions. Both of these cases constitute single-frequency methods of magnetization and the nature of the iron losses which occur are well known.

In much equipment, however, the iron is magnetized simultaneously from two or more sources, whose frequencies may not be integrally related. The nature of all cases of multi-frequency magnetization and the iron losses which occur are not widely known and there is little literature on the subject.

The various conditions of two-frequency core magnetization are considered as the magnitude and frequency of one component is altered. The effects of phase difference between the two component frequencies upon the time-average iron-loss power can only have significance when the two frequencies are integrally related. Accordingly the cores were magnetized at f_1 and nf_1. The values of n which were used for the main investigation of combined magnetization conditions were 2 and 3. Throughout all these tests the cores were magnetized under sine-current conditions to enable an adaptation of the standard transductor connection to be used. In this way the individual or total core loss components can be directly obtained. It is found that as the phase angle is altered, large variations are obtained in the individual loss components. These variations are investigated for

various values of magnetizing force over a complete range of phase angle. Of special interest are the conditions which give a reduction in the core loss at either frequency under combined magnetization when compared with the corresponding single-frequency values.

To enable an estimation of core loss conditions to be obtained theoretically, the B-H relationship for the core material is defined to include the effects of hysteresis loss. The loss is then obtained for various conditions of combined magnetization which is compared with the corresponding single-frequency case. The theoretical conditions considered in Part I are investigated practically in Part II. Originality is claimed for the presentation of the comprehensive series of results under two-frequency magnetization and also for the method of core connection to enable these to be simply measured.

The work was carried out in the Electrical Engineering Department from 1947 to 1952. The author wishes to thank Professor B. Hague, D.Sc., for much helpful encouragement during this period and for permission to utilize the equipment of the laboratory. Dr. J.E. Parton is also thanked for many helpful discussions during the course of this work.

COMBINED MAGNETIZATION OF MAGNETIC MATERIALS

PART I.

AN INVESTIGATION OF SINE-CURRENT COMBINED MAGNETIZATION OF MAGNETIC MATERIALS.

PART II.

EXPERIMENTAL RESULTS

PART II (Continued)

EXPERIMENTAL RESULTS

PART I.

AN INVESTIGATION OF SINE-CURRENT COMBINED MAGNETIZATION OF MAGNETIC MATERIALS.

CHAPTER I.

INTRODUCTION.

For circuit calculations involving magnetic materials it is often permissible to replace the actual relationship between the core flux-density and the magnetizing force by a single-valued function relating B and H. While this simplification enables normal mathematical methods to be used in the solution of non-linear circuits, it completely ignores the effects of core loss. The magnitude of this loss for some of the modern core materials is relatively small and the above assumption does give a satisfactory solution, e.g. in magnetic amplifier circuits. For standard core materials, however, this loss cannot be neglected and it is the object of this work to investigate the core-loss conditions which occur when a magnetic material is subjected to combined magnetization.

A typical hysteresis loop for a core material is shown in Fig. 1. The loop extends between the limits $\pm$ Hm of the magnetizing force which varies cyclically.

Fig. 1.

It should be noted that the magnetizing force wave contains only one maximum and minimum per cycle, i.e. the wave is not re-entrant.

When the wave possesses a number of maxima and minima, then a complex hysteresis loop will be formed due to the presence of minor loops. A typical loop formed by a magnetizing force $h = h_1 \cos\omega t + h_3 \cos 3\omega t$ is shown in Fig. 2.

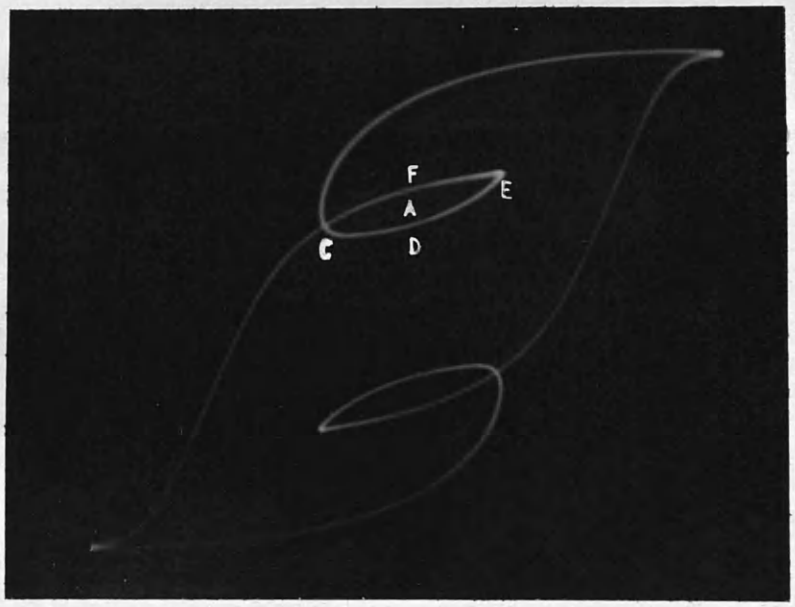

Complex loop

Flux density Magnetizing force

Fig. 2.

The magnetizing force wave has subsidiary minimum values at h' and h'' and subsidiary maxima at h''' and h^{12}. The absolute maximum and minimum occur at ± Hm. The formation of the minor loop (A) may be readily followed with reference to the magnetizing force wave. Consider the sequence of operations from + Hm. The magnetizing force is decreasing with a corresponding decrease in B until h'' is reached, when h increases and traces out the portion CDE of the minor loop. After the subsidiary maximum at h''' the magnetizing force decreases to a value equal to h'' and traces out the section EFC of the minor loop, which is now closed. Thereafter further change in h traces out the main loop until the next subsidiary maximum is reached.

It is obvious from the complex loop shape that a single-valued function cannot now be used to represent conditions in the magnetic material. Recourse must be made to expressions which represent the complete loop before any circuit calculations for combined magnetization conditions can be carried out. It must be assumed that the general form of the minor loops will be the same as the main loop obtained under single frequency magnetization for the same amplitudes.

The normal mode of operation of a saturable reactor comprises a special case of combined magnetization, when one of the components has zero frequency.

CHAPTER 2.

TYPES OF TWO-FREQUENCY LOOPS.

When a magnetic material is subjected to a magnetising force

$$h = h_1 \cos(\omega t + \phi) + h_n \cos(n\omega t + \psi)$$

The form of the hysteresis loops produced depends on the values of h_1, h_n, n, ϕ and ψ.

Case 1. $h_n = 0$

The normal single frequency hysteresis loop is formed. As ω is increased, a family of loops will be produced (neglecting any effects due to eddy-currents). This will be considered as the basic loop generated at a frequency $\frac{\omega}{2\pi}$ in the following cases.

Case 2. $h_1 \gg h_n \qquad n < 1 > \frac{1}{2}$

The resulting magnetizing force wave is shown in Fig. 3 when a slightly lower frequency magnetizing force wave is combined with the basic wave.

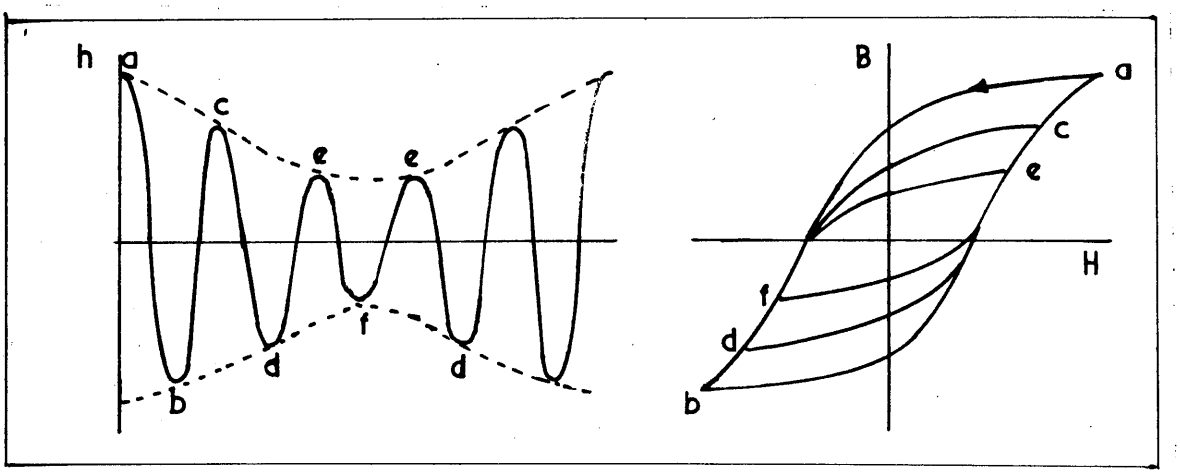

Fig. 3.

The maximum magnetizing force varies cyclically between $h_1 + h_n$ and $h_1 - h_n$ and over one complete cycle of the magnetizing force a series of half loops will be traced out, all differing slightly. (The undulations in the magnetizing force wave will occur at the higher frequency, i.e. f_1). The resulting loops formed are shown in Fig. 3.

Case 3. $h_1 = h_n$, $n < 1 > \frac{1}{3}$

This is the limiting value of case 2, since the magnetizing force varies cyclically from a maximum value of $(h_n + h_1)$ to zero. This causes the hysteresis loop to take the form of a spiral, which vanishes when the total magnetizing force reaches zero and then develops a similar curve outward as the magnetizing force is increasing (Fig. 4).

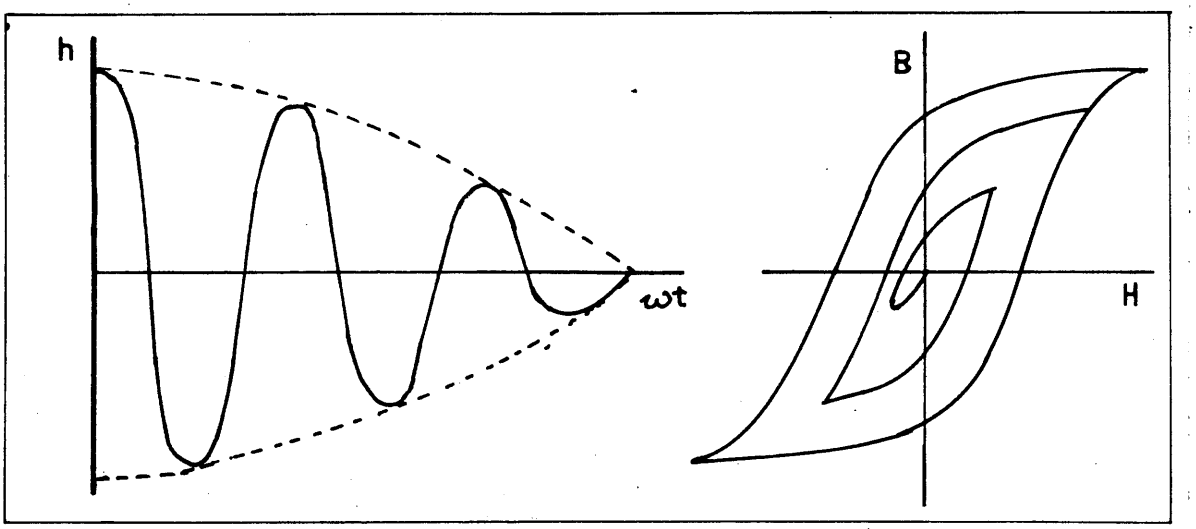

Fig. 4.

Case 4. $h_1 \ll h_n \qquad n < 1 > \frac{1}{2}$

The basic loop amplitude is considerably reduced and the resulting loops formed will be similar to Case 2, except that the undulations in the magnetizing force wave will occur at the frequency of the component h_n.

Case 5. $h_1 \ll h_n \qquad n > 1$

This condition sets up loops which are almost identical, except for the low frequency shift as shown in Fig. 5.

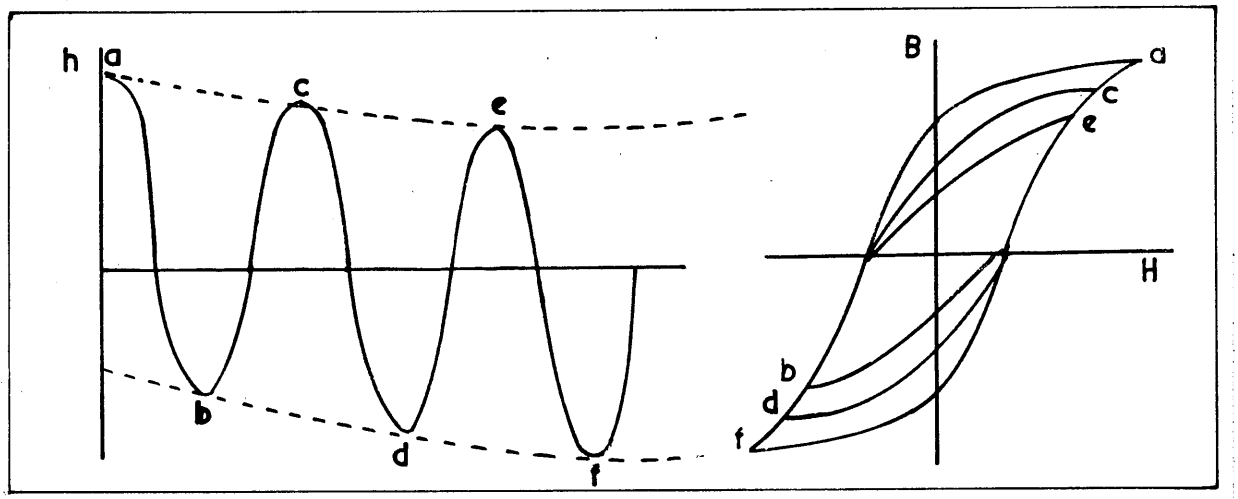

Fig. 5.

Case 6. $h_1 > h_n \qquad n \geqslant 2$

For this case, the value of h_1 should not be very much larger than h_n (say $h_1 = 2h_n$). Minor loops will be formed under this condition of magnetization, provided that the h wave is re-entrant.* A typical loop is shown in Fig. 6.

---

* For the required conditions to cause minor loops to be formed, see Chapter 3.

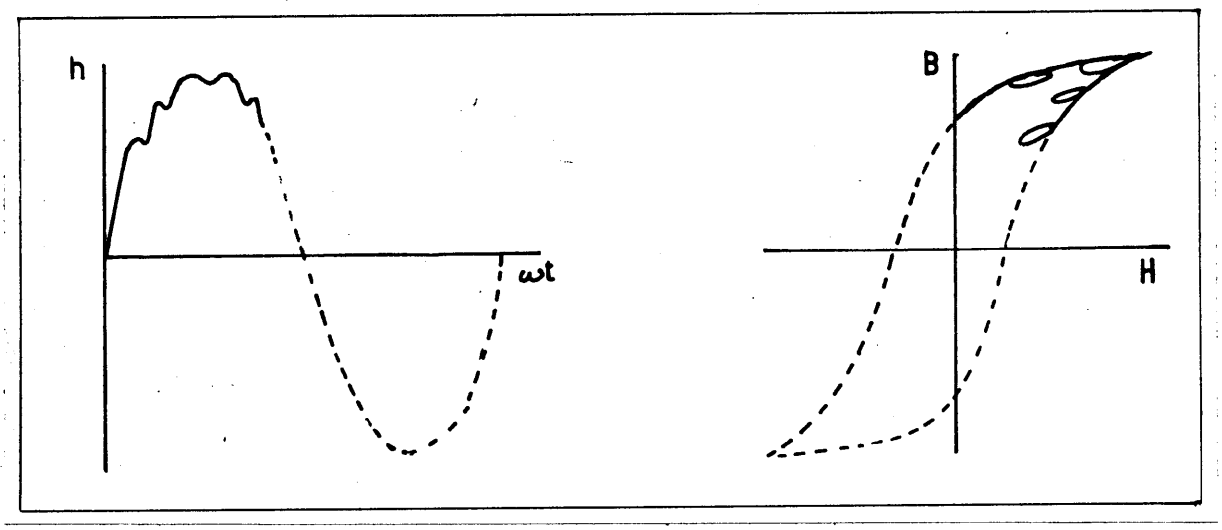

Fig. 6.

If the two frequencies of magnetization are not locked together, the minor loops will not be formed at the same point on the main loop in each cycle, but will drift round the low frequency loop. Obviously, as the frequency of h_n is increased the distance between adjacent minor loops will be decreased. Due to the different rate of change of h_1 between zero and maximum values, the minor loops tend to be longer near the maximum value of h_1 when compared with the corresponding loops in the neighbourhood of zero h.

If the total magnetizing force is defined as $h = h_1 \sin\omega t + h_n \sin n\omega t$ then the maximum number of complete minor loops which may be formed is $(n - 1)$.

As the magnitude of h_n is reduced, the amplitude of the minor loops is correspondingly reduced and this causes the minor loops at $h = 0$ to disappear. Further reduction of h_n causes more minor loops to disappear until Case 7 is reached.

Case 7. $h_1 \gg h_n \qquad n \geqslant 2$

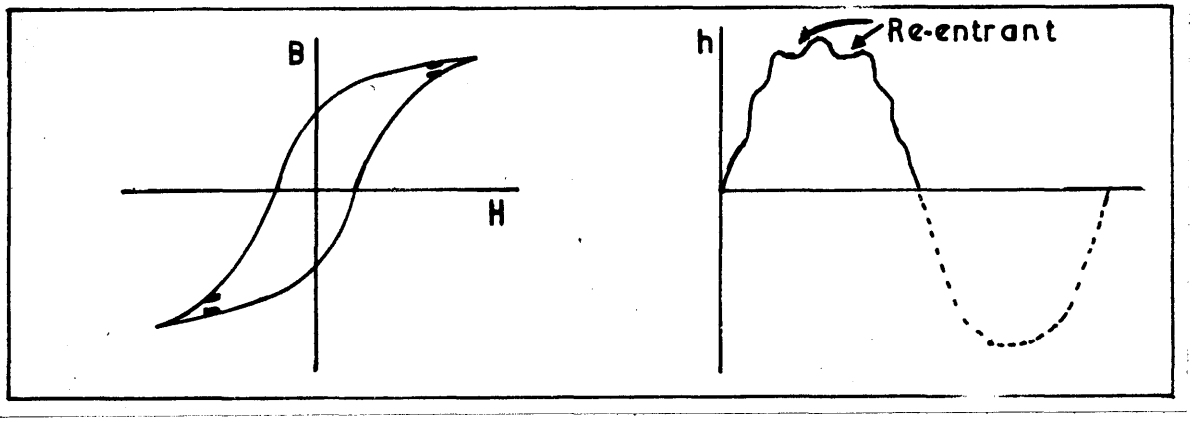

Fig. 7.

For this Case, the total magnetizing force wave is only re-entrant at values near maximum positive and negative h. This causes the few very small minor loops, as shown in Fig. 7, to be generated. As h_n is reduced to zero, the basic single frequency loop is obtained.

Case 8. $n = 0; \quad h_1 > h_o; \quad h_o + v_e.$

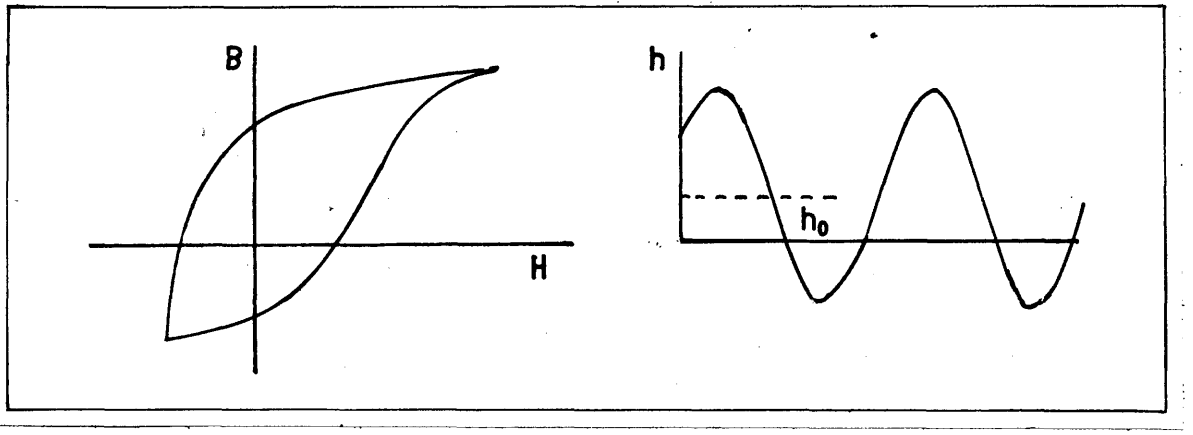

Fig. 8.

Case 8a. $n = 0$; $h_1 < h_o$; $h_o + v_e$.

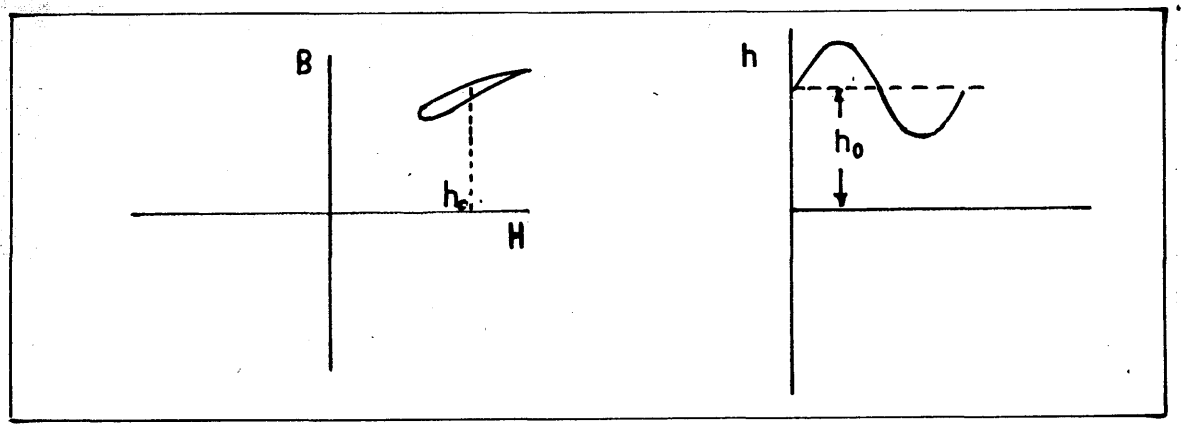

Fig. 9.

This is the mode of operation of the saturable reactor cores used in magnetic amplifiers, magnetic modulators etc. No minor loop is formed, but the main loop is unsymmetrical due to the presence of the d.c. component of magnetization. If the polarity of the d.c. component is reversed, then the loops shown in Figs. 8 and 9 are altered to give Figs. 10 and 11.

$n = 0$; $h_1 > h_o$; $h_o - v_e$.

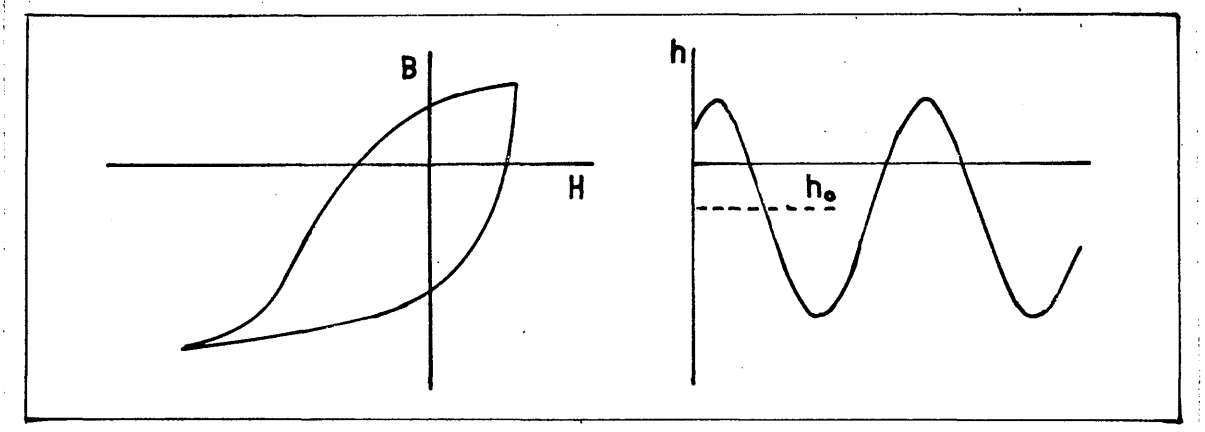

Fig. 10.

$n = 0$; $h_1 < h_o$; $h_o - v_e$.

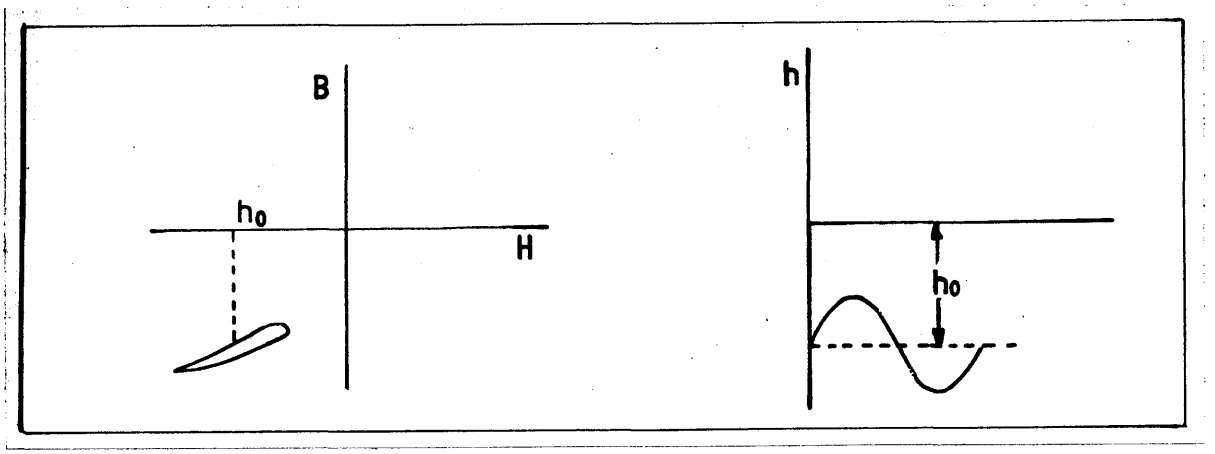

Fig. 11.

In the preceding general cases, the two magnetizing forces acting on the magnetic material were at frequencies f_1 and f_2 where $f_2 \neq nf_1$, n an integer. For the purpose of calculations and experiments in Parts I and II, the general cases of combined magnetization which will be considered in detail require that the condition $f_2 = nf_1$ will hold. This implies that for a given phase position between the two magnetizing forces the minor loops will always occur at the same point on the major loop, i.e. the hysteretic phenomena are singly periodic. This condition will be obtained if the frequencies of the two sources energizing the cores are electrically locked together. The necessary circuit details to obtain this synchronization are considered in Part II, Appendix (b).

CHAPTER 3.

EFFECTS OF PHASE CHANGE.

Let the total core magnetizing force wave be defined as

$$h = h_1 \sin(\omega t + \varphi_1) + h_n \sin(n\omega t + \varphi_n)$$

which may be simplified to give

$$h = h_1 \sin\omega t + h_n \sin(n\omega t + n\theta)$$

(n is assumed to be an integer of value > 1).

The phase angle of the higher frequency component will be considered a variable. This enables all possible phase positions to be obtained when θ varies between 0 and $\frac{2\pi}{n}$ measured with respect to ωt. It should be noted that after θ has been increased by $\frac{2\pi}{n}$ the total loop will have the same shape, with minor loops in the same relative positions as previously. To illustrate this, a loop is shown in Fig. 12(a) when a magnetizing force $h = h_1 \sin\omega t + h_3 \sin(3\omega t + n\theta)$ (where $\theta = 0$) is applied to a core. The corresponding loop when $\theta = \frac{2\pi}{n}$ is shown in Fig. 12(b).

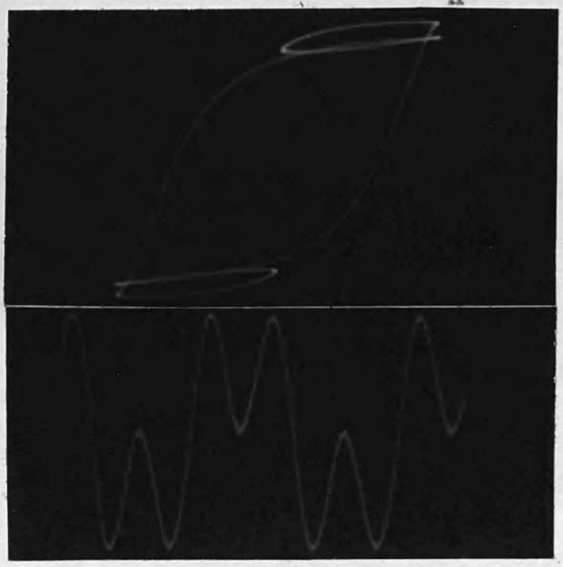

Fig. 12(a)

$h = h_1 \sin\omega t + h_3 \sin 3\omega t$

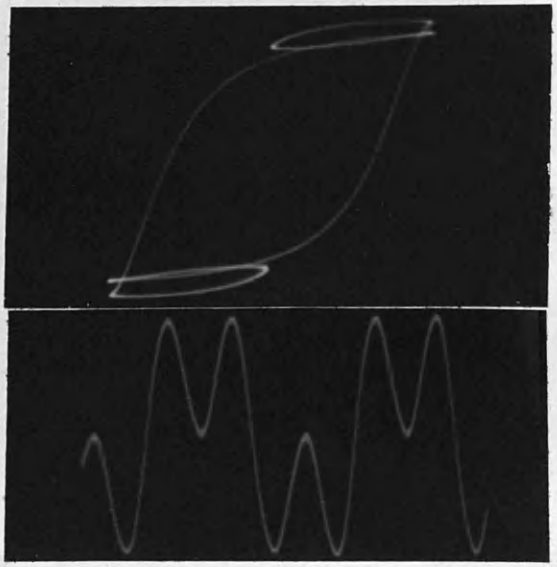

Fig. 12(b)

$h_1 = h_1 \sin\omega t + h_3 \sin(3\omega t + 2\pi)$

During this change of phase angle the minor loops moved round the major loop, as shown in Fig. 12(b).

It can be seen that a complete cycle of changes will be effected if the fundamental is moved $\frac{2\pi}{n}$ radians, the higher-frequency component remaining fixed.

In the following sections the magnetizing force will be expressed in the general form $h = h_1 \sin(\omega t + \varphi) + h_n \sin n\omega t$, the phase angle change being considered with reference to the fundamental quantity. In the experimental tests (see Part II) the phase of the fundamental is altered with respect to the higher frequency component.

As the frequency of the magnetizing force h_n is increased, a larger number of minor loops will be formed, and the quantity by which the fundamental phase angle must be altered to give one complete cycle becomes smaller and smaller. This indicates a smaller range of minor loop movement along the major loop before any one loop position is repeated. When the frequency of h_n is greater than ten times the frequency of h_1, the phase change effects have practically disappeared.*

Conditions for minor loops to be formed.

Case 1. n large

Since the phase effect is negligible, let the magnetizing force be given by

$$h = h_1 \cos\omega t + h_n \cos n\omega t \qquad (1)$$

As shown earlier, the last minor loops to disappear are those in the

---

* For experimental results, see Part II, Chapter 2.

vicinity of the major loop tips, thus correspondingly, they are the first to be formed. When the amplitude of h_n is reduced, any two adjacent minor maximum (or minimum) values of total magnetizing force tend to reach a common value, which implies that there is no change in slope between these points. The minor loop at that point will disappear when this condition is reached.

The minor loops will first appear where $\frac{dh}{dt} = 0$. This occurs at H_{max} but, as shown in Fig. 13, this does not give a minor loop point for the magnetization condition of Equation 1. The first minor loop will be formed when $n\omega t = \pi$.

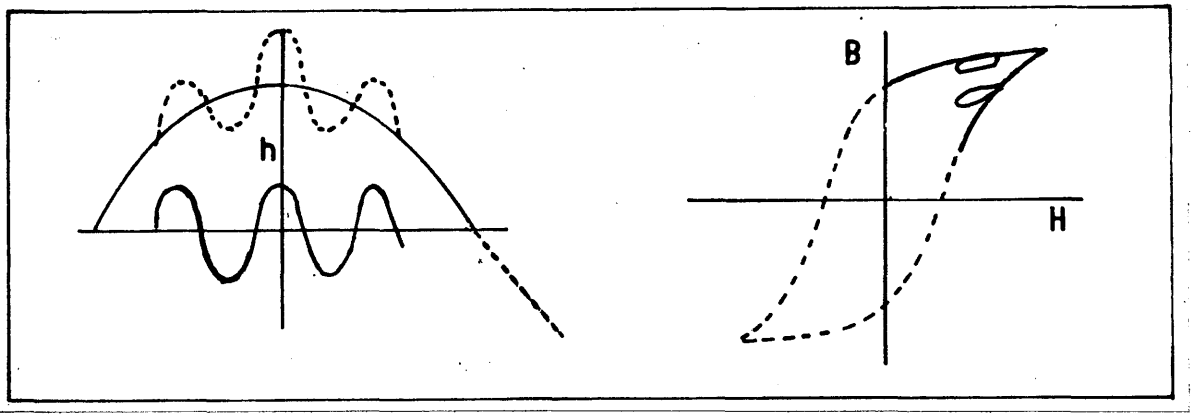

Fig. 13

The value of $\frac{dh}{dt} = -\omega h_1 \sin\omega t - n\omega h_n \sin n\omega t = 0$ and the conditions for which the minor loop will just disappear are given when sin n $\omega t = -1$.

i.e. $h_1 \sin \omega t = nh_n$

$$\therefore \quad \omega t = \sin^{-1} \frac{nh_n}{h_1} \qquad (2)$$

If $\frac{nh_n}{h_1} > 1$ all the minor loops are formed in the cycle, since there is no real solution for ωt in (2).

Case 2. When n is small.

The assumptions made in Case 1 are no longer valid and the magnetizing force must be defined as

$$h = h_1 \cos(\omega t + \varphi) + h_n \cos n\omega t \qquad (3)$$

Let $h_n = k\, h_1 \quad (k > 0)$

$$\therefore \quad \frac{dh}{dt} = -h_1 \left[\omega \sin(\omega t + \varphi) + k\, n\omega \sin n\, \omega t\right] \qquad (4)$$

$$= 0$$

For given values of n and k, equation 4 must be satisfied to enable minor loops to be formed, but care must be taken to distinguish between the absolute maximum and minimum values of h and the intermediate ones, which define the minor loop positions.

The value of k must be always real and from equation 4

$$k = -\frac{\sin(\omega t + \varphi)}{n \sin n\, \omega t}$$

$$\therefore \quad \frac{-\sin(\omega t + \varphi)}{n \sin n\, \omega t} \geqslant 0$$

As shown earlier, the first minor loops to be formed are those at the tips of the major loop, corresponding to a magnetizing force

$$h = h_1 \sin \omega t + h_n \sin n\, \omega t \qquad (5)$$

$$= h_1 \cos\left(\omega t + \frac{\pi}{n}\right) + h_n \cos n\, \omega t \qquad \left(\varphi = \frac{\pi}{n}\right)$$

$$= h_1 \left[\cos\left(\omega t + \frac{\pi}{n}\right) + k \cos n\, \omega t\right] \qquad \left(k = \frac{h_n}{h_1}\right) \qquad (6)$$

If the value of k is such that minor loops are just formed, then as the phase angle φ is altered by $\frac{\pi}{n}$ to give

$$h = h_1 (\cos \omega t + k \cos n\omega t) \qquad (7)$$

the minor loops will disappear. If the value of k is altered to k' such that minor loops are formed for equation 7, then as the phase angle is altered the minor loops will continue to be formed for all values of ϕ. Equations 6 and 7 define the range of k for a given n to cause minor loop formation for one value of ϕ or for all values of ϕ. It should be noted that $k' > k$.

Case 1.

Minimum value of k to cause minor loop formation at the tip of the major loop.

The case when n = 3 will be considered in detail. Let the magnetizing force wave be

$$h = h_1 \sin \omega t + h_3 \sin 3\omega t \quad \text{from (5)}$$

$$= h_1 \sin \omega t + kh_1 \sin 3\omega t \quad (h_3 = kh_1) \tag{8}$$

giving two minor loops for suitable values of h_3.

$$\therefore \frac{dh}{dt} = \omega h_1 \cos\omega t + 3\omega h_3 \cos 3\omega t = 0$$

$$\therefore \cos \omega t + 3k \cos 3\omega t = 0$$

$$\therefore \cos \omega t (1 - 9k) + 12k \cos^3 \omega t = 0$$

$$\therefore \cos \omega t = 0 \tag{9}$$

i.e. $\omega t = \frac{\pi}{2}$ corresponding to (a) the subsidiary minimum value $h = h_1 - h_3$ when h_3 is large enough to cause minor loop formation. (b) maximum value of h when h_3 is small, i.e., when no minor loop is formed.

Also $$\cos \omega t = \sqrt{\frac{9k - 1}{12k}} \tag{10}$$

$\therefore$ For minor loops to be formed, this must give a value of $\omega t \neq \frac{\pi}{2}$ corresponding to conditions in Fig. 14(a).

$\therefore$ k must be greater than $\frac{1}{9}$. (If $k = \frac{1}{9}$, $\omega t = \frac{\pi}{2}$ and the h wave is not re-entrant).

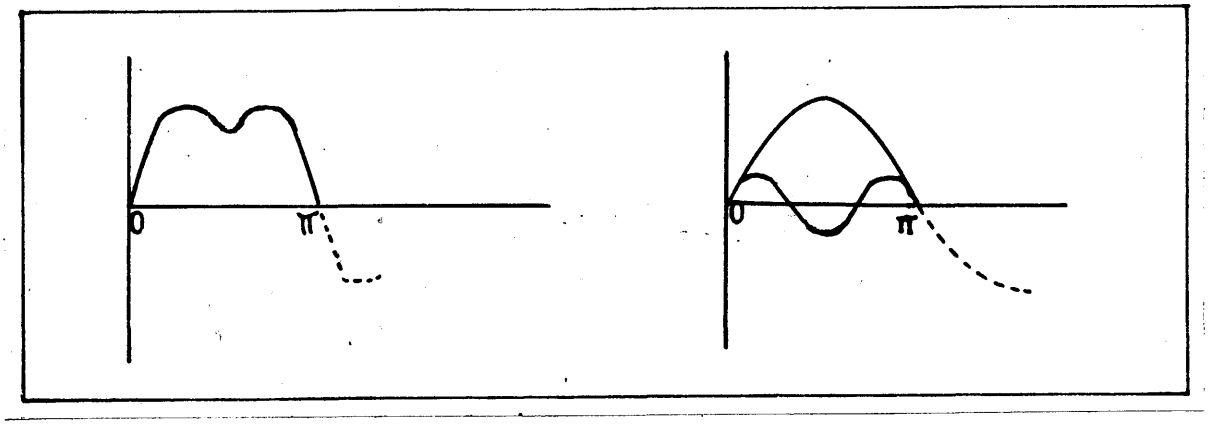

Fig. 14.

From equation 10 the value of ωt at which the first minor loop commences to be formed may be obtained for a given value of k. This loop ends when $\theta' = \pi - \omega t$. The second minor loop is formed when $\theta'' = (\pi + \omega t)$ and ends at $\theta = (2\pi - \omega t)$.

As the value of k is varied over the range $0 \rightarrow 1$, the peak value of the core magnetizing force (H_m) alters. Values of H_m, $\theta \rightarrow \theta'$, the start and finish of the first minor loop are given in the table below for values of k.

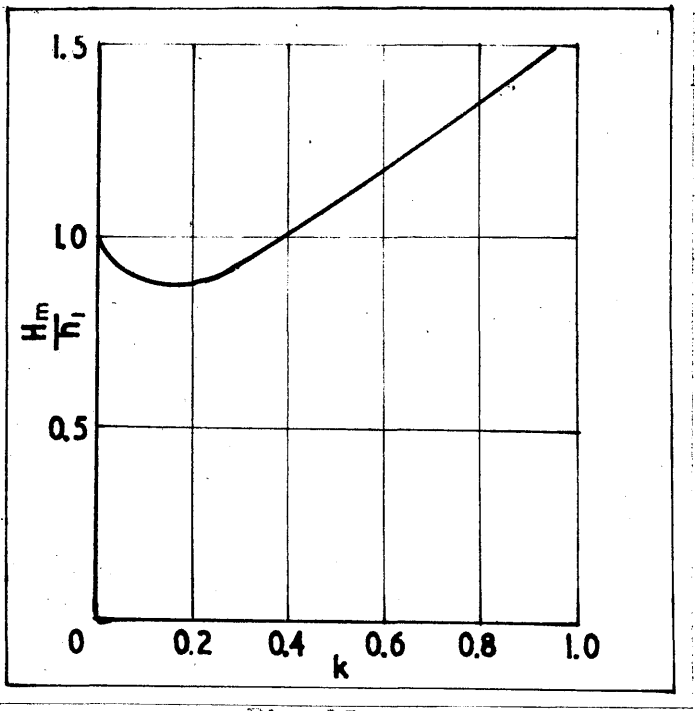

Fig. 15.
Variation of peak magnetizing force.

k	$\sqrt{\frac{9k-1}{12k}}$	θ	θ'	H_m	
0		90°	90°	h_1	)no minor loop
0.111	0.0	90°	90°	$0.889h_1$	) " " "
0.15	0.441	63° 50'	116° 10'	$0.867h_1$	
0.2	0.575	54° 54'	125° 6'	$0.871h_1$	
0.3	0.684	46° 51'	133° 9'	$0.920h_1$	
0.4	0.738	42° 27'	137° 33'	$0.993h_1$	
0.5	0.765	40° 6'	139° 54'	$1.075h_1$	
0.6	0.784	38° 22'	141° 38'	$1.166h_1$	
0.7	0.794	37° 26'	142° 34'	$1.254h_1$	
0.8	0.806	36° 18'	143° 42'	$1.348h_1$	
0.9	0.813	35° 36'	144° 24'	$1.442h_1$	
1.0	0.817	35° 12'	144° 48'	$1.539h_1$	
Very large n.	0.866	30°	150°	nh_1	

For the magnetization conditions of equation 8, Fig. 15 shows that under combined magnetization the value of H_m is less than h_1 over the range of $k > 0 < 0.41$, while minor loops are formed only over the portion of this range for $k > 0.111$. It is, therefore, possible that over a portion of this range there may be a reduction in low frequency loss under combined magnetization. (See Chapter 4).

Case 2.

Minimum value of k to cause minor loop formation at any point on the major loop.

To obtain this condition, the magnetizing force is given by equation 7 (where n = 3),

i.e. $h = h_1 \cos\omega t + h_3 \cos 3\omega t$

$$= h_1 (\cos \omega t + k \cos 3\omega t)$$

$$\therefore \frac{dh}{dt} = 0 = \sin \omega t + 3k \sin 3\omega t$$

$$\therefore \quad 12k \sin^3 \omega t - (1 + 9k) \sin \omega t = 0$$

$$\therefore \quad \sin \omega t = 0, \text{ i.e. } \omega t = 0. \qquad (11)$$

This gives maximum value $h_1 + h_3$

Also

$$\sin \omega t = \sqrt{\frac{1 + 9k}{12k}} \qquad (12)$$

$\therefore$ For $\sin \omega t < 1$ the minimum value of k which satisfies equation 12 is $1 + 9k = 12k$ $(\sin \omega t = 1)$, i.e., $k > \frac{1}{3}$.

Provided $k > \frac{1}{3}$ minor loops are formed for this condition of magnetization. The value of H_m obtained is always greater than the low frequency component h_1. Values of H_m, θ and θ', the start and finish of the first minor loops, are given below for values of k.

k	$\sqrt{\frac{1 + 9k}{12k}}$	θ	θ'	H_m
0	1	-	-	$1.0h_1$
0.333	1	90°	90°	$1.333h_1$
0.4	0.98	78° 31'	101° 29'	$1.40h_1$
0.5	0.955	72° 44'	107° 16'	$1.50h_1$
0.6	0.94	70° 31'	109° 57'	$1.6h_1$
0.7	0.931	68° 36'	111° 24'	$1.7h_1$
0.8	0.924	67° 31'	112° 29'	$1.8h_1$
0.9	0.918	66° 38'	113° 23'	$1.9h_1$
1.0	0.913	65° 56'	114° 4'	$2.0h_1$
Very large n	0.866	60°	120°	nh_1

If $k > \frac{1}{3}$ minor loops are formed for any relative phase angle φ when the magnetizing force is $h = h_1 \sin(\omega t + \varphi) + kh_1 \sin 3\omega t$.

Similar results may be obtained for the case when n = 2.

Let $h = h_1 \cos \omega t + h_2 \cos 2\omega t$.

This gives a minor loop situated at the lower tip of the major loop as shown in Fig. 16. It should be noted that the loop is no longer symmetrical.

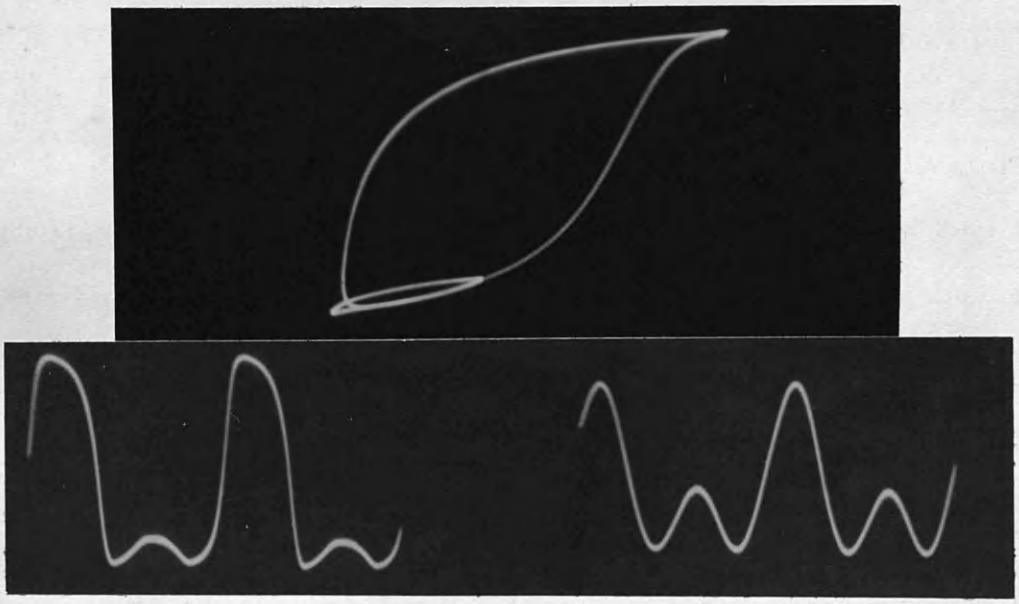

Fig. 16.

$$\frac{dh}{dt} = \omega h_1 \sin \omega t + 2\omega h_2 \sin 2\omega t$$

$\therefore$ $\sin \omega t + 4k \sin 2\omega t = 0 \quad (h_2 = kh_1)$

$\therefore$ Conditions for zero slope: i) $\sin \omega t = 0$, i.e., $\omega t = 0$. This gives the maximum value of magnetizing force $H_m = h_1 + h_2$.

ii) $4k \cos \omega t = -1$. The minimum value of k will occur when $\cos \omega t = -1$, i.e. $k = \frac{1}{4}$.

For minor loop formation under the above conditions of magnetizing force k must be greater than 0.25.

The values of ωt at which the minor loop commences and finishes are given for various values of k. In addition the values of the positive and negative H_m and the peak to peak magnetizing force are given for the range of k from 0 to 1. These results are shown graphically in Figs. 17 and 18. (The minor loop starts at θ and finishes at θ').

k	cos ωt	θ	θ'	H_m ($\omega t = 0$)	H_m ($\omega t = 0$)	Peak - Peak
0	-	180°	180°	h_1	h_1	$2h_1$
0.25	-1	180°	180°	$1.25h_1$	$-0.75h_1$	$2h_1$
0.3	-0.834	146° 30'	213° 30'	$1.3h_1$	$-0.717h_1$	$2.017h_1$
0.4	-0.625	128° 41'	231° 19'	$1.4h_1$	$-0.712h_1$	$2.112h_1$
0.5	-0.50	120°	240°	$1.5h_1$	$-0.75h_1$	$2.25h_1$
0.6	-0.416	114° 35'	245° 25'	$1.6h_1$	$-0.808h_1$	$2.408h_1$
0.8	-0.312	108° 11'	251° 49'	$1.8h_1$	$-0.95h_1$	$2.756h_1$
1.0	-0.25	104° 29'	255° 31'	$2.0h_1$	$-1.125h_1$	$3.125h_1$

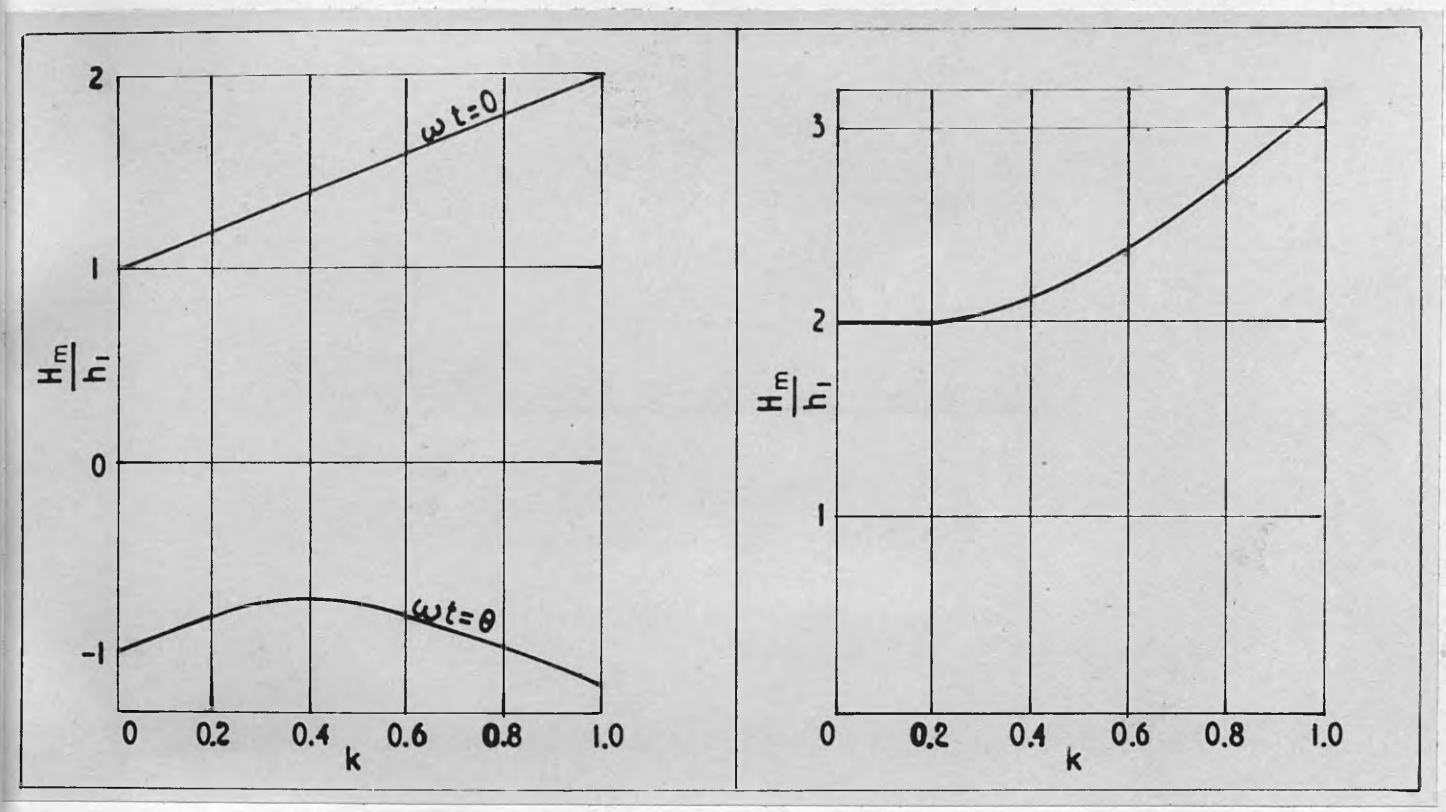

Fig. 17.
Variation of magnetizing force.

Fig. 18.
Variation of peak to peak magnetizing force.

Similarly, if $h = h_1 \sin \omega t + h_2 \sin 2\omega t$, the minor loop is situated as shown in Fig. 19. In this case, the major loop extends between $\pm H_m$.

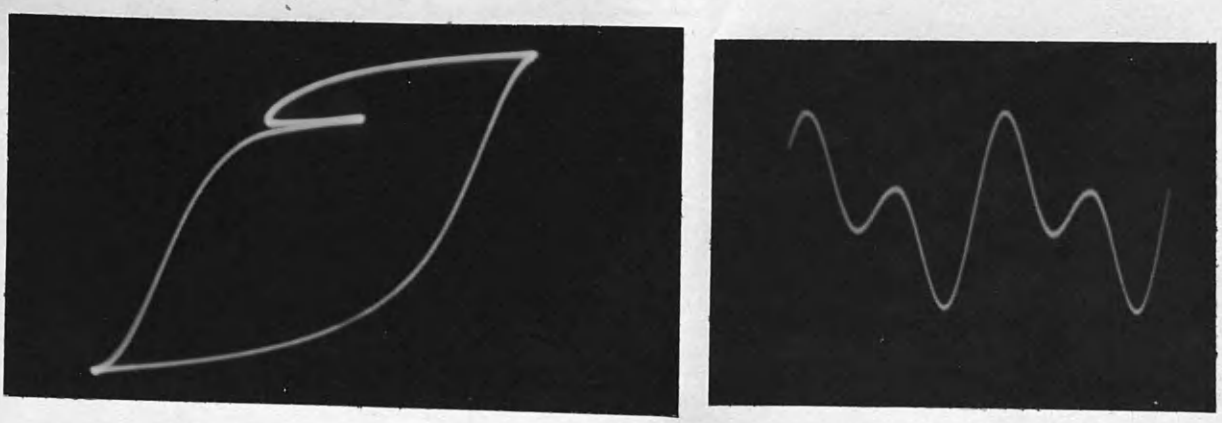

Fig. 19.

$$\therefore \quad \frac{dh}{dt} = \cos \omega t + 2k \cos 2\omega t = 0 \qquad (h_2 = kh_1)$$

$$= 4k \cos^2 \omega t + \cos\omega t - 2k = 0$$

$\therefore$ Conditions for zero slope are

$$\cos \omega t = \frac{-1 \pm \sqrt{1 + 32k^2}}{8k}$$

The range of k for minor loop formation is obtained from the above equation. When k is greater than 0.5, two solutions are obtained for ωt and hence a minor loop will be set up. The values of ωt at which the minor loop starts to be formed and the values of H_m are given for the range of k values.

k	cos ωt		θ	θ''	H_m
0	0			90°	h_1
0.1	0.187			79° 13'	$1.018h_1$
0.2	0.319			71° 24'	$1.069h_1$
0.3	0.404			66° 10'	$1.135h_1$
0.4	0.468			62° 6'	$1.215h_1$
0.5	0.5,	-1	180°	60°	$1.3h_1$
0.6	0.528,	-0.95	161° 48'	58° 8'	$1.386h_1$
0.7	0.554,	-0.91	155° 30'	56° 19'	$1.476h_1$
0.8	0.576,	-0.878	151° 24'	55° 32'	$1.57h_1$
0.9	0.578,	-0.86	149° 19'	54° 42'	$1.66h_1$
1.0	0.594,	-0.845	147° 40'	53° 33'	$1.76h_1$
Very large = n	0.707,	-0.707	135°	45°	nh_1

(θ gives start of minor loop)

(θ'' gives position of H_m)

The variation of H_m with k is shown in Fig. 20.

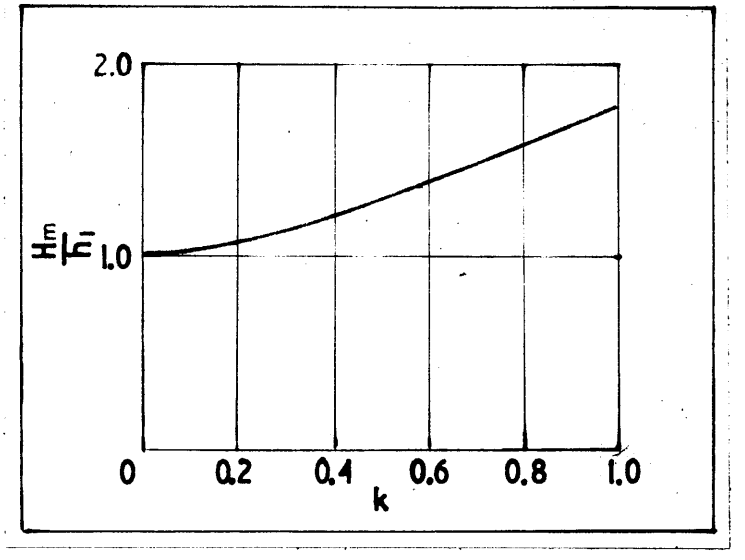

Fig. 20.

General case.

To obtain the values of ωt corresponding to $\frac{dh}{dt} = 0$ when

$h = h_1 \cos(\omega t + \varphi) + h_n \cos n\omega t$

$$\therefore \frac{dh}{dt} = -\omega h_1 \sin(\omega t + \varphi) - \omega n h_n \sin n\omega t$$

$$= 0$$

$$\therefore K \sin(\omega t + \varphi) + n \sin n\omega t = 0$$

where $K = \frac{h_1}{h_n}$.

$$\therefore A \sin \omega t + B \cos \omega t + n \sin n\omega t = 0 \qquad (13)$$

where $A = K \cos \varphi$ and $B = K \sin \varphi$.

Divide equation 13 by $\cos^n \omega t$

$$\therefore A \sin \omega t \sec^n \omega t + B \cos \omega t \sec^n \omega t + n \sec^n \omega t \sin n\omega t = 0 \qquad (14)$$

From De Moivre's theorem by equating imaginary parts

$$\sin n\omega t = n \cos^{n-1} \omega t \sin \omega t - \frac{n(n-1)(n-2)}{3!} \cos^{n-3} \omega t \sin^3 \omega t + \ldots\ldots + (-1)^{\frac{n-1}{2}} \sin^n \omega t \qquad (15)$$

for n odd,

and when n is even

$$\sin n\omega t = n \cos^{n-1} \omega t \sin \omega t - \frac{n(n-1)(n-2)}{3!} \cos^{n-3} \omega t \sin^3 \omega t + \ldots\ldots + (-1)^{\frac{n-2}{2}} n \cos \omega t \sin^{n-1} \omega t \qquad (16)$$

Consider case 1 when n is odd.

Let $t = \tan \omega t$, then by substitution of equation 15 into equation 14, the following is obtained

$$A\, t \sec^{n-1} \omega t + B \sec^{n-1} \omega t + n\left[nt - \frac{n(n-1)(n-2)}{3!} t^3 + \ldots\ldots + (-1)^{\frac{n-1}{2}} t^n \right] = 0$$

and since $\sec^2 \omega t = 1 + t^2$

$$\therefore \quad \sec^{n-1} \omega t = (1 + t^2)^{\frac{n-1}{2}}$$

$$\therefore \quad (At + B)(1 + t^2)^{\frac{n-1}{2}} + n\left[nt - \frac{n(n-1)(n-2)}{3!} t^3 + \ldots\ldots + (-1)^{\frac{n-1}{2}} t^n \right] = 0 \qquad (17)$$

Case 2. n even

Let $t = \tan \frac{\omega t}{2}$

$$\therefore \quad \tan \omega t = \frac{2t}{1 + t^2} \quad \text{and} \quad \sec^2 \omega t = \frac{1 + t^2}{1 - t^2}$$

$\therefore$ By the above substitution and from equations 16 and 14, the general expression obtained is

$$A \left(\frac{2t}{1-t^2}\right) \left(\frac{1 + t^2}{1 - t^2}\right)^{n-1} + B \left(\frac{1 + t^2}{1 - t^2}\right)^{n-1} + n\left[n \frac{2t}{1 + t^2} - \frac{n(n-1)(n-2)}{3!} \left(\frac{2t}{1-t^2} \right)^3 \ldots \right.$$

$$\left. \ldots\ldots - (1)^{\frac{n-2}{n}} n \left(\frac{2t}{1-t^2}\right)^{n-1} \right] = 0 \qquad (18)$$

Multiplying equation 18 by $(1 - t^2)^n$ gives

$$(1 + t^2)^{n-1} \left[2At + B(1-t^2) \right]$$
$$+ n \left[n(1-t^2)^{n-1}\, 2t - \frac{n(n-1)\,(n-2)}{3!} (1-t^2)^{n-3}\, (2t)^3 \right.$$
$$\left. \ldots\ldots\ldots + (-1)^{\frac{n-2}{2}}\, n\, (1-t^2)\, (2t)^{n-1} \right] = 0 \qquad (19)$$

From equations 17 and 19 by appropriate substitution, the values of ωt are obtained at which the magnetizing force wave has zero slope. This will give all points at which minor loops may be formed, in addition to the position of maximum positive and negative values of the magnetizing force h.

The general requirement for a minor loop to be formed for a magnetizing force $h = h_1 (\sin \omega t + k \sin n\omega t)$ is that k must be greater than $\frac{1}{n^2}$. Similarly if $h = h_1 (\cos\omega t + k \cos n\omega t)$, k must be greater than $\frac{1}{n}$. Hence if minor loops are to be formed for any value of phase angle φ then the value of k must exceed $\frac{1}{n}$.

From the foregoing it is obvious that to obtain the maximum effect of phase change upon core characteristics under the assumed conditions of magnetization, (see Chapter 2, case 6), the frequencies of h_n and h_1 should be in the ratio 2:1. (The 1:1 case is excluded). Results are considered for this case in Part II. The more practical case of combined magnetization in alternating current circuits is due in most cases to odd harmonic components of the magnetizing wave and consequently the case in which $h = h_1 \cos (\omega t + \varphi) + h_3 \cos 3\omega t$ is considered in greater detail experimentally and theoretically.

CHAPTER 4

EXPRESSION FOR THE CORE LOSS OF A MAGNETIC MATERIAL WHEN UNDERGOING COMBINED MAGNETIZATION.

The magnetizing force wave is defined as

$$h = h_1 \cos\omega t + h_n \cos n\,\omega t \tag{20}$$

In view of assumptions made in this calculation to give loop symmetry, only values of n odd are considered.

General expressions for B and H which represent the hysteresis loop are [1]

$$B_1(h, H_m) = a_{10}h - a_{02}h^2 + a_{11}hH_m + a_{02}H_m^2 + a_{30}h^3 - a_{03}h^2 H_m + a_{12}hH_m^2 + a_{03}H_m^3 \tag{21}$$

and

$$B_2(h, H_m) = a_{10}h + a_{02}h^2 + a_{11}hH_m - a_{02}H_m^2 + a_{30}h^3 + a_{03}h^2 H_m + a_{12}hH_m^2 - a_{03}H_m^3$$

where H_m is the peak value of core magnetizing force, and a_{nn} are core constants.

The following constants may be substituted in these expressions.

$$\begin{aligned} A &= a_{02}H_m^2 + a_{03}H_m^3 = B(0, H_m) \\ C &= a_{10} + a_{11}H_m + a_{12}H_m^2 \\ D &= a_{30}H_m^3 \\ F &= -(a_{02} + a_{03}H_m) \end{aligned} \tag{22}$$

Thus

$$\begin{aligned} B_1(h,H_m) &= B(0,H_m) + Ch + Fh^2 + a_{30}h^3 + \ldots \\ B_2(h,H_m) &= -B(0,H_m) + Ch - Fh^2 + a_{30}h^3 \ldots \end{aligned} \tag{23}$$

For h substitute equation 20

$$\therefore B_1(h,H_m) = B(0,H_m) + C(h_1\cos\omega t + h_n\cos n\,\omega t)$$
$$+ F(h_1^2\cos^2\omega t + h_n^2\cos^2 n\,\omega t + 2h_1h_n\cos\omega t\cos n\,\omega t)$$
$$+ a_{30}(h_1^3\cos^3\omega t + h_n^3\cos^3 n\,\omega t + 3h_1h_n^2\cos\omega t\cos^2 n\,\omega t$$
$$+ 3h_1^2 h_n\cos^2\omega t\cos n\,\omega t) \qquad (24)$$

and $B_2(h,H_m) = -B(0,H_m) + C(h_1\cos\omega t + h_n\cos n\omega t)$
$$-F(h_1^2\cos^2\omega t + h_n^2\cos^2 n\omega t + 2h_1h_n\cos\omega t\cos n\,\omega t)$$
$$+ a_{30}(h_1^3\cos^3\omega t + h_n^3\cos^3 n\omega t + 3h_1h_n^2\cos\omega t\cos^2 n\omega t$$
$$+ 3h_1^2 h_n\cos^2\omega t\cos n\omega t)$$

$\therefore$ Consider only the expression for $B_1(H,H_m)$

$$= B(0,H_m) + Ch_1\cos\omega t + Ch_n\cos n\omega t + \frac{Fh_1^2}{2} \qquad (25)$$
$$+ \frac{Fh_1^2}{2}\cos 2\omega t + \frac{Fh_n^2}{2} + \frac{Fh_n^2}{2}\cos 2\,n\omega t$$
$$+ Fh_1 h_n\cos(n+1)\omega t + Fh_1 h_n\cos(n-1)\omega t +$$
$$\frac{^{30}30h_1^3}{4}\cos\omega t + \frac{^{a}30h_1^3}{4}\cos 3\omega t + \frac{3a_{30}H_n^3}{4}\cos n\omega t$$
$$+ \frac{^{a}30h_n^3}{4}\cos 3n\omega t + \frac{3a_{30}h_1h_n^2}{2}\cos\omega t + \frac{3a_{30}h_1h_n^2}{4}\cos(2n+1)\omega t$$
$$+ \frac{3a_{30}h_1h_n^2}{4}\cos(2n-1)\omega t + \frac{3a_{30}h_1^2h_n}{2}\cos n\,\omega t +$$
$$+ \frac{3a_{30}h_1^2h_n}{4}\cos(n+2)\omega t + \frac{3a_{30}h_1^2h_n}{4}\cos(n-2)\omega t$$

$\therefore$ Collecting terms

$$B_1(h,H_m) = \left[B(0,H_m) + \frac{F\,h_1^2 + Fh_n^2}{2}\right]$$
$$+ \left[Ch_1 + \frac{3a_{30}h_1^3}{4} + \frac{3a_{30}h_1h_n^2}{2}\right]\cos\omega t \qquad (26)$$
$$+ \frac{Fh_1^2}{2}\cos 2\,\omega t$$
$$+ \frac{^{a}30h_1^3}{4}\cos 3\,\omega t$$

$$+ \frac{3a_{30}h_1^2h_n}{4} \cos (n-2)\omega t$$

$$+ Fh_1h_n \cos (n-1)\omega t$$

$$+ \left[Ch_n + \frac{3a_{30}h_n^3}{4} + \frac{3a_{30}h_1^2h_n}{2}\right] \cos n\omega t$$

$$+ Fh_1h_n \cos (n+1)\omega t$$

$$+ \frac{3a_{30}h_1^2h_n}{4} \cos (n+2)\omega t$$

$$+ \frac{3a_{30}h_1h_n^2}{4} \cos (2n-1)\omega t$$

$$+ \frac{Fh_n^2}{2} \cos 2n\omega t$$

$$+ \frac{3a_{30}h_1h_n^2}{4} \cos (2n+1)\omega t$$

$$+ \frac{a_{30}h_n^3}{4} \cos 3n\omega t$$

Hence the general expression for $B_1(h, H_m)$ is

$$\alpha + \beta \cos \omega t + \gamma \cos 2\omega t + \delta \cos 3\omega t + \varepsilon \cos n\omega t \qquad (27)$$
$$+ \zeta \cos 2n\omega t + \eta \cos 3n\omega t + \theta \left[\cos (n+1)\omega t + \cos (n-1)\omega t\right]$$
$$+ \iota \left[\cos (n+2)\omega t + \cos (n-2)\omega t\right] + \kappa \left[\cos (2n+1)\omega t + \cos (2n-1)\omega t\right]$$

in which the constants have the following values.

$$\alpha = B(0, H_m) + \frac{F}{2}(h_1^2 + h_n^2)$$

$$\beta = Ch_1 + \frac{3a_{30}h_1^3}{4} + \frac{3a_{30}h_1h_n^2}{2}$$

$$\gamma = \frac{Fh_1^2}{2}$$

$$\delta = \frac{a_{30}h_1^3}{4}$$

$$\varepsilon = Ch_n + \frac{3a_{30}h_n^3}{4} + \frac{3a_{30}h_1^2h_n}{2}$$

$$\zeta = \frac{Fh_n^2}{2}$$

$$\eta = \frac{a_{30}h_n^3}{4}$$

$$\theta = Fh_1h_n$$

$$i = \frac{3a_{30}h_1h_n^2}{4}$$

$$\mathcal{K} = \frac{3a_{30}h_1h_n^2}{4}$$

Similarly for $B_2(h, H_m)$

$$= -\alpha + \beta \cos\omega t - \gamma \cos 2\omega t + \delta \cos 3\omega t + \varepsilon \cos n\omega t \qquad (29)$$
$$- \zeta \cos 2 n\omega t + \eta \cos 3n \omega t - \theta \left[\cos(n + 1)\, \omega t + \cos (n-1)\, \omega t\right]$$
$$+ i \left[\cos(n + 2)\, \omega t + \cos(n-2)\, \omega t\right] + \mathcal{K}\left[\cos (2n + 1)\, \omega t + \cos(2n-1)\, \omega t\right]$$

These two equations for the B - H relationship may be combined in a Fourier series valid over one complete cycle.

$$B = \frac{a_0}{2} + \sum (a_k \cos k\, \omega t + b_k \sin k\, \omega t) \qquad (30)$$

For n odd

$$a_k = \frac{2}{\pi}\int_0^{\pi}\Big\{\beta \cos \omega t + \delta \cos 3\omega t + \varepsilon \cos n\omega t + \eta \cos 3\, n\omega t \qquad (31)$$
$$+ i\left[\cos (n + 2)\, \omega t + \cos (n - 2)\, \omega t\right] + \mathcal{K}\left[\cos (2n + 1)\, \omega t\right.$$
$$\left. + \cos (2n - 1)\, \omega t\right]\Big\} \cos k\omega t\, d\, (\omega t)$$

and

$$b_k = \frac{2}{\pi}\int_0^{\pi}\Big\{\alpha + \gamma \cos 2\omega t + \zeta \cos 2n\omega t + \theta\left[\cos (n + 1)\, \omega t \qquad (32)$$
$$+ \cos (n - 1)\, \omega t\right]\Big\} \sin k\, \omega t\, d\, (\omega t)$$

The general form of the solution for B is

$$= a_1 \cos \omega t + a_3 \cos 3\omega t + \ldots \qquad (33)$$
$$+ b_1 \sin \omega t + b_3 \sin 3\omega t + \ldots$$

Since $e = TA\frac{dB}{dt}$ T = coil turns

A = cross sectional area of core

$$= TA\left[-\omega a_1 \sin \omega t - 3\omega a \sin 3\, \omega t \ldots \qquad (34)\right.$$
$$\left. + \omega b_1 \cos \omega t + 3\, \omega b_3 \cos 3\omega t + \ldots\right]$$

To obtain the fundamental frequency component of core loss, it is only necessary to evaluate the coefficient b_1 as the applied magnetizing force was $h = h_1 \cos \omega t + h_n \cos n \omega t$.

Evaluation of b_1.

In the expression for b_k put $k = 1$

$$\therefore \quad b_1 = \frac{2}{\pi}\int_0^{\pi}\Big\{ \alpha \sin \omega t + \gamma \cos 2\omega t \sin \omega t + \zeta \cos 2n \omega t \sin \omega t + \theta\big[\cos (n + 1) \omega t \sin \omega t + \cos (n - 1) \omega t \sin \omega t\big]\Big\} \, d(\omega t)$$

$$= \frac{2}{\pi}\int_0^{\pi}\Big\{ \alpha \sin \omega t + \frac{\gamma}{2}(\sin 3\omega t - \sin \omega t) + \frac{\zeta}{2}\big[\sin (2n + 1) \omega t - \sin (2n - 1) \omega t\big] + \frac{\theta}{2}\big[\sin (n + 2) \omega t - \sin n\omega t + \sin n \omega t - \sin (n - 2) \omega t\big]\Big\} \, d(\omega t)$$

$$= \frac{4}{\pi}\Big[\alpha - \frac{\gamma}{3} - \frac{2\theta}{n^2 - 4} - \frac{\zeta}{4n^2 - 1}\Big] \qquad (35)$$

Substituting values for the constants from equation 28 gives

$$b_1 = \frac{4}{\pi}\Big[B(0, H_m) + \frac{F}{2}(h_1^2 + h_n^2) - \frac{Fh_1^2}{6} - \frac{2Fh_1h_n}{n^2 - 4} - \frac{Fh_n^2}{2(4n^2 - 1)}\Big]$$

$$= \frac{4}{\pi}\Big[B(0, H_m) - (a_{02} + a_{03} H_m)\Big(\frac{h_1^2}{3} + \frac{2n^2 - 1}{4n^2 - 1} h_n^2 - \frac{2h_1h_n}{n^2 - 4}\Big)\Big] \qquad (36)$$

From equation 34 the hysteresis loss in the core contributed by the low frequency component is $E_1 I_1 \cos \varphi$, and the r.m.s. value of the in-phase component of voltage is $\frac{TA\omega b_1}{\sqrt{2}}$ (since magnetizing force is $h = h_1 \cos \omega t + h_n \cos n \omega t$).

$$\therefore \quad \text{Loss} = \frac{TA\omega}{\sqrt{2}} b_1 I_1 \text{ watts}, \qquad (37)$$

where $I_1 = \frac{h_1 l}{\sqrt{2}T}$

(neglecting eddy current effects).

Equation 36 gives the general solution for b_1 for any odd value of n. The case which is considered in detail experimentally is when n = 3.

$\therefore$ Put n = 3 in equation 36.

$$\therefore \quad b_1 = \frac{4}{\pi}\left[B(0,Hm) + \frac{F}{2}(h_1^2 + h_3^2) - \frac{Fh_1^2}{6} - \frac{2Fh_1h_3}{5} - \frac{Fh_3^2}{70}\right]$$

$$= \frac{4}{\pi}\left[B(0,H_m) + F\left(\frac{1}{3}h_1^2 - \frac{2}{5}h_1h_3 + \frac{17}{35}h_3^2\right)\right]$$

Substituting the value for F from equation 22.

$$\therefore \quad b_1 = \frac{4}{\pi}\left[B(0,H_m) - (a_{02} + a_{03}H_m)\left(\frac{1}{3}h_1^2 - \frac{2}{5}h_1h_3 + \frac{17}{35}h_3^2\right)\right] \qquad (38)$$

Note

If $h_3 = 0$, then $h_1 = H_m$ and the value for b_1 reduces to

$$\frac{4}{\pi}\left[B(0,H_m) - \frac{1}{3}(a_{02}H_m^2 + a_{03}H_m^3)\right]$$

$$= \frac{4}{\pi}\left[B(0,H_m) - \frac{1}{3}B(0,H_m)\right]$$

$$= \frac{8}{3\pi}B(0,H_m)$$

for the case of single frequency magnetization.

Effect of phase change on loss coefficient.

Consider the case when n = 3. In equation 24 of the previous case, substitute

$$h = h_1 \sin \omega t + h_3 \sin 3\omega t \qquad (39)$$

$$\therefore \quad B_1(h,H_m) = B(0,H_m) + C(h_1 \sin \omega t + h_3 \sin 3\omega t)$$
$$+ F(h_1^2 \sin^2 \omega t + h_3^2 \sin^2 3\omega t$$
$$+ 2h_1h_3^2 \sin \omega t \sin 3\omega t)$$
$$+ a_{30}(h_1^3 \sin^3 \omega t + h_3^3 \sin^3 3\omega t$$
$$+ 3h_1h_3^2 \sin \omega t \sin^2 3\omega t$$
$$+ 3h_1^2 h_3 \sin^2 \omega t \sin^3 \omega t).$$

$$= B(0,Hm) + Ch_1 \sin \omega t + Ch_3 \sin 3\omega t + \frac{1}{2} Fh_1^2 - \frac{1}{2} Fh_1^2 \cos 2\omega t + \frac{1}{2} Fh_3^2$$
$$- \frac{1}{2} Fh_3^2 \cos 6\omega t + Fh_1 h_3 \cos 2\omega t - Fh_1 h_3 \cos 4\omega t$$
$$+ \frac{3}{4} a_{30} h_1^3 \sin \omega t - \frac{1}{4} a_{30} h_1^3 \sin 3\omega t + \frac{3}{4} a_{30} h_3^3 \sin 3\omega t$$
$$- \frac{1}{4} a_{30} h_3^3 \sin 9\omega t + \frac{3}{2} a_{30} h_1 h_3^2 \sin \omega t - \frac{3}{4} a_{30} h_1 h_3^2 \sin 7\omega t$$
$$+ \frac{3}{4} a_{30} h_1 h_3^2 \sin 5\omega t + \frac{3}{2} a_{30} h_1^2 h_3 \sin 3\omega t - \frac{3}{4} a_{30} h_1^2 h_3 \sin 5\omega t$$
$$- \frac{3}{4} a_{30} h_1^2 h_3 \sin \omega t$$

Collecting terms.

$$B_1(h,H_m) = \frac{1}{2} Fh_1^2 + \frac{1}{2} Fh_3^2 + B(0,H_m) \qquad (41)$$
$$+\left[Ch_1 + \frac{3}{4} a_{30} h_1^3 + \frac{3}{2} a_{30} h_1 h_3^2 - \frac{3}{4} a_{30} h_1^2 h_3 \right] \sin \omega t$$
$$+\left[-\frac{1}{2} Fh_1^2 + Fh_1 h_3 \right] \cos 2\omega t$$
$$+\left[Ch_3 - \frac{1}{4} a_{30} h_1^3 + \frac{3}{4} a_{30} h_3^3 + \frac{3}{2} a_{30} h_1^2 h_3 \right] \sin 3\omega t$$
$$+\left[-Fh_1 h_3 \right] \cos 4\omega t$$
$$+\left[\frac{3}{4} a_{30} h_1 h_3^2 - \frac{3}{4} a_{30} h_1^2 h_3 \right] \sin 5\omega t$$
$$+\left[-\frac{1}{2} Fh_3^2 \right] \cos 6\omega t$$
$$+\left[-\frac{3}{4} a_{30} h_1 h_3^2 \right] \sin 7\omega t$$
$$+\left[-\frac{1}{4} a_{30} h_3^3 \right] \sin 9\omega t$$

$\therefore$ $B_1(h,H_m) = \alpha + \beta \sin \omega t + \gamma \cos 2\omega t + \delta \sin 3\omega t + \varepsilon \cos 4\omega t$
$$+ \zeta \sin 5\omega t + \eta \cos 6\omega t + \theta \sin 7\omega t + \iota \sin 9\omega t \qquad (42)$$

Similarly

$$B_2(h,H_m) = -\alpha + \beta \sin \omega t - \gamma \cos 2\omega t + \delta \sin 3\omega t - \varepsilon \cos 4\omega t$$
$$+ \zeta \sin 5\omega t - \eta \cos 6\omega t + \theta \sin 7\omega t + \iota \sin 9\omega t$$

$\therefore$ Combining these two equations in the usual manner

$$B = \frac{a_0}{2} + \sum (a_k \cos k\omega t + b_k \sin k\omega t)$$

$$\therefore a_k = \frac{1}{\pi} \int_0^{2\pi} f(\omega t) \cos k\omega t \, d(\omega t)$$

$$b_k = \frac{1}{\pi} \int_0^{2\pi} f(\omega t) \sin k\omega t \, d(\omega t)$$

Since $B = B_1$ from $\frac{\pi}{2}$ to $\frac{3\pi}{2}$ and $B = B_2$ from $\frac{-\pi}{2}$ to $\frac{\pi}{2}$

$$\therefore \quad \pi a_k = \int_{\frac{-\pi}{2}}^{\frac{\pi}{2}} B_2(h,H_m) \cos k\,\omega t \, d(\omega t) + \int_{\frac{\pi}{2}}^{\frac{3\pi}{2}} B_1(h,H_m) \cos k\omega t \, d(\omega t) \quad (43)$$

$$\pi b_k = \int_{\frac{-\pi}{2}}^{\frac{\pi}{2}} B_2(h,H_m) \sin k\,\omega t \, d(\omega t) + \int_{\frac{\pi}{2}}^{\frac{3\pi}{2}} B_1(h,H_m) \sin k\,\omega t \, d(\omega t)$$

$\therefore$ General form of solution for B is

$$= a_1 \cos \omega t + a_3 \cos 3\omega t + \ldots$$

$$+ b_1 \sin \omega t + b_3 \sin 3\omega t + \ldots$$

Since magnetizing force wave is defined as

$$h = h_1 \sin \omega t + h_3 \sin 3\omega t$$

$\therefore$ to obtain the fundamental loss component, it is only necessary to evaluate the a_1 term in the general expression for B.

$$\therefore \quad a_1 = \frac{1}{\pi}\Big[\int_{\frac{-\pi}{2}}^{\frac{\pi}{2}} -\alpha + \beta \sin \omega t - \gamma \cos 2\,\omega t + \delta \sin 3\omega t - \varepsilon \cos 4\omega t \quad (44)$$

$$+ \zeta \sin 5\omega t - \eta \cos 6\omega t + \theta \sin 7\omega t + \iota \sin 9\omega t) \cos\omega t \, d(\omega t)$$

$$+ \int_{\frac{\pi}{2}}^{\frac{3\pi}{2}} \alpha + B \sin \omega t + \gamma \cos 2\omega t + \delta \sin 3\omega t + \varepsilon \cos 4\omega t$$

$$+ \zeta \sin 5\omega t + \eta \cos 6\omega t + \theta \sin 7\omega t + \iota \sin 9\omega t) \cos\omega t \, d(\omega t)\Big]$$

$$a_1 = \frac{1}{\pi}\Big[\int_{\frac{-\pi}{2}}^{\frac{\pi}{2}} -\alpha \cos \omega t + \frac{\beta}{2} \sin 2\omega t - \frac{\gamma}{2} (\cos 3\omega t + \cos\omega t) + \frac{\delta}{2} (\sin 4\omega t + \sin 2\omega t) \quad (45)$$

$$- \frac{\varepsilon}{2} (\cos 5\omega t + \cos 3\omega t) + \frac{\zeta}{2} (\sin 6\omega t + \sin 4\omega t)$$

$$- \frac{\eta}{2} (\cos 7\omega t + \cos 5\omega t) + \frac{\theta}{2} (\sin 8\omega t + \sin 6\omega t)$$

$$+ \frac{\iota}{2} (\sin 10\,\omega t + \sin 8\omega t) \, d(\omega t) +$$

$$+ \int_{\frac{\pi}{2}}^{\frac{3\pi}{2}} \alpha \cos \omega t + \frac{\beta}{2} \sin 2\omega t + \frac{\gamma}{2} (\cos 3\,\omega t + \cos \omega t) + \frac{\delta}{2} (\sin 4\omega t + \sin 7\omega t)$$

$$+ \frac{\epsilon}{2}(\cos 5\omega t + \cos 3\omega t) + \frac{\zeta}{2}(\sin 6\omega t + \sin 4\omega t)$$
$$+ \frac{\eta}{2}(\cos 7\omega t + \cos 5\omega t) + \frac{\theta}{2}(\sin 8\omega t + \sin 6\omega t)$$
$$+ \frac{\iota}{2}(\sin 10\omega t + \sin 8\omega t)\ d\omega t\Big]$$

$$= -\frac{4}{\pi}\left[\alpha + \frac{\gamma}{3} - \frac{\epsilon}{15} + \frac{\eta}{35}\right]$$

$$= -\frac{4}{\pi}\Big[B(0,H_m) + \left(\frac{1}{2}Fh_1^2 + Fh_3^2\right) + \frac{\left(-\frac{1}{2}Fh_1^2 + Fh_1h_3\right)}{3}$$
$$- \left(\frac{-Fh_1h_3}{15}\right) + \left(-\frac{1}{70}Fh_3^2\right)\Big]$$

$$= -\frac{4}{\pi}\Big[B(0,H_m) + \frac{1}{2}Fh_1^2 + \frac{1}{2}Fh_3^2 - \frac{1}{6}Fh_1^2 + \frac{1}{3}Fh_1h_3$$
$$+ \frac{Fh_1h_3}{15} - \frac{1}{70}Fh_3^2\Big]$$

$$= -\frac{4}{\pi}\Big[B(0,H_m) + F\left(\frac{1}{3}h_1^2 + \frac{17}{35}h_3^2 + \frac{2}{5}h_1h_3\right)\Big]$$

$$= -\frac{4}{\pi}\Big[B(0,H_m) - (a_{02} + a_{03}H_m)\left(\frac{1}{3}h_1^2 + \frac{17}{35}h_3^2 + \frac{2}{5}h_1h_3\right)\Big] \qquad (46)$$

Note

If $h_3 = 0$, $h_1 = H_m$ and the expression again reduces to

$$\frac{4}{\pi}\left[B(0,H_m) - \frac{1}{3}B(0,H_m)\right]$$
$$= \frac{8}{3\pi}B(0,H_m) \text{ for single frequency magnetization.}$$

The two cases considered may be combined and the effect of a change in the relative phase of one component studied in detail if the magnetizing force in Case 2, equation 39, is taken as the basic reference, i.e. $h = h_1 \sin \omega t + h_3 \sin 3\omega t$. The magnetizing force for case 1 may then be written as

$$h = h_1 \sin(\omega t + 60^\circ) + h_3 \sin 3\omega t \ . \quad (\text{i.e. } \varphi = 60^\circ) \qquad (47)$$

These two magnetizing force values give the limiting conditions of core magnetization. Equation 39 gives minor loops situated at the tips of the major loop (see Fig. 21). As shown in Chapter 2, for small values of h_3, the minor loops formed in this position are the last to disappear as h_3

is reduced. Additionally, this phase position gives the minimum value of H_m for given values of h_1 and h_3 and hence it would be expected that the low frequency core loss would be a minimum at this point.

The other extreme case, equation 47, gives a loop as shown in Fig. 22. The maximum value of total core magnetizing force for given h_1 and h_3 values is obtained in this phase position, which also gives the maximum low frequency core loss.

Fig. 21. $h = h_1 \sin \omega t + h_3 \sin 3\omega t$

Fig. 22. $h = h_1 \sin (\omega t + \frac{\pi}{3}) + h_3 \sin 3 \omega t$

The magnetizing force waves and loss loops obtained in the two extreme cases of combined magnetization (when n = 3) are shown in Figs. 21 and 22.

Effect of the higher frequency component of magnetizing force on the low frequency loss term.

1a) If the core is subjected to a magnetizing force $h = h_1 \cos \omega t + h_3 \cos 3\omega t$, the peak value of magnetizing force is $H_m = h_1 + h_3$. The loop shape obtained is shown in Fig. 22. The loss term b_1 as obtained from equation 38 may be compared with the corresponding term obtained when the core is energised by $h = h_1 \cos \omega t$, i.e. single frequency excitation with the same value of h_1 as above. This will show if the low frequency component of loss is increased due to the presence of the higher frequency term. In this case, since $H_m > h_1$ an increase in loss would be expected.

$$b_1 = \frac{4}{\pi} \left[B(0,H_m) - (a_{02} + a_{03} H_m) \left(\frac{1}{3} h_1^2 - \frac{2h_1 h_3}{5} + \frac{17}{35} h_3^2 \right) \right]$$

(from equation 38)

Let $k_3 = kh_1$ and substitute for B (OH) from equation 22 $(k > 0 < 1)$

$\therefore$ Since $B(0,H_m) = a_{02} H_m^2 + a_{03} H_m^3$ where $H_m = h_1 + h_3 = h_1 (1 + k)$

$$= a_{02} (h_1 + h_3)^2 + a_{03} (h_1 + h_3)^3$$

$$= a_{02} h_1^2 (1 + k)^2 + a_{03} h_1^3 (1 + k)^3 \qquad (48)$$

and $(a_{02} + a_{03} H_m) \left(\frac{1}{3} h_1^2 - \frac{2h_1 h_3}{5} + \frac{17}{35} h_3^2 \right)$

$$= \left[a_{02} + a_{03} (1 + k) h_1 \right] \left(\frac{1}{3} h_1^2 - \frac{2k h_1^2}{5} + \frac{17}{35} k^2 h_1^2 \right)$$

$$= \left[a_{02} + a_{03} (1 + k) h_1 \right] \left[h_1^2 \left(\frac{1}{3} - \frac{2k}{5} + \frac{17}{35} k^2 \right) \right]$$

$$= a_{02} h_1^2 \left(\frac{1}{3} - \frac{2k}{5} + \frac{17}{35} k^2 \right) + a_{03} h_1^3 (1 + k) \left(\frac{1}{3} - \frac{2k}{5} + \frac{17}{35} k^2 \right) \qquad (49)$$

$\therefore$ From equations 48 and 49.

$$b_1 = \frac{4}{\pi}\Big[a_{02}h_1^2\,(1+k)^2 + a_{03}h_1^3\,(1+k)^3 - a_{02}h_1^2\left(\frac{1}{3} - \frac{2k}{5} + \frac{17}{35}k^2\right) - a_{03}h_1^3\,(1+k)\left(\frac{1}{3} - \frac{2k}{5} + \frac{17}{35}k^2\right)\Big]$$

$$= \frac{4}{\pi}\Big\{a_{02}h_1^2\left[(1+k)^2 - \left(\frac{1}{3} - \frac{2k}{5} + \frac{17}{35}k^2\right)\right] + a_{03}h_1^3\,(1+k)\left[(1+k)^2 - \left(\frac{1}{3} - \frac{2k}{5} + \frac{17}{35}k^2\right)\right]\Big\}$$

$$= \frac{4}{\pi}\left[P\,a_{02}h_1^2 + P\,(1+k)\,a_{03}h_1^3\right] \qquad (50)$$

Where $P = \left[(1+k)^2 - \left(\frac{1}{3} - \frac{2k}{5} + \frac{17}{35}k^2\right)\right]$

$\therefore$ $b_1 = \frac{4}{\pi}\left[\left(\frac{2}{3} + \frac{12}{5}k + \frac{18}{35}k^2\right)a_{02}h_1^2 + \left(\frac{2}{3} + \frac{46}{15}k + \frac{102}{35}k^2 + \frac{18}{35}k^3\right)a_{03}h_1^3\right]$ (51)

From the single frequency case for the same value of low frequency magnetizing force

$$b_1^1 = \frac{8}{3\pi}\,B(0,H_m) \qquad (H_m = h_1)$$

$$= \frac{4}{\pi}\left[\frac{2}{3}a_{02}h_1^2 + \frac{2}{3}a_{03}h_1^3\right]$$

$\therefore$ If there was to be any reduction in low frequency core loss due to the superimposed magnetizing force, then either P or P (1 + k) or both, require to be less than $\frac{2}{3}$ for a value of k, which must be positive.

Consider expression for $P = (1+k)^2 - \left(\frac{1}{3} - \frac{2k}{5} + \frac{17}{35}k^2\right)$

$$= 1 + k^2 + 2k - \frac{1}{3} + \frac{2k}{5} - \frac{17}{35}k^2$$

$$= \frac{2}{3} + \frac{12}{5}k + \frac{18}{35}k^2$$

$\therefore$ Provided k is positive this equation will always be greater than $\frac{2}{3}$. Similarly $(1+k)\,P > \frac{2}{3}$. The low frequency core loss is increased by $(b_1 - b_1^1)$ as k is varied.

Where $(b_1 - b_1^1) = \frac{4}{\pi}\left[\left(\frac{12}{5}k + \frac{18}{35}k^2\right)a_{02}h_1^2 + \left(\frac{46}{15}k + \frac{102}{35}k^2 + \frac{18}{35}k^3\right)a_{03}h_1^3\right]$ (52)

Variation of the increase in coefficients with the value of k

k	$\frac{12}{5}k$ $= 2.4k$	$\frac{18}{35}k^2$ $=0.515k^2$	$\frac{12}{5}k + \frac{18}{35}k^2$	$\frac{46}{15}k$ $=3.07k$	$\frac{102}{35}k^2$ $=2.92k^2$	$0.515k^2$	$\frac{46}{15}k + \frac{102}{35} + \frac{18}{35}k^3$
0	0	0	0	0	0	0	0
0.1	0.24	0.005	0.245	0.307	0.029	0.0005	0.336
0.2	0.48	0.0206	0.506	0.614	0.116	0.004	0.734
0.4	0.9	0.0825	0.982	1.23	0.465	0.034	1.729
0.6	1.44	0.186	1.62	1.84	1.05	0.11	3.00
0.8	1.92	0.33	2.25	2.46	1.86	0.26	4.58
1.0	2.4	0.515	2.92	3.07	2.92	0.51	6.50

For this condition of combined magnetization the presence of the higher frequency term causes an increase in the low frequency loss.

1b) Assume the single frequency loop has the same peak to peak values of magnetizing force as the combined loop, i.e. single frequency case $h_1' = H_m \cos \omega t$ and combined magnetization, $h = h_1 \cos \omega t + h_3 \cos 3\omega t$

where $H_m = h_1 + h_3$

$= h_1 (1 + k)$

For combined magnetization the value of b_1 is the same as previously obtained (equation 51). The single frequency value is obtained below.

$$b_1'' = \frac{8}{3\pi} B(0, H_m) = \frac{8}{3\pi} B[0, h_1 (1 + k)]$$

$$\therefore \quad b_1'' = \frac{4}{\pi} \left[\frac{2}{3} a_{02} h_1^2 (1 + k)^2 + \frac{2}{3} a_{03} h_1^3 (1 + k)^3\right]$$

$$= \frac{4}{\pi} \left[\left(\frac{2}{3} + \frac{4}{3}k + \frac{2}{3}k^2\right) a_{02} h_1^2 + \left(\frac{2}{3} + 2k + 2k^2 + \frac{2}{3}k^2\right) a_{03} h_1^3\right] \quad (53)$$

Comparing the values of b_1'' with b_1 obtained previously, the increase in fundamental loss is now given by $b_1 - b_1''$.

$\therefore$ The low frequency loss is increased by

$$\frac{4}{\pi}\left\{\left[\left(\frac{2}{3}-\frac{2}{3}\right)+\left(\frac{12}{5}-\frac{4}{3}\right)k+\left(\frac{18}{35}-\frac{2}{3}\right)k^2\right] a_{02} h_1^2 + \left[\left(\frac{2}{3}-\frac{2}{3}\right)+\left(\frac{46}{15}-2\right)k+\left(\frac{102}{35}-2\right)k^2+\left(\frac{18}{35}-\frac{2}{3}\right)k^3\right] a_{03} h_1^3\right\}$$

$$= \frac{4}{\pi}\left[(0.94k - 0.151k^2)\, a_{02} h_1^2 + (2.07k + 0.92k^2 - 0.151k^3)\, a_{03} h_1^3\right]$$

The values of the increase in the coefficients a_{02} and a_{03} for values of k are given below

			a_{02}				a_{03}
k	0.94k	$0.151k^2$	$0.94k - 0.151k^2$	2.07k	$0.92k^2$	$0.151k^3$	$2.07k + 0.92k^2 - 0.151k^3$
0	0	0	0	0	0	0	0
0.1	0.094	0.001	0.093	0.207	0.009	0.0001	0.216
0.2	0.188	0.006	0.182	0.414	0.037	0.0012	0.45
0.4	0.376	0.024	0.352	0.83	0.148	0.0097	0.968
0.6	0.564	0.054	0.510	1.24	0.33	0.0326	1.54
0.8	0.75	0.097	0.653	1.66	0.59	0.077	2.17
1.0	0.94	0.151	0.789	2.07	0.92	0.151	2.84

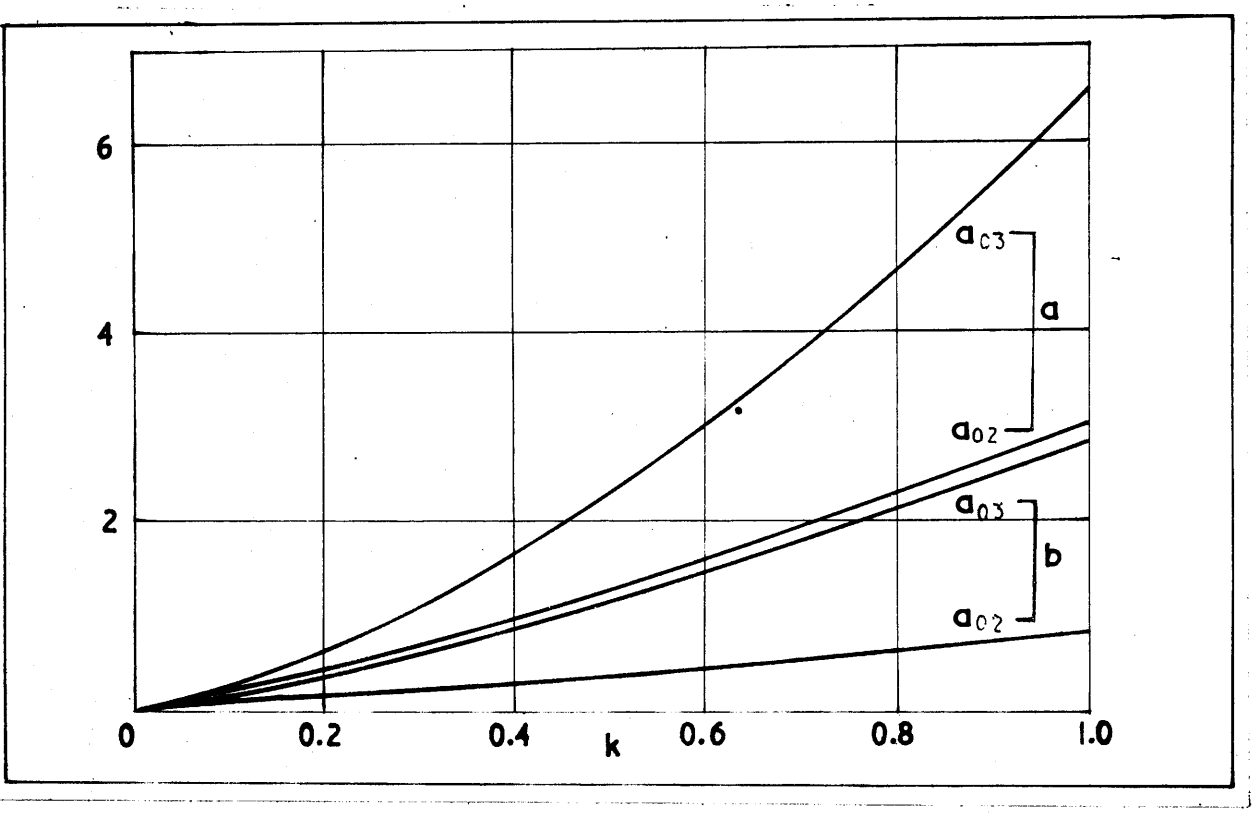

Fig. 23.
Variation of loss coefficients.

It is seen from Fig. 23 that, while the above coefficient values give a smaller increase in low frequency loss than in the previous case, there is still an appreciable increase in loss for all values of k, when the core magnetization is $h = h_1 (\cos \omega t + k \cos 3 \omega t)$.

2) Consider now the conditions where there may be a reduction in low frequency loss, i.e. when $h = h_1 (\sin \omega t + k \sin 3 \omega t)$. For a range of k values H_m is now less than h_1. For a given value of k, the value of H_m may be obtained in terms of h_1. A table showing these values is given in Chapter 3.

The single frequency magnetizing force will be taken as $h = h_1 \sin \omega t$ and the loss coefficient b_1 is given by

$$\frac{4}{\pi}\left[\frac{2}{3}\quad B(0,H_m)\right] \qquad \text{from equation 46}$$

$$= \frac{4}{\pi}\left[0.66a_{02}\,h_1^{\,2} + 0.66a_{03}\,h_1^{\,2}\right]$$

Under combined magnetization conditions, no general expression can be obtained for the change in loss with variation of k due to the dependence of H_m on k. Numerical cases will be considered and the condition illustrated graphically.

Let k = 0.15, i.e. $h = h_1 (\sin \omega t + 0.15 \sin 3\omega t)$ where $h_3 = kh_1$

Now from Chapter 3, the value of $H_m = 0.867h_1$

$$\therefore \quad a_1 = \frac{4}{\pi}\left[B(0,H_m) - (a_{02} + a_{03} H_m)\left(\frac{1}{3}h_1^{\,2} + \frac{2}{5}h_1h_3 + \frac{17}{35}h_3^{\,2}\right)\right]$$

from equation 46.

Substituting for h_3, k and H_m.

$$B(0,H_m) = 0.867^2\, a_{02}\, h_1^{\,2} + (0.867)^3\, a_{03}\, h_1^{\,3} \tag{54}$$

$$= 0.75\, a_{02}\, h_1^{\,2} + 0.65\, a_{03}\, h_1^{\,3}$$

$$\left(\frac{1}{3}h_1^{\,2} + \frac{2}{5}h_1h_3 + \frac{17}{35}h_3^{\,2}\right) = h_1^{\,2}\,(0.33 + 0.4k + 0.486k^2) \tag{55}$$

$$= 0.401h_1^{\,2}$$

$$(a_{02} + a_{03} H_m)\,(0.401h_1^{\,2}) = 0.401a_{02}\, h_1^{\,2} + 0.347a_{03}\, h_1^{\,3} \tag{56}$$

From equations 54 and 56.

$$a_1 = \frac{4}{\pi}\left[(0.75 - 0.401)\, a_{02}\, h_1^{\,2} + (0.65 - 0.347)\, a_{03}\, h_1^{\,3}\right]$$

$$= \frac{4}{\pi}\left[0.349a_{02}\, h_1^{\,2} + 0.303\, a_{03}\, h_1^{\,3}\right] \tag{57}$$

Comparing the coefficients of equation 57 with 0.66, the single frequency value, it is seen that under combined magnetization conditions there is a reduction in loss when $h = h_1 (\sin\omega t + k \sin 3\omega t)$ for k = 0.15 if a_{02} and a_{03} are both positive.

The corresponding results for various values of k are given below and are shown on Fig. 24.

k	H_m	a_{02}	a_{03}
0.0	h_1	0.66	0.66
0.15	$0.867h_1$	0.349	0.303
0.30	$0.92h_1$	0.356	0.329
0.50	$1.075h_1$	0.51	0.55
0.80	$1.348h_1$	0.85	1.15
1.0	$1.539h_1$	1.14	1.76

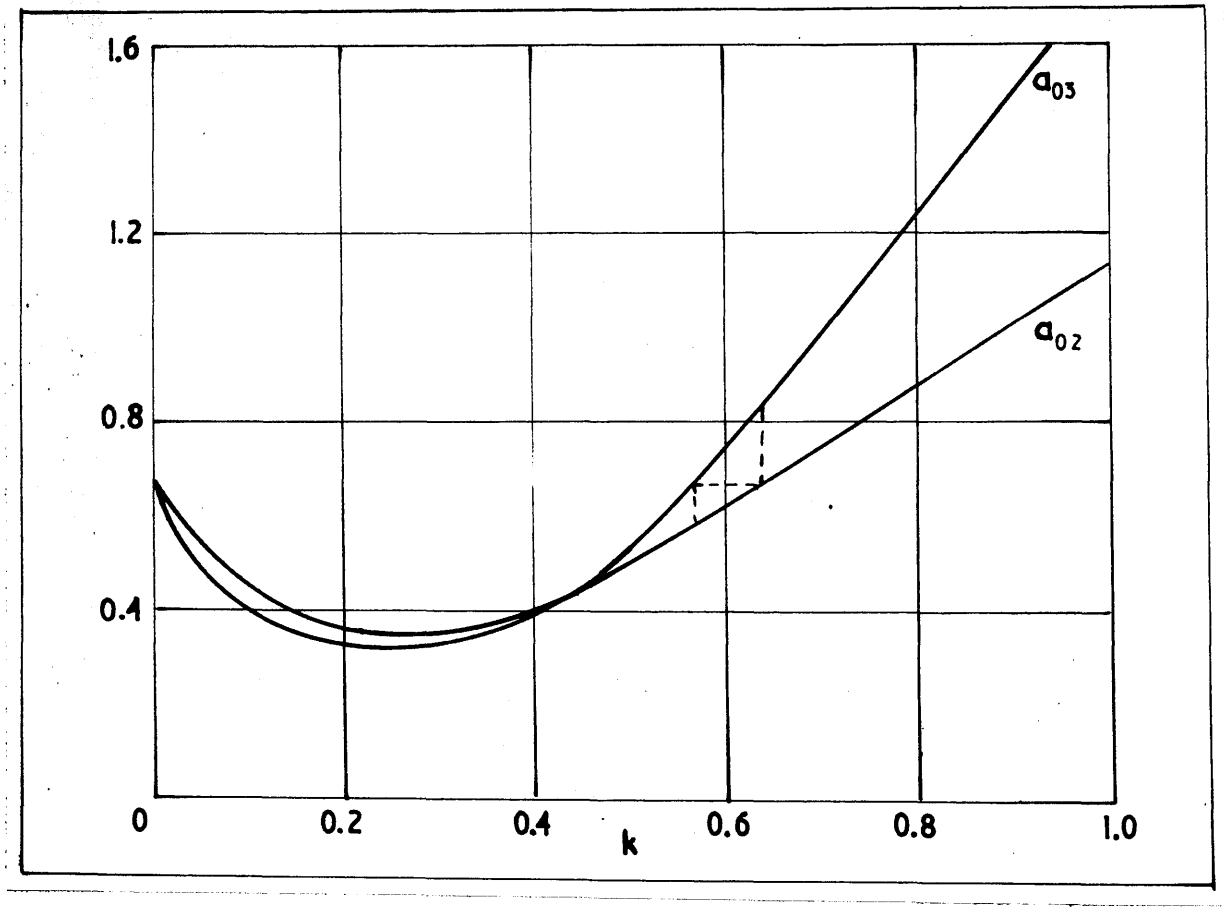

Fig. 24.
[illegible]tion of loss coefficients.

From Fig. 24 it is seen that a reduction in loss is possible over a wide range of k if a_{02} and a_{03} are both positive. (This reduction is quite independent of the numerical value of these constants). For most core materials a_{02} is positive and a_{03} negative. To obtain a reduction in W_{50} under these conditions and independent of the numerical value of the constants requires $a_{02} < 0.66$ and $a_{03} > 0.66$ for the same value of h_1 (i.e. single frequency case $h = h_1 \sin \omega t$, combined magnetization $h = h_1 (\sin \omega t + k \sin 3 \omega t)$). This condition is satisfied when k is > 0.58 and < 0.66. The value of a_{03} obtained experimentally is usually small in comparison with a_{02}. If it can be neglected, then a reduction in loss will occur over the range of k from 0 to 0.66. It should be noted that minor loops are only formed when $k > 0.111$ (See Chapter 3).

It has been shown that under conditions of combined magnetization, the low frequency component of core loss may be reduced, under certain conditions of relative phase angle and magnitudes of the magnetizing forces, when compared with the core loss value obtained for single frequency magnetization at the <u>same</u> fundamental magnetizing force. It has also been shown that under these conditions the peak core magnetizing force may be less than that obtained in the single frequency case. It may be suggested that this reduction in loss could be attributed only to the reduction in H_m, although from Fig. 24 it is seen that a reduction still occurs when $H_m > h_1$, i.e. for $k > 0.58$. The a_1 coefficients obtained on Page 42 would then require to be compared not with 0.66 the coefficient value for the original value of h_1, but with the

coefficients obtained below for the value of H_m obtained for each value of k.

i.e. original $a_1 = \frac{4}{\pi}\left[0.66\ B(0,H_m)\right] = \frac{4}{\pi}\left(0.66\ a_{02} H_m^2 + 0.66\ a_{03} H_m^3\right)$

For H_m substitute values given in the table on Page

e.g. $k = 0.15 \quad a_1'' = \frac{4}{\pi}\left[0.66\ a_{02}\ (0.867h_1)^2 + 0.66\ a_{03}\ (0.867h_1)^3\right]$

$= \frac{4}{\pi}\left(0.496\ a_{02}\ h_1^2 + 0.43\ a_{03}\ h_1^3\right)$

The complete range of these coefficients is given below

k	H_m	a_{02}''	a_{03}''
0	h_1	0.66	0.66
0.15	$0.867h_1$	0.496	0.43
0.3	$0.92h_1$	0.56	0.515
0.5	$1.075h_1$	0.763	0.82
0.8	$1.348h_1$	1.19	1.61
1.0	$1.539h_1$	1.57	2.4

From the above table it is seen that, if the single frequency loss is compared with the loss under combined magnetization for the same maximum magnetizing force, a reduction is obtained under the latter condition for all values of k considered, i.e. $> 0 \leqslant 1$. The variation of coefficients a_{02}'', a_{03}'' and a_{02}, a_{03} (from Page 42) are shown to a base of k in Fig. 25.

It is considered that this latter method of comparison is less suitable and does not fully illustrate the change in core conditions from single to combined magnetization.

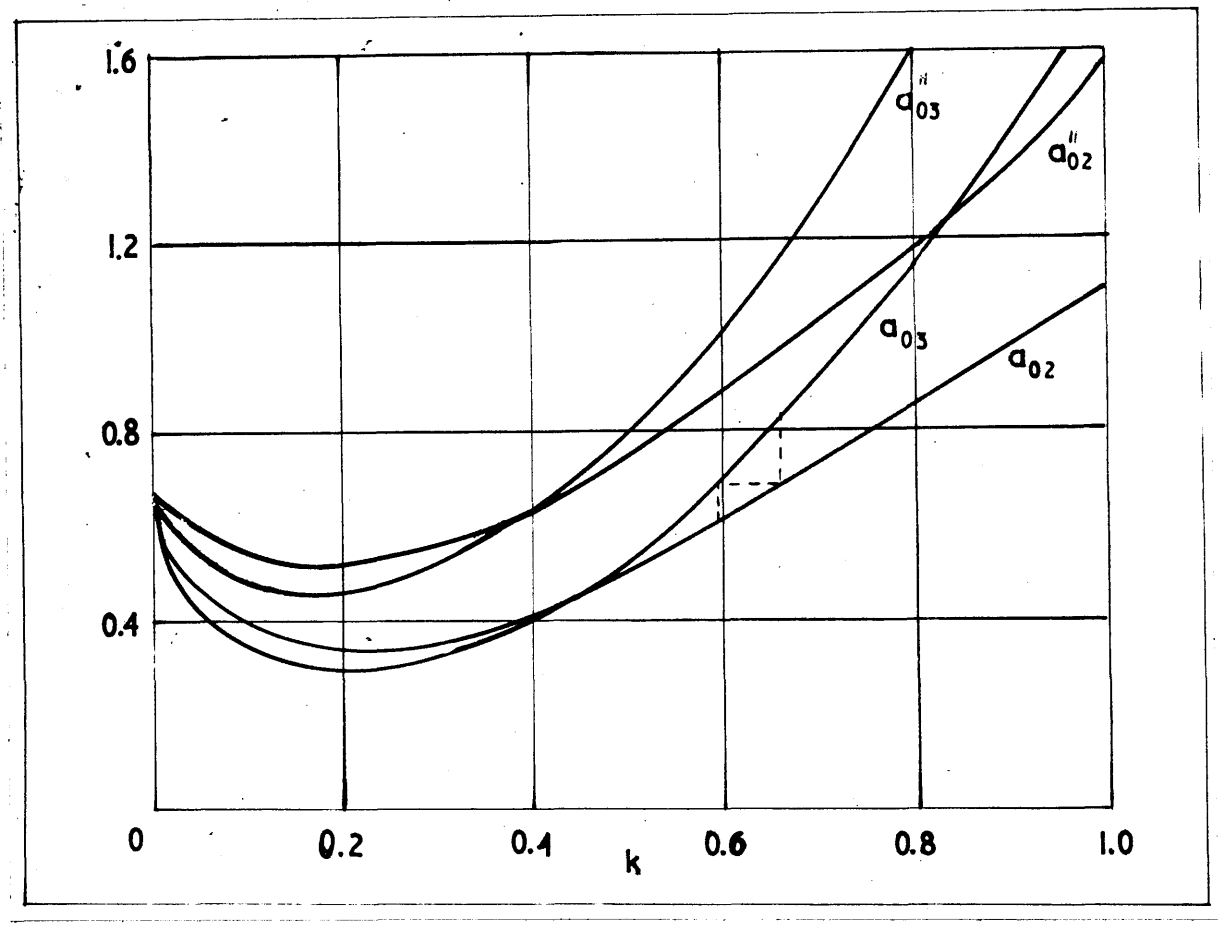

Fig. 2b.
Variation of loss coefficients.

It must be borne in mind that the foregoing results for the changes in the core loss values are obtained on the assumptions that the minor loops follow the same defining equations as the major loop and, additionally, that there is no change in the magnetic properties of the core as defined by the core constants a_{02} and a_{03} due to the presence of the higher frequency magnetizing force.

Up to this point, only the fundamental loss term has been considered since the main point of interest is the conditions required to give a reduction in the low frequency core loss. To determine the corresponding

loss term due to the higher frequency magnetizing force, b_3 may be evaluated from equation 32 for $h = h_1 \cos \omega t + h_3 \cos 3\omega t$,

i.e. $$b_3 = \frac{2}{\pi}\int_0^{\pi}\Big[\alpha \sin 3\omega t + \gamma \cos 2\omega t \sin 3\omega t + \xi \cos 6\omega t \sin 3\omega t + \theta(\cos 4\omega t \sin 3\omega t + \cos 2\omega t \sin 3\omega t\Big] d(\omega t)$$

$$= \frac{2}{\pi}\int_0^{\pi}\Big[\alpha \sin 3\omega t + \frac{\gamma}{2}(\sin 5\omega t + \sin \omega t) + \frac{\xi}{2}(\sin 9\omega t - \sin 3\omega t) + \frac{\theta}{2}(\sin 7\omega t - \sin \omega t) + \frac{\theta}{2}(\sin 5\omega t + \sin \omega t)\Big] d(\omega t)$$

$$= \frac{4}{\pi}\left(\frac{1}{3}\alpha + \frac{3}{5}\gamma - \frac{1}{9}\xi + \frac{6}{35}\theta\right)$$

Substituting constants from equation 26.

$$b_3 = \frac{4}{\pi}\left[\frac{1}{3}\left\{B(0,H_m) + \frac{Fh_1^2 + Fh_3^2}{2}\right\} + \frac{3}{5}\,\frac{Fh_1^2}{2} - \frac{1}{9}\,\frac{Fh_3^2}{2} + \frac{6}{35}\,Fh_1h_3\right]$$

$$= \frac{4}{\pi}\left[\frac{1}{3}\,B(0,H_m) + F\left(\frac{7}{15}\,h_1^2 + \frac{1}{9}\,h_3^2 + \frac{6}{35}\,h_1h_3\right)\right]$$

Substituting for F from equation 22.

$$= \frac{4}{\pi}\left[\frac{1}{3}\,B(0,H_m) - (a_{02} + a_{03}\,H_m)\left(\frac{7}{15}\,h_1^2 + \frac{1}{9}\,h_3^2 + \frac{6}{35}\,h_1h_3\right)\right] \qquad (58)$$

This expression gives the magnitude of one component of the 3ωt flux density wave. As shown by equation 37, this coefficient is proportional to the loss component at that frequency.

$$\therefore \quad \text{Core Loss} = \frac{3TA\omega\, b_3}{\sqrt{2}}\, I_3 \text{ watts.} \quad \text{where } I_3 = \frac{h_3 l}{\sqrt{2T}} \qquad (59)$$

(Neglecting eddy current effects as previously).

The corresponding value of loss term (a_3) for the core magnetization condition $h = h_1 \sin \omega t + h_3 \sin 3\omega t$ may be similarly obtained from equation 44.

$$a_3 = \frac{2}{\pi}\int_{-\frac{\pi}{2}}^{\frac{\pi}{2}} -(\alpha \cos 3\omega t + \gamma \cos 2\omega t \cos 3\omega t + \xi \cos 4\omega t \cos 3\omega t + \eta \cos 6\omega t \cos 3\omega t)\, d(\omega t)$$

$$= \frac{-4}{\pi}\left[\frac{1}{3}\,B(0,H_m) - (a_{02} + a_{03}\,H_m)\left(-\frac{2}{15}\,h_1^2 + \frac{1}{18}\,h_3^2 + \frac{1}{35}\,h_1h_3\right)\right] \qquad (60)$$

Comparing equations 58 and 60, it is seen that since $h_1 > h_3$ hence the value of a_3 will be greater than b_3, since equation 60 can be rewritten as

$$a_3 = -\frac{4}{\pi}\left[\frac{1}{3}B(0,H_m) + (a_{02} + a_{03}H_m)\left(\frac{2}{15}h_1^2 - \frac{1}{18}h_3^2 - \frac{1}{35}h_1h_3\right)\right]$$

The last two terms in this expression are so small that they may be neglected.

The variation of the 3ωt loss coefficients may be compared with the corresponding fundamental loss coefficients. It is seen that, when the fundamental loss is at a maximum ($h = h_1 \cos \omega t + h_3 \cos 3\omega t$), the 3ωt loss term is a minimum. Similarly, when the fundamental loss is at a minimum ($h = h_1 \sin \omega t + h_3 \sin 3\omega t$) the 3ωt term is a maximum.

These theoretical results are verified experimentally in Part II.

CHAPTER 5

SPECIAL CASE OF CORE MAGNETIZATION WHEN n = 0, i.e. A.C. AND D.C. MAGNETIZING FORCE.

The core magnetizing force for this condition will be defined as $h = h_0 + h_1 \sin \omega t$, which produces the well-known unsymmetrical hysteresis loop as shown in Fig. 26.

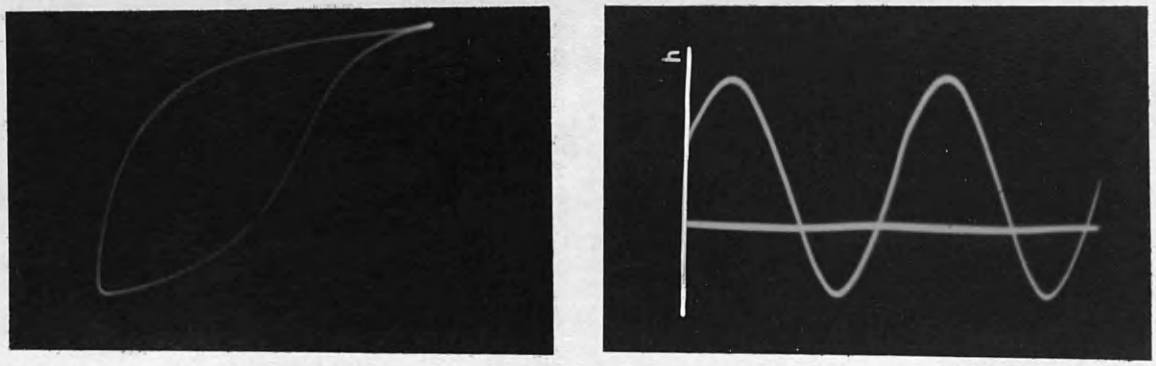

Fig. 26.

The core loss in this case cannot be obtained from the expressions in Chapter 4, since these assumed a symmetrical loop shape. It is obvious that the core loss is dependent on the values of h_0, h_1 and the resultant + b_m and $-b_m$ magnitudes obtained. Due to the d.c. component, the hysteresis loss is increased for the same $\pm b_m$ values, the loss increasing as h_0 is increased, i.e. when the loop occurs in the saturated region, for the same $\pm b_m$ its area can be three times that at the origin when $h_0 = 0$, see Fig. 27 which illustrates typical conditions when the peak to peak loop flux density is 0.1 weber/sq.m. for silicon iron.

Fig. 27.
Variations in loop area, as h_0 is altered, for the same amplitude of core flux density.

When the peak to peak flux density value is increased, the resulting change in core loss as h_0 varies, is much reduced until when the loop extends well into the saturated region, both positively and negatively, the change in loss value is extremely small. This condition is obtained in a parallel-connected transductor on short-circuit.

To obtain a mathematical expression for the loss under this condition of magnetization is not practical and recourse is made to empirical formulae. It must be pointed out that the core materials used in magnetic amplifiers, modulators, magnetometers etc., have very small core loss values, which are usually neglected. The B - H relationship is then defined as a single-valued function. For the normal core materials, e.g. stalloy etc., a formula based on Steinmetz' equation gives an estimation of the loss. One form of this, due to Ball[2], is

$$P = (\eta + \alpha B_0^{\ y}) B^x \qquad (61)$$

where B_0 = polarizing flux density

and B = half the total flux density amplitude

P = loss in the loop

x = 1.6

y = 1.9

Equation 61 is based on the single frequency magnetization hysteresis loss obtained from Steinmetz' equation ($P = \eta B^x$). The value of the exponent x is not constant over the range of B, but varies between wide limits (1.6 → 2). To this term is added an additional factor to account for the increased loss when the core is subjected to unsymmetrical magnetization. It has been shown[2] that the exponent y in this term is also not constant over the flux density range, but varies from 1.8 → 2.1.

When the exponent values 1.6 and 1.9 are taken for x and y respectively, the errors over the complete range of flux density values for silicon iron core materials vary from 0 → 12%. This enables an estimation of the hysteresis loss to be readily obtained.

CHAPTER 6

REDUCTION OF LOW-FREQUENCY COMPONENT OF HYSTERESIS LOSS

The reduction of hysteresis loss noted in Chapter 4 was obtained on the assumption that the core material constants, defining the B - H relationships were unaltered under conditions of combined magnetization. It is suggested that there may be a further reduction in the low frequency component of loss due to "domain shake up" by the higher frequency component, causing a reduction in molecular friction to the lower frequency component. No means are available of assessing theoretically the magnitude of this effect, but it would be thought that when the two frequencies of the applied magnetization are relatively close together the reduction in loss due to this cause would be small.

The effects of the higher-frequency magnetizing force on the core may be compared with the effect of mechanical vibration on magnetic properties of materials. It is well known that, when a soft iron wire is subjected to mechanical vibration, its retentivity is almost completely removed and the B - H curve of the material no longer possesses the usual lower bend region, as shown in Fig. 28.

For harder magnetic materials, this effect is not so pronounced.

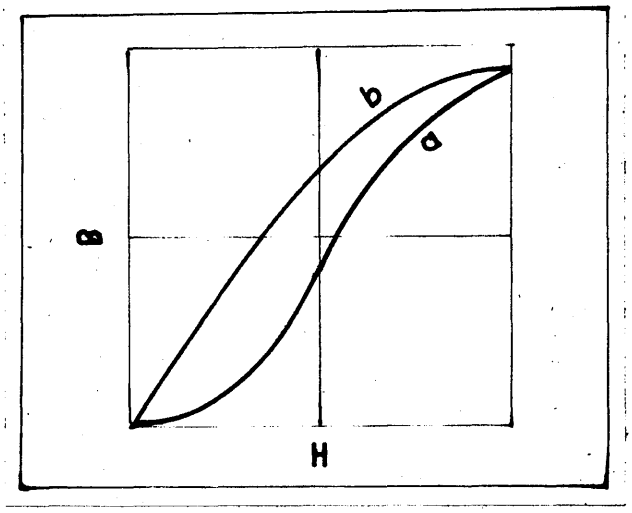

Fig. 28
B - H Curve for soft annealed iron wire

a) Normal
b) With mechanical vibration.

The corresponding electrical effect was illustrated by Gerosa and Finzi[3] in 1891. A soft iron wire inside a solenoid was subjected to two magnetizing forces. An alternating current was passed through the wire, which set up circular alternating magnetization and direct current in the solenoid caused longitudinal magnetization. It was observed[3] that the susceptibility to longitudinal magnetization was increased due to the action of the alternating component. The violent domain displacement due to this component destroyed nearly all traces of hysteresis, as measured by the longitudinal magnetizing force.

A very convincing curve is given by Ewing[4] which shows the effect on the hysteresis loop obtained when an iron wire is subjected to normal reversals of longitudinal magnetization (Fig. 29, curve a) and when an alternating longitudinal current is also applied (curve b). It is seen that the normal loop collapses into practically a single line relationship between B and H.

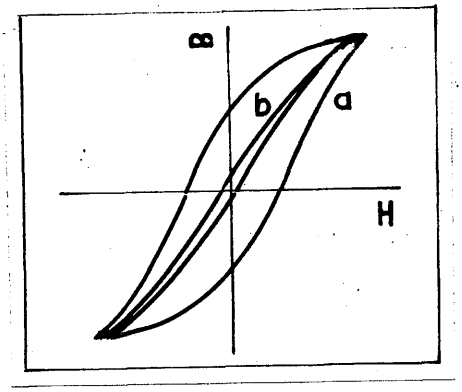

Fig. 29.

In Part II, Chapter 6, experimental results are obtained when the core material is subjected to combined magnetization at 50 and 1450 c/s and it is seen that no reduction in low frequency core loss occurs until the material is operating beyond the knee of the magnetization curve. From the results for fixed h_1 and h_n (h.f. test 1, Page126), over a wide range of frequency there is no change in the low frequency core loss, which indicates that if there should be any reduction in loss due to "domain shake up", it is independent of the "frequency of shake". This would indicate that for normal core materials operating under combined magnetization conditions as above, the reduction in core loss is not primarily due to the presence of the high frequency component itself, but is dependent on the core operating in the saturated region. It is suggested, therefore, that the high frequency component of magnetization affects the alignment of the magnetic moments of the domains, enabling them to follow the change in the low frequency magnetizing force more easily. This causes a reduction in hysteresis loss.

CHAPTER 7

VOLTAGE AND FLUX DENSITY HARMONIC COMPONENTS

The experimental circuit used to investigate the effects of phase change under combined magnetization conditions is shown in Fig. 30. Two identical cores are used, each with similar windings. Full details of the actual construction of the test specimens are given in Part II, Chapter 1.

Each set of energizing windings is connected in series and supplied from high impedance sources with current waveforms,

$$i_1 = \hat{i}_1 \sin \omega t$$

$$i_n = \hat{i}_n \sin n\omega t$$

This method of energizing the cores is based on the saturable reactor method of connection but under the above conditions it is necessary to investigate the actual voltage components appearing across the supply terminals due to the flow of the above current in the cores.

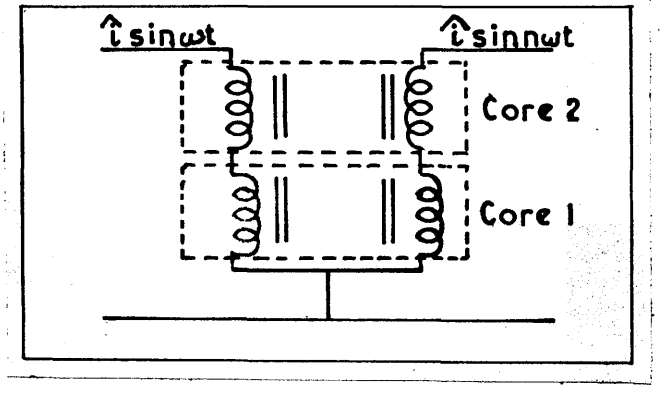

Fig. 30.
Basic circuit.

The ideal mode of operation would give no voltage at the frequency of source 1 or harmonics of it across source 2 terminals and similarly for source 1 terminals. Under these conditions there can be no flow of harmonic power from source 1 to source 2 or vice versa. To obtain this condition with the given current waveform, the cores would require to present linear impedances, which is not the case due to the effects of the core material. The voltage across each winding on the specimens will, therefore, contain harmonics. If these harmonic voltages cause currents to flow back through the sources, then two effects occur. Firstly, due to the harmonic current flow the core magnetization is no longer $h = h_1 \sin \omega t + h_n \sin n\omega t$ and, secondly, there will be a power loss in the source caused by the harmonic current. This harmonic power must be supplied from the fundamental power delivered to the cores, as a result of which the measurements of core loss obtained will be greater than the true loss since,

Fundamental power input to specimen = Total core loss + harmonic power.

The effect of harmonic power flow will, therefore, be to <u>increase</u> the <u>measured</u> fundamental component of core loss. This fact must be borne in mind when the high frequency test results (Part II, Chapter 6) are considered. (See also Part II, Chapter 7).

To obtain analytically the voltage components across the source terminals under combined magnetization conditions, the core B - H relationship will be represented by

$$B = aH + bH^3 + cH^5 \quad \text{(where a, b and c are constants)} \qquad (62)$$

This expression neglects hysteresis and eddy current effects but enables an estimation of flux-density harmonic components to be readily obtained.

The magnetizing force for core 1, Fig. 30, is given by

$$h = h_1 \sin \omega t + h_n \sin n\omega t \qquad (63)$$

and the corresponding magnetizing force for core 2 is

$$h = h_1 \sin \omega t - h_n \sin n\omega t \qquad (64)$$

(since nωt winding on core 2 is reversed).

Substitute equation 63 for H in equation 62.

$\therefore$ Core 1 flux density

$$\begin{aligned} b_1 &= a(h_1 \sin \omega t + h_n \sin n\omega t) + b\,(h_1 \sin \omega t + h_n \sin n\omega t)^3 \\ &\quad + c\,(h_1 \sin \omega t + h_n \sin n\omega t)^5 \\ &= a\,h_1 \sin \omega t + a\,h_n \sin n\omega t + b\,h_1^3 \sin^3 \omega t + b\,h_n^3 \sin^3 n\omega t \\ &\quad + 3b\,h_1 h_n^2 \sin \omega t \sin^2 n\omega t + 3b\,h_1^2 h_n \sin^2 \omega t \sin n\omega t \\ &\quad + c\,h_1^5 \sin^5 \omega t + c\,h_n^5 \sin^5 n\omega t + 5c\,h_1^4 h_n \sin^4 \omega t \sin n\omega t \\ &\quad + 10c\,h_1^3 h_n^2 \sin^3 \omega t \sin^2 n\omega t + 10\,c\,h_1^2 h_n^3 \sin^2 \omega t \sin^3 n\omega t \\ &\quad + 5c\,h_1 h_n^4 \sin \omega t \sin^4 n\omega t \end{aligned}$$

Expanding and collecting terms

$$\begin{aligned} \therefore b_1 = \sin \omega t \Big(& a\,h_1 + \tfrac{3}{4} b\,h_1^3 + \tfrac{3}{2} b\,h_1 h_n^2 + \tfrac{5}{8} c\,h_1^5 \\ & + \tfrac{15}{4} c\,h_1^3 h_n^2 + \tfrac{15}{8} c\,h_1 h_n^4 \Big) \\ & + \sin 3\omega t \left(-\tfrac{1}{4} b\,h_1^3 - \tfrac{5}{16} c\,h_1^5 - \tfrac{5}{4} c\,h_1^3 h_n^2\right) \\ & + \sin 5\omega t \left(\tfrac{1}{16} c\,h_1^5\right) \\ & + \sin (n-4)\omega t \left(\tfrac{5}{16} c\,h_1^4 h_n\right) \\ & + \sin (n-2)\omega t \left(-\tfrac{3}{4} b\,h_1^2 h_n - \tfrac{5}{4} c\,h_1^4 h_n - \tfrac{15}{8} c\,h_1^2 h_n^3\right) \end{aligned}$$

$$+ \sin n\omega t \left(a h_n + \frac{3}{4} b h_n^3 + \frac{3}{2} b h_1^2 h_n + \frac{5}{8} c h_n^5 + \frac{15}{8} c h_1^4 h_n + \frac{15}{4} c h_1^2 h_n^3\right)$$

$$+ \sin (n+2)\omega t \left(-\frac{3}{4} b h_1^2 h_n - \frac{5}{4} c h_1^4 h_n - \frac{15}{8} c h_1^2 h_n^3\right)$$

$$+ \sin (n+4)\omega t \left(\frac{5}{16} c h_1^4 h_n\right)$$

$$+ \sin (2n-3)\omega t \left(-\frac{5}{8} c h_1^3 h_n^2\right)$$

$$+ \sin (2n-1)\omega t \left(\frac{3}{4} b h_1 h_n^2 + \frac{15}{8} c h_1^2 h_n^2 + \frac{5}{4} c h_1 h_n^4\right)$$

$$+ \sin (2n+1)\omega t \left(-\frac{3}{4} b h_1 h_n^2 - \frac{15}{8} c h_1^3 h_n^2 - \frac{5}{4} c h_1 h_n^4\right)$$

$$+ \sin (2n+3)\omega t \left(\frac{5}{8} c h_1^3 h_n^2\right)$$

$$+ \sin (3n-2)\omega t \left(\frac{5}{8} c h_1^2 h_n^3\right)$$

$$+ \sin 3n\omega t \left(-\frac{1}{4} b h_n^3 - \frac{5}{16} c h_n^5 - \frac{5}{4} c h_1^2 h_n^3\right)$$

$$+ \sin (3n+2)\omega t \left(\frac{5}{8} c h_1^2 h_n^3\right)$$

$$+ \sin (4n-1)\omega t \left(-\frac{5}{16} c h_1 h_n^4\right)$$

$$+ \sin (4n+1)\omega t \left(\frac{5}{16} c h_1 h_n^4\right)$$

$$+ \sin 5n\omega t \left(\frac{1}{16} c h_n^5\right)$$

The above expression gives the complete solution for the flux density from the given B - H relationship, when the applied magnetizing force is given by equation 63, i.e.

$$b_1 = A \sin \omega t - C \sin 3\omega t + D \sin 5\omega t + E \sin (n-4)\omega t \qquad (65)$$

$$-F \sin (n-2)\omega t + G \sin n\omega t - F \sin (n+2)\omega t$$

$$+E \sin (n+4)\omega t - J \sin (2n-3)\omega t + K \sin (2n-1)\omega t$$

$$-K \sin (2n+1)\omega t + J \sin (2n+3)\omega t + L \sin (3n-2)\omega t$$

$$-M \sin 3n\omega t + L \sin (3n+2)\omega t - N \sin (4n-1)\omega t$$

$$+N \sin (4n+1)\omega t + P \sin 5n\omega t$$

(The values of the constants are obtained from the above equation)

From equation 65 (which gives the general solution for the components of the flux density wave) it can be seen that in addition to the harmonic components produced due to the magnetizing force components ωt and $n\omega t$, intermodulation components are introduced, i.e. $(n - 4)\ \omega t$, $(n + 4)\ \omega t$; $(n - 2)\ \omega t$, $(n + 2)\ \omega t$; $(2n - 3)\ \omega t$, $(2n + 3)\ \omega t$; $(2n - 1)\ \omega t$, $(2n + 1)\ \omega t$; $(3n - 2)\ \omega t$, $(3n + 2)\ \omega t$; $(4n - 1)\ \omega t$, $(4n + 1)\ \omega t$,

due to the combined magnetization condition. When n is small, the above components give rise to a complete series of odd harmonic components, A typical case when n = 3 is considered on Page 61 .

When n is large, the additional components occur at frequencies just above and just below the higher frequency harmonic components. Similarly for core 2 when the magnetizing force is given by equation 64.

$$b_2 = a(h_1 \sin \omega t - h_n \sin n\omega t) + b(h_1 \sin \omega t - h_n \sin n\omega t)^3 + c(h_1 \sin \omega t - h_n \sin n\omega t)^5$$

Expanding and collecting terms as previously gives the general form of the core flux density as

$$\begin{aligned} b_2 = {} & A \sin \omega t - C \sin 3\omega t + D \sin 5\ \omega t - E \sin (n - 4)\ \omega t \\ & + F \sin (n - 2)\ \omega t - G \sin n\omega t + F \sin (n + 2)\ \omega t \\ & - E \sin (n + 4)\ \omega t - J \sin (2n - 3)\ \omega t + K \sin (2n - 1)\ \omega t \\ & - K \sin (2n + 1)\ \omega t + J \sin (2n + 3)\ \omega t - L \sin (3n - 2)\ \omega t \\ & + M \sin 3\ n\omega t - L \sin (3n + 2)\ \omega t - N \sin (4n - 1)\ \omega t \\ & + N \sin (4n + 1)\ \omega t - P \sin 5\ n\omega t \end{aligned}$$

The values of the constants in this expression are identical with those obtained for b_1.

Under single frequency magnetization, the corresponding flux density components are given below.

Let $h = h_1 \sin \omega t$

$$b = a (h_1 \sin \omega t) + b (h_1 \sin \omega t)^3 + c (h_1 \sin \omega t)^5$$

$$= \sin \omega t \left(a h_1 + \frac{3}{4} b h_1^3 + \frac{5}{8} c h_1^5\right)$$

$$+ \sin 3\omega t \left(-\frac{1}{4} b h_1^3 - \frac{5}{16} c h_1^5\right)$$

$$+ \sin 5\omega t \left(\frac{1}{16} c h_1^5\right)$$

$$= A' \sin \omega t + C' \sin 3\omega t + D' \sin 5\omega t$$

This can also be obtained from the general case by putting $h_n = 0$.

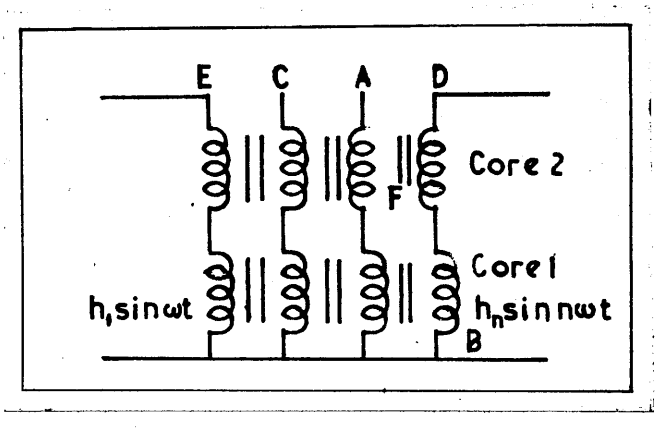

Fig. 31.

The voltage appearing across A - B under the assumed conditions of magnetization may be readily obtained from the foregoing expressions for flux density.

Core 1. magnetizing force = $h_1 \sin \omega t + h_n \sin n\omega t$

Core 2. magnetizing force = $h_1 \sin \omega t - h_n \sin n\omega t$

Voltage across AB $= N_1 \frac{d\varphi_1}{dt} - N_2 \frac{d\varphi_2}{dt} = N_1 A \left(\frac{db_1}{dt} - \frac{db_2}{dt} \right)$

$= N_1 A \frac{d}{dt} (b_1 - b_2)$ (if $N_1 = N_2$)

(A = core cross-sectional area. sq.m.).

$= 2 N_1 A \frac{d}{dt} (E \sin (n - 4) \omega t - F \sin (n - 2) \omega t + G \sin n\omega t$

$-F \sin (n + 2) \omega t + E \sin (n + 4) \omega t + L \sin (3n - 2) \omega t$

$-M \sin 3n\omega t + L \sin (3n + 2) \omega t + P \sin 5 n\omega t)$

$= 2\omega N_1 A (nG \cos n\omega t - 3n M \cos 3n \omega t + 5n P \cos 5 n\omega t$ (66)

$+ (n - 4) E \cos (n - 4) \omega t - (n - 2) F \cos (n - 2) \omega t$

$- (n + 2) F \cos (n + 2) \omega t + (n + 4) E \cos (n + 4) \omega t$

$+ (3n - 2) L \cos (3n - 2) \omega t + (3n + 2) L \cos (3n + 2) \omega t)$

Similarly, the voltage across CB

$= N_1 \left[\frac{d\varphi_1}{dt} + \frac{d\varphi_2}{dt} \right]$ $(N_1 = N_2)$

$= 2\omega N_1 A (A \cos \omega t - 3C \cos 3\omega t + 5D \cos 5\omega t - (2n - 3) J \cos (2n-3) \omega t$

$+ (2n - 1) K \cos (2n - 1) \omega t - (2n + 1) K \cos (2n + 1) \omega t$ (67)

$+ (2n + 3) J \cos (2n + 3) \omega t - (4n - 1) N \cos (4n - 1) \omega t$

$+ (4n + 1) N \cos (4n + 1) \omega t$

Hence it can be seen from the above expressions that the voltages appearing across each set of energizing windings on the cores (CB and DB in Fig. 31) contain fundamental + Harmonic components of <u>one</u> supply and additionally certain "intermodulation products" as given above. (Neglecting winding resistances).

The voltage across one core only, i.e. FB

$N_1 \frac{d\varphi_1}{dt} = N_1 A \frac{db_1}{dt}$

$$= N_1 A\omega \left[A \cos \omega t - 3C \cos 3\omega t + 5D \cos 5\omega t + (n-4)\, E \cos (n-4)\, \omega t \right.$$
$$- (n-2)\, F \cos (n-2)\, \omega t + n\, G \cos n\omega t - (n+2)\, F \cos (n+2)\, \omega t$$
$$+ (n+4)\, E \cos (n+4)\, \omega t - (2n-3)\, J \cos (2n-3)\, \omega t$$
$$+ (2n-1)\, K \cos (2n-1)\, \omega t - (2n+1)\, K \cos (2n+1)\, \omega t \qquad (68)$$
$$+ (2n+3)\, J \cos (2n+3)\, \omega t + (3n-2)\, L \cos (3n-2)\, \omega t$$
$$- 3nM \cos 3\, n\omega t + (3n+2)\, L \cos (3n+2)\, \omega t - (4n-1)\, N \cos (4n-1)\omega t$$
$$\left. + (4n+1)\, N \cos (4n+1)\, \omega t + 5\, nP \cos 5\, n\omega t \right]$$

From equations 66 and 67 it is seen that the effect of the back-to-back connection when compared with single-core excitation (equation 68) prevents a large percentage of the harmonic voltage terms generated in each core from appearing across the source terminals.

For the case when n is large, the voltage appearing across the "ωt" source consists of harmonics of ωt + higher order terms in n. Similarly, the voltage across the "n ωt" source consists of harmonics of n ωt + higher order terms in n. If large air-cored inductances are inserted in the supply circuits, the impedance presented to the harmonic voltages will restrict the flow of harmonic current to negligible proportions.

When n is small the intermodulation products give rise to voltage components at the harmonic frequencies of each source, this case is illustrated for n = 3,

then $$v_1 = 2\omega N_1 A\, (A \cos \omega t - 3\,(C + J) \cos 3\, \omega t$$
$$+ 5\,(D + K) \cos 5\, \omega t - 7\, K \cos 7\, \omega t + 9\, J \cos 9\, \omega t \qquad (69)$$
$$- 11\, N \cos 11\, \omega t + 13\, N \cos 13\, \omega t)$$

and $v_3 = 2\omega N_1 A\ (-E + F) \cos \omega t + 3G \cos 3\omega t - 5F \cos 5\omega t$

$+ 9\ (E + L) \cos 7\omega t - 9\ M \cos 9\omega t + 11\ L \cos 11\omega t$ (70)

$+ 15\ P \cos 15\omega t)$

From these equations it would at first sight appear that the use of the back-to-back connection was of little advantage due to the presence of $3\omega t$ and ωt terms across the ωt and $3\omega t$ sources respectively. The magnitude of the coefficients of these terms is small and it is found that they do not in any way detract from the method, provided the source impedances are relatively large in comparison with the core winding impedance.

The corresponding voltage across one core winding (i.e., FB, Fig.31) when n = 3 is obtained from equation 68.

$= N_1 A\omega\ (\ (A - E - F) \cos \omega t - 3\ (C + J - G) \cos 3\omega t$

$+ 5\ (D + K - F) \cos 5\omega t - 7\ (K - E - L) \cos 7\omega t$ (71)

$+ 9\ (J - M) \cos 9\omega t + 11\ (L - N) \cos 11\omega t$

$+ 13\ N \cos 13\omega t + 15\ P \cos 15\omega t)$

From this equation it is seen that the effect of the intermodulation when n = 3 is to alter the magnitude of the true harmonic terms (ωt, $3\omega t$, $5\omega t$, $9\omega t$) by amounts depending on the magnitudes of h_1, h_3 and the core constants b and c. The remaining terms $7\omega t$, $11\omega t$ and $13\omega t$ are set up solely by intermodulation, since the normal core harmonic components are only considered up to and including the 5th in this analysis.

Note.

The values of the constants A, C and D under combined magnetization differ from A', C', D' (see Page 59) obtained for single frequency

excitation, but the change is NOT due to the effect of the intermodulation terms, as shown by the general expression for b_1 on Page 57 (equation 65).

The above theory has been developed on the assumption that hysteresis and eddy current effects are absent. While this is not the case in practice, it does indicate the effect of the back-to-back methods of connection. Due to core losses there will not be perfect balance between cores for any frequency, as the flux density is a double-valued function of the magnetizing force.

PART II

EXPERIMENTAL RESULTS.

CHAPTER 1.

GENERAL CIRCUIT DETAILS.

From the theoretical considerations of Part I, Chapter 4, it is seen that under certain conditions of combined magnetization the low-frequency component of core loss may be reduced below the single frequency value by the action of the higher frequency term. These results have been investigated experimentally, using the basic circuit shown in Fig. 3 (See also Part I, Chapter 7).

Core construction.

Two exactly similar specimens of special Lohys were assembled. To ensure that each core had the same magnetic properties, the 64 ring stampings used were sub-divided and mixed until two cores of equal weight with 32 stampings each were obtained. As the insuline coating on the stampings showed signs of deterioration, rings of tracing paper (0.0025" thick) were inserted between the stampings. Before the windings were put on, each core was half-lapped with insulating tape. Each winding was distributed evenly round the complete core circumference.

Specimen details.

Stampings: 19 cm O.D.
16 cm I.D.
0.014" nominal thickness

Core weight 639 gm each

Core area 1) From ring thickness 1.524 cm^2
2) From core weight (assuming density 7.80 gm/cm^3) 1.495 cm^2

Mean path length		54.9 cm		
Windings:	1)	400^T	30 S.W.G.	Lumex
	2)	100^T	7/0.0075"	Durawire
	3)	400^T	22 S.W.G.	D.S.C. enamel
	4)	100^T	18 S.W.G.	Lumex

To illustrate fully the effects of phase change upon the core loss values under conditions of combined magnetization, a series of tests was carried out with various values of magnetizing force components to illustrate the loss variations as the relative phase angle is altered. To enable the phase angle to be controlled, it is necessary to utilize two supplies whose frequencies are locked to one another. The necessary circuits etc. to enable 50 and 100 c/s, and 50 and 150 c/s to be obtained practically with provision for accurate and easy change of phase angle are described in Appendix (b)

The cores are magnetized under sine current conditions throughout these tests. While it is realized that this condition of magnetization is not always obtained, the choice of test method rests between sine flux, or sine current, with the normal practical condition between these two ideals. Under combined magnetization the test method used, i.e. back-to-back connection, is ideally suited to the case with sine current. With the cores in series, as in Fig. 3, although sinusoidal supply voltages could be obtained, the individual core voltages and hence the flux would not be sinusoidal. The sum of the voltages across the two cores would add together to give the sinusoidal supply voltage. It might be suggested that this

could be overcome by connecting the windings in parallel. Obviously if both low frequency and high frequency windings are connected in parallel as in Fig. 1, the main asset of the back-back connection is lost since each supply will inject its own voltage components into the other source and also cause a large circulating current in the windings. This method is obviously useless.

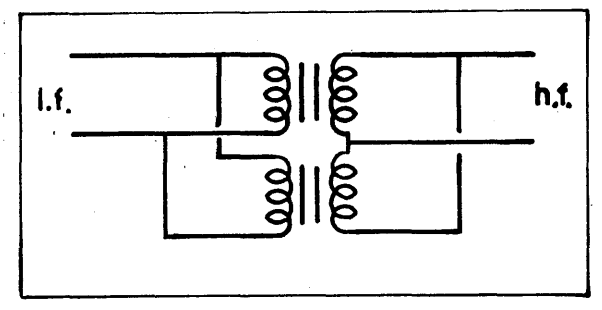

Fig. 1.

If one set of windings is connected in series, the circuit for a parallel connected saturable reactor is obtained. For two-frequency excitation ($f_2 > 0$) a circulating current will still be obtained in the parallel branch, while the core excitation from the high frequency source is no longer sine flux. (See Fig. 2). This method is, therefore, not suitable.

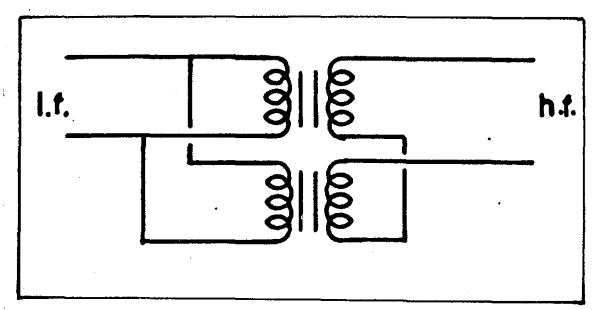

Fig. 2.

In view of the above, it is seen that to utilize fully the back-back method of connection the two cores must have their windings series connected and energised under sine current conditions. This connection is used for all the tests carried out on the cores (See Fig. 3).

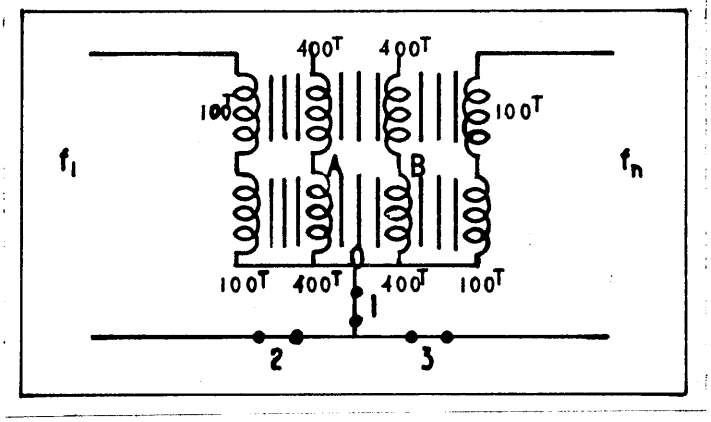

Fig. 3.

By means of ammeter switches at 1, 2 and 3 the components of the total current wave can be obtained. For a.c. potentiometer measurements a standard resistance is inserted at 1 and the two components of the magnetizing force obtained, the voltage components being measured from the voltage across the 400^T search coils AO or BO. This voltage is the total core voltage containing f_1, f_n and harmonics of both these components.

For wattmeter readings the two core-loss components are obtained by inserting the current coil at 2, to give W_{f_1} and at 3 for W_{f_n} with the voltage coil connected across the 400^T winding AO or BO. The sum of these two loss values will equal W_T which is obtained by inserting the current coil in position 1.

CHAPTER 2

EFFECT OF PHASE AS THE FREQUENCY OF THE SUPERIMPOSED MAGNETIZING FORCE IS VARIED.

Since only the maximum and minimum values of the core loss component are required, it is not necessary to have locked frequency supplies to illustrate this effect. A motor generator set was used to obtain frequencies over the range 100 - 250 c/s. The circuit diagram of the set is shown in Fig. 4. The speed of the set was altered by armature resistance and to maintain the torque, the field current was increased as the armature current was reduced.

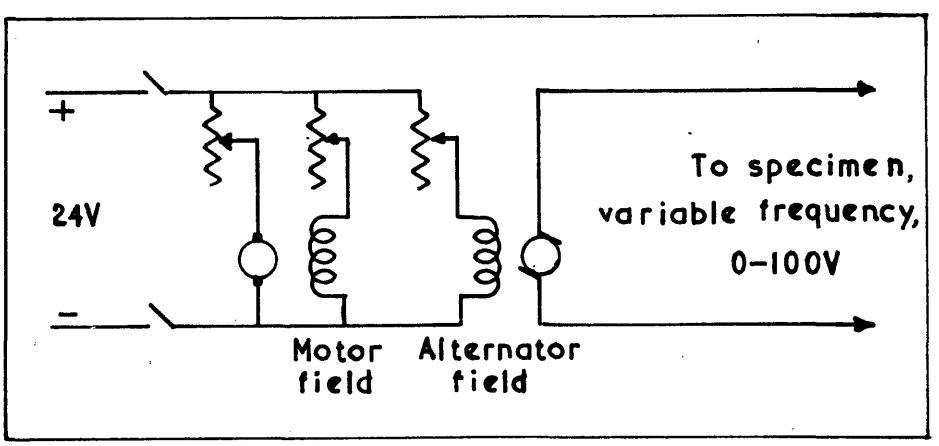

Fig. 4.

With the cores energized in the normal manner from the 50-c/s supply and the motor-generator set, the frequency of the latter was adjusted to give a slow drift of the core loss from maximum to minimum values. The core loss components were obtained from the maximum and minimum readings of the wattmeter, whose voltage coil was permanently across the 400^{T}

winding. The current coil was inserted by the ammeter switch into each supply lead and the total current circuit as shown in Fig. 3.

I_{50} = 0.6A. I superimposed = 0.3A.

f c/s		0	50	100	150	200	250	1450
W_{50}	Max	0.55	1.57	1.20	1.44	1.10	1.03	0.91
	Min	0.55	0.26	0.70	0.66	1.04	0.98	0.91
W_{hf}	Max	0	0.92	0.33	0.65	0.55	0.63	-
	Min	0	0.5	0.21	0.3	0.52	0.6	-
W_T	Max	0.55	1.64	1.44	1.78	1.65	1.65	-
	Min	0.55	0.19	1.03	1.28	1.54	1.58	-
$k_{50} = W_{50} \frac{Max}{Min}$		1	6.05	1.71	2.18	1.06	1.05	1.0
$k_{hf} = W_{hf} \frac{Max}{Min}$		1	1.84	1.57	2.17	1.06	1.05	1.0
$k_{total} = W_T \frac{Max}{Min}$		1	8.65	1.40	1.39	1.07	1.04	1.0

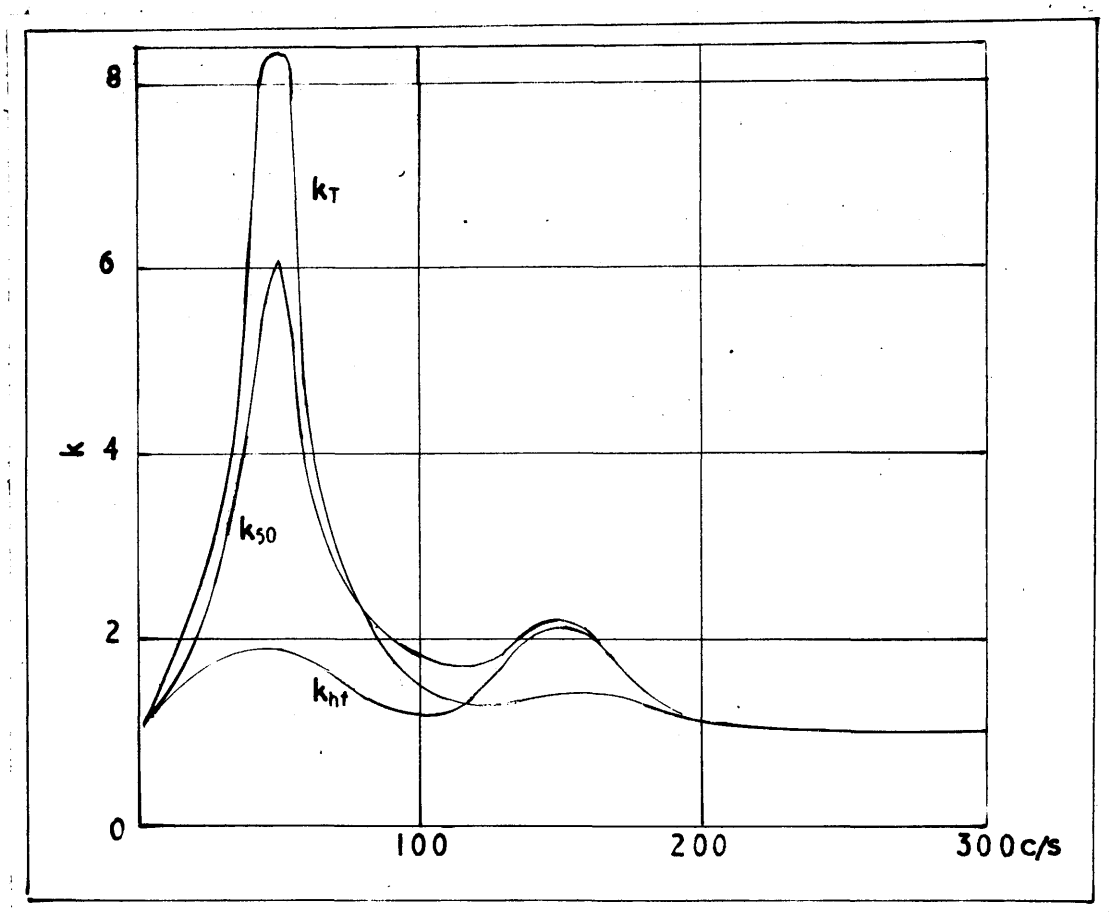

Fig. 5.

From the values of k_{total} (Fig. 5), it is seen that the effects of phase change have practically ceased to alter the total core loss when the frequency ratio is 5/1, for the values of magnetizing force in this test. For all values, the limit of the range in which the phase of the higher frequency component with respect to the lower f_1, affects the total core loss may be taken as $10f_1$. The peak which occurs at f_1 on the graph for k_{total} is, of course, dependent on the values of h_1 and h_{hf}. For the case when $h_1 = h_{hf}$ the value of k is ∞ at f_1 since

the maximum and minimum h values are $2h_1$ and zero when the frequencies of the two components are equal.

The increase in the values of k_{50} and k_{hf} when the frequency is 150 c/s is due to a combination of the 150-c/s voltage component from the 3rd harmonic of the 50-c/s supply and the fundamental of the 150-c/s supply. These both contribute to the core loss at 150 c/s.

Conditions which give the largest change in core loss with phase angle occur when $hf = 3f_1$. This is, of course, discounting the condition when $hf = f_1$ since this is not a true case of combined magnetization which assumes two magnetizing forces of different frequencies. Core conditions when $hf = f_1$ are obtained in the normal manner for single-frequency excitation. The case when $hf = 3f_1$ is accordingly fully investigated and additionally, the case when $hf = 2f_1$.

There is no harmonic interference for this latter case, as core 1 magnetization gives rise to odd terms and core 2 to even harmonic terms in the flux density wave.

CHAPTER 3

VARIATION OF MAXIMUM AND MINIMUM CORE LOSS COMPONENTS OVER THE RANGE OF MAGNETIZING FORCE VALUES.

The cores were energized from the 50-c/s and 150-c/s supplies in the normal manner and the relative phase-angle altered to give maximum and minimum core loss values (total, 50 and 150-c/s components). When the cores are not operating in the saturated region it would be expected that maximum and minimum values would be obtained, when $h = h_1 \sin(\omega t + 60^{\circ}) + h_3 \sin 3\omega t$ and $h = h_1 \sin \omega t + h_3 \sin 3\omega t$ respectively. This is seen to be the case. As the cores are taken into the saturated region, the effects of the eddy currents cause a non-uniform flux distribution across the core-section and since the magnitude of this loss is proportional to the r.m.s. voltage induced in a search coil winding, it is seen that the maximum core loss can occur at a value of phase angle which does not give B_m but gives the maximum value of $B_{r.m.s.}$ (See also Chapter 4 for values of $E_{r.m.s.}$). Additionally, it is assumed that the core is being subjected throughout to the magnetizing force which is measured in terms of the value at the surface of the core. It must, of course, be borne in mind that in general the peaks of the observable values of B and H do not synchronize.

Variation of maximum and minimum values of total core loss with superimposed magnetizing force for various values of 50-c/s magnetizing force.

I_{150}	0.05	0.1	0.2	0.3	0.4	0.5	0.55	A
W_T/core max	1.09	1.24	1.51	1.78	2.06	2.31	2.46	W
H_{50} = 109.2 φ	55°	40°	45°	45°	43°	40°	40°	
I_{50} = 0.6A								
W_T/core min	0.88	0.88	1.05	1.28	1.53	1.78	1.98	W
φ	0	-5°	-10°	-10°	-18°	-20°	-30°	
W_T/core max	0.68	0.84	1.11	1.42	1.73	2.06	2.26	W
H_{50} = 81.9 φ	58°	56°	53°	52°	53°	50°	50°	
I_{50} = 0.45A								
W_T/core min	0.48	0.51	0.7	0.99	1.33	1.7	1.92	W
φ	0	0	-5°	-5°	-15°	-30°	-30°	
W_T/core max	0.26	0.4	0.68	0.98	1.36	1.88	2.37	W
H_{50} = 54.6 φ	60°	60°	60°	60°	60°	60°	60°	
I_{50} = 0.3A								
W_T/core min	0.14	0.2	0.41	0.71	1.1	1.56	1.92	W
φ	0	0	0	-5°	-10°	-10°	-10°	
I_{50}								
0.6 α_T	0.81	0.71	0.69	0.72	0.74	0.78	0.80	
0.45 α_T	0.71	0.61	0.63	0.69	0.77	0.82	0.85	
0.3 α_T	0.54	0.50	0.60	0.73	0.81	0.83	0.81	

$$\alpha_T = \frac{W_T/\text{core min}}{W_T/\text{core max}}$$

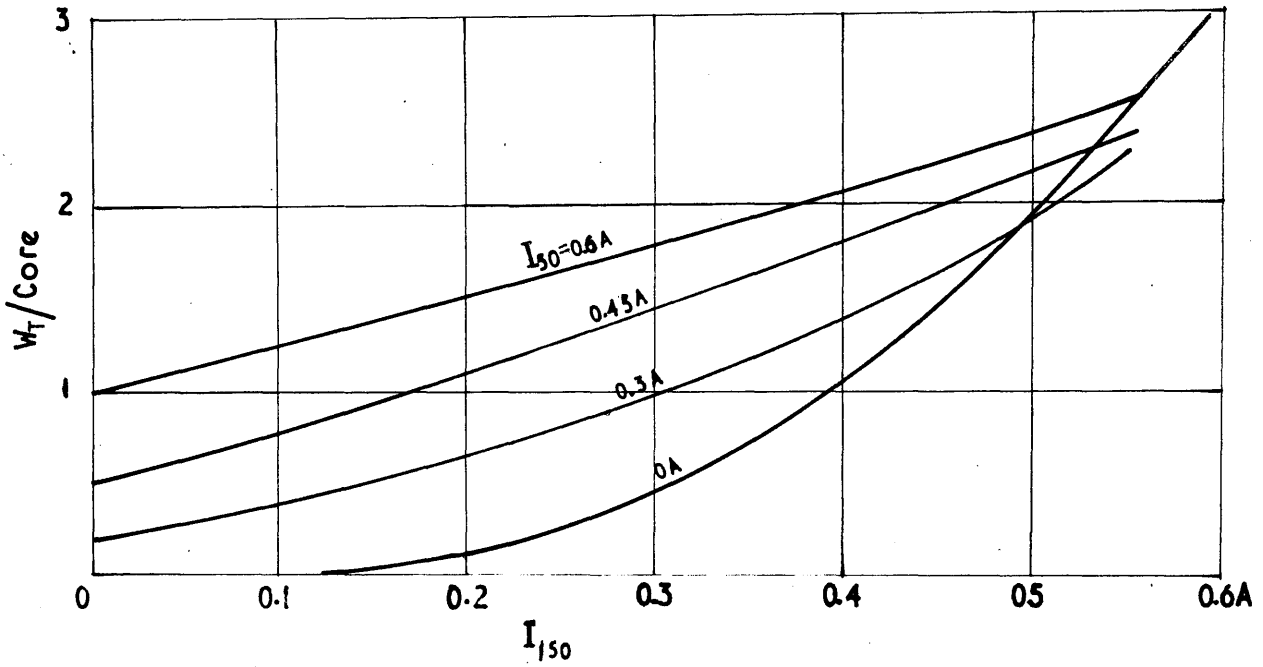

Fig. 6.

Variation of $W_{T.MAX}$

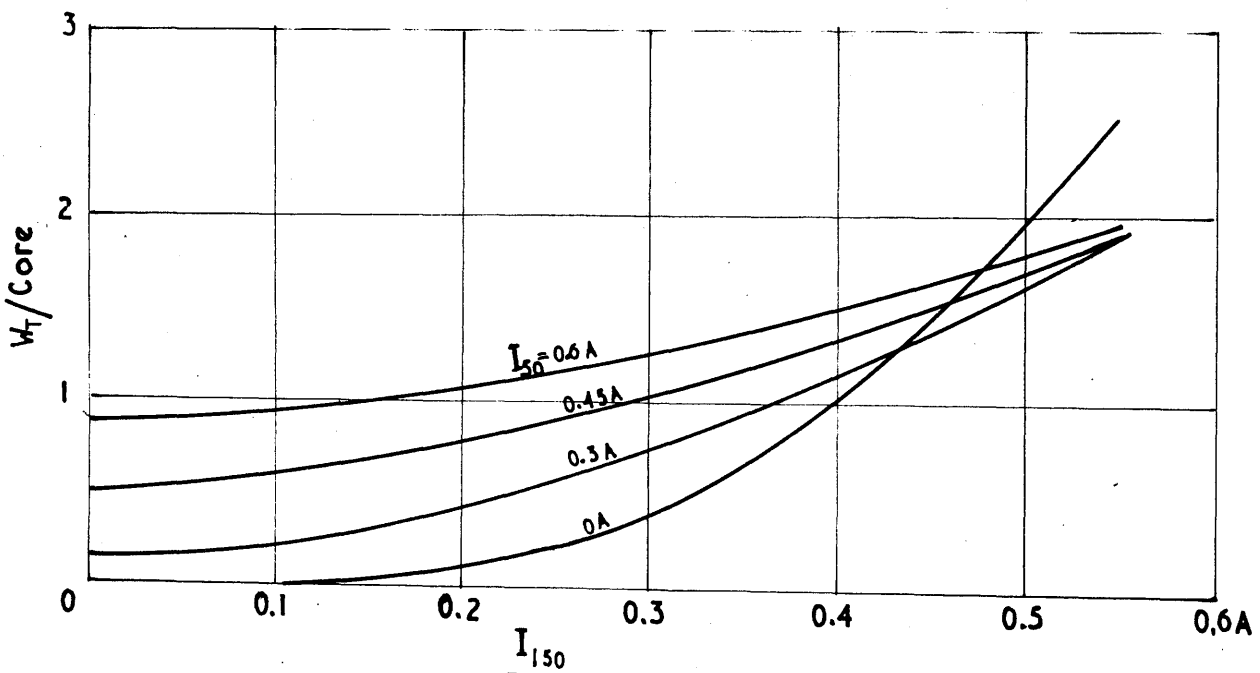

Fig.7.

Variation of $W_{T.MIN}$

From Figs. 6 and 7 it is seen that for the lower range of I_{150} the core loss is always greater than the value obtained under single frequency excitation. As the higher frequency component is increased, the total core loss approaches the value for $I_{50} = 0$. The value of I_{150} at which this condition is obtained depends on the lower frequency magnetizing force, as shown graphically in Figs. 6 and 7. The minimum values of W_T are obtained at lower values of H_{150} for the same H_{50}, than the maximum values. For large values of H_{150} the maximum and minimum values of total core loss tend to the values obtained under single frequency conditions (i.e. $H_{50} = 0$). It should be noted that for each value of H_{50} under combined magnetization, there is one value of the 150-c/s component which causes no change in core loss when H_{50} is removed. This value is given by the intersection of the $H_{50} = 0$ curve with those for various values of H_{50}. Further increase of H_{150} causes an overall reduction in core loss under combined magnetization compared with the corresponding loss for single frequency conditions at 150 c/s. As the magnitude of H_{150} is further increased, this reduction will be reduced since, as stated above, these curves tend to the $H_{50} = 0$ curve for very large values of H_{150}.

When the ratio $\frac{W_{Tmin}}{W_{Tmax}}$ is plotted to a base of H_{150} it is seen (Fig. 8) that the smaller the value of the 50-c/s magnetizing force, the larger is the difference between maximum and minimum core loss values for small values of H_{150}, but it is obvious that as H_{50} is further reduced this condition must be reversed. In the limit when $H_{50} = 0$ the value of α_T is unity for all values of H_{150}.

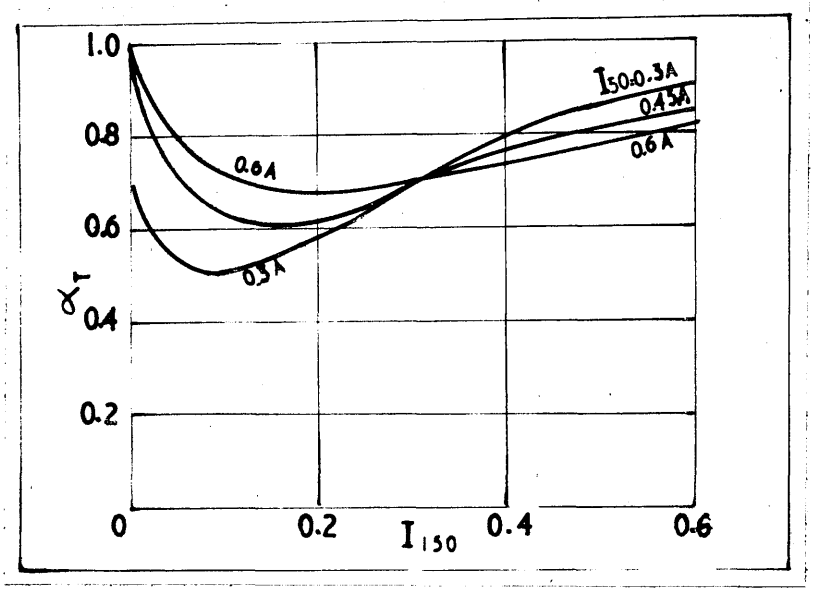

Fig. 8.
Variation of α_T with I_{150}

Variation of maximum and minimum values of 50-c/s component of core loss.

	I_{150}	0.05	0.10	0.15	0.2	0.25	0.3	0.4	0.5	0.6
	W_{50max}	1.08	1.22	1.31	1.38	1.42	1.44	1.42	1.34	1.28
H_{50} = 109.2A	φ	60°	60°	60°	60°	60°	58°	52°	44°	42°
I_{50} = 0.6A	W_{50min}	0.85	0.71	0.69	0.69	0.67	0.66	0.58	0.47	0.44
	φ	0°	0°	0°	0°	-6°	-8°	-18°	-30°	-30°
	W_{50max}	0.69	0.79	0.87	0.93	0.96	0.96	0.93	0.87	0.76
H_{50} = 81.9	φ	60°	60°	60°	60°	60°	57°	52°	46°	38°
I_{50} = 0.45A	W_{50min}	0.44	0.38	0.41	0.43	0.44	0.45	0.42	0.36	0.25
	φ	0°	0°	0°	-4°	-9°	-12°	-13°	-24°	-33°

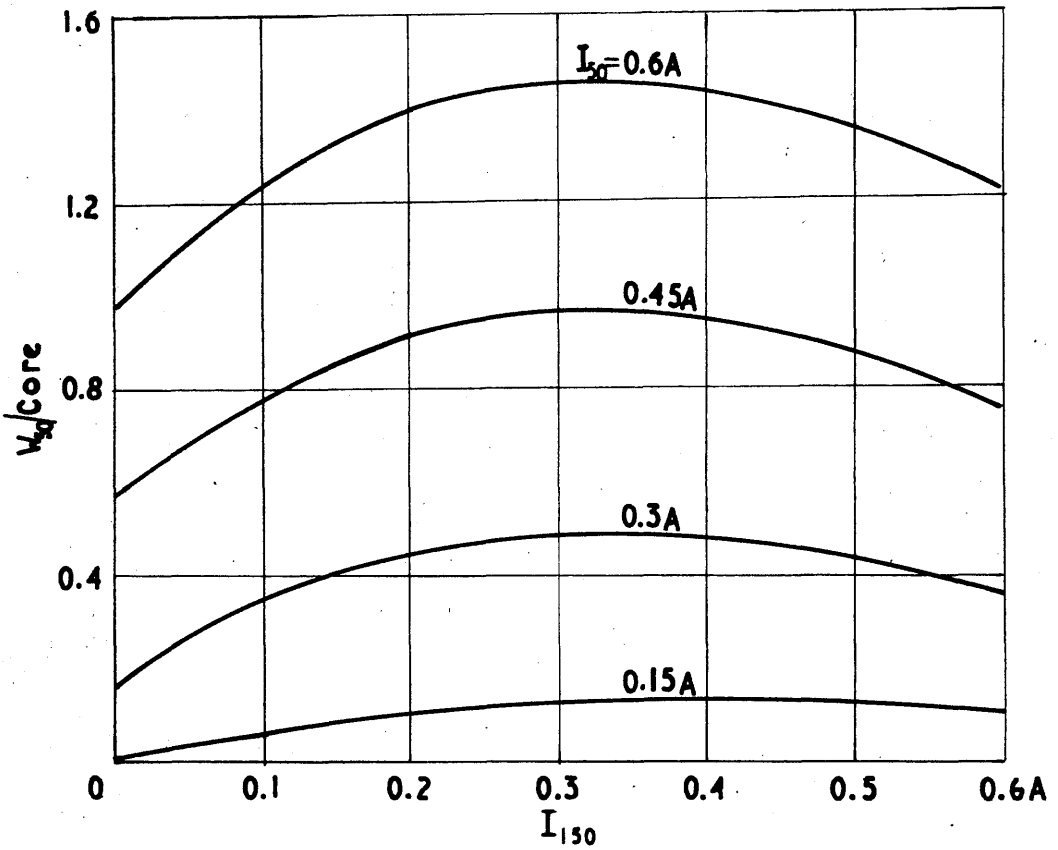

Fig. 9.
Variation of $W_{50.MAX.}$

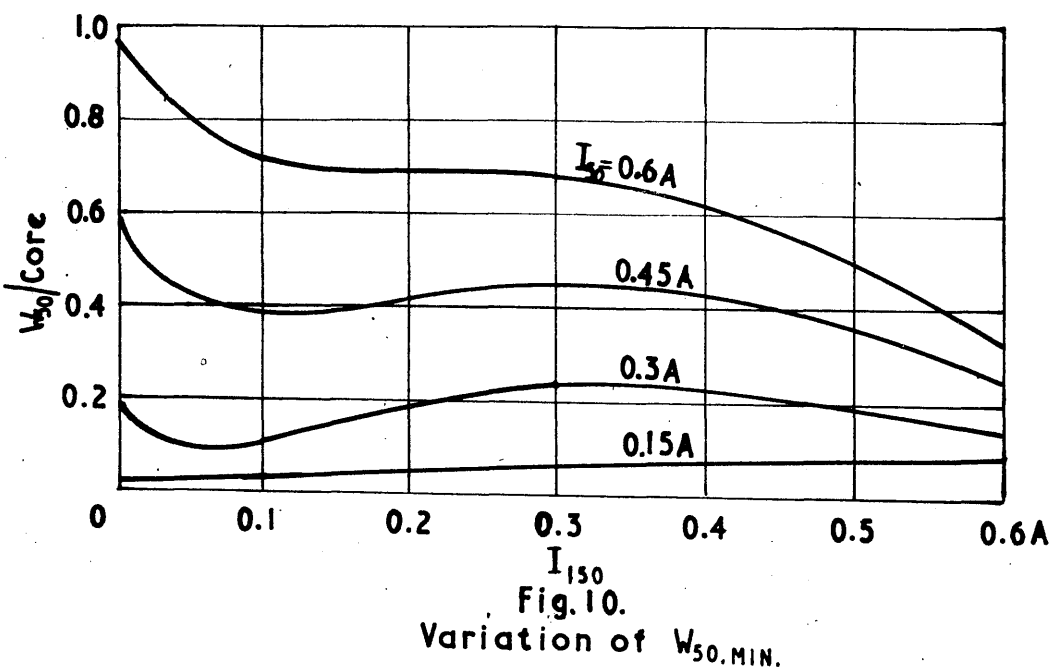

Fig. 10.
Variation of $W_{50.MIN.}$

(Contd) I_{150}	0.05	0.10	0.15	0.2	0.25	0.3	0.4	0.5	0.6
W_{50max}	0.25	0.335	0.395	0.435	0.465	0.485	0.48	0.44	0.36
H_{50} = 54.6 φ	60°	60°	60°	60°	60°	55°	40°	35°	35°
I_{50} = 0.3A W_{50min}	0.11	0.12	0.145	0.18	0.205	0.22	0.20	0.175	0.1
φ	0°	0°	0°	0°	0°	-10°	-11°	-25°	-40°
W_{50max}	0.025	0.045	0.07	0.10	0.11	0.12	0.13	0.125	0.1
φ	60°	60°	60°	60°	60°	52°	50°	30°	
I_{50} = 0.15A W_{50min}	0.01	0.01	0.02	0.04	0.05	0.065	0.08	0.08	
φ	0°	0°	0°	0°	0°	-10°	-17°	-18°	

I_{50}									
0.6	α_{50}	0.79	0.58	0.526	0.5	0.47	0.45	0.41	0.35	0.34
0.45	α_{50}	0.635	0.48	0.47	0.46	0.46	0.47	0.45	0.41	0.33
0.3	α_{50}	0.44	0.36	0.37	0.41	0.44	0.45	0.42	0.40	0.28
0.15	α_{50}	0.4	0.22	0.28	0.4	0.45	0.54	0.61	0.64	

$$\alpha_{50} = \frac{W_{50/\text{core min}}}{W_{50/\text{core max.}}}$$

The variation of the minimum component (Fig. 10) is of most interest since in this way it is possible to control the core loss by altering the magnitude and phase of the superimposed component. Once the core reaches the saturated state it is seen that for all values of 50-c/s magnetizing force, this loss component rapidly decreases. This occurs when the core flux is severely distorted due to large 150-c/s component. The shape of these curves is seen to be similar to those obtained from the high frequency tests (Chapter 6), where all phase effects can be neglected. The first minimum value of W_{50min}, occurring at a low value of H_{150} will correspond to

maximum core permeability, which is obtained for the same value of H_m for all values of H_{50}.

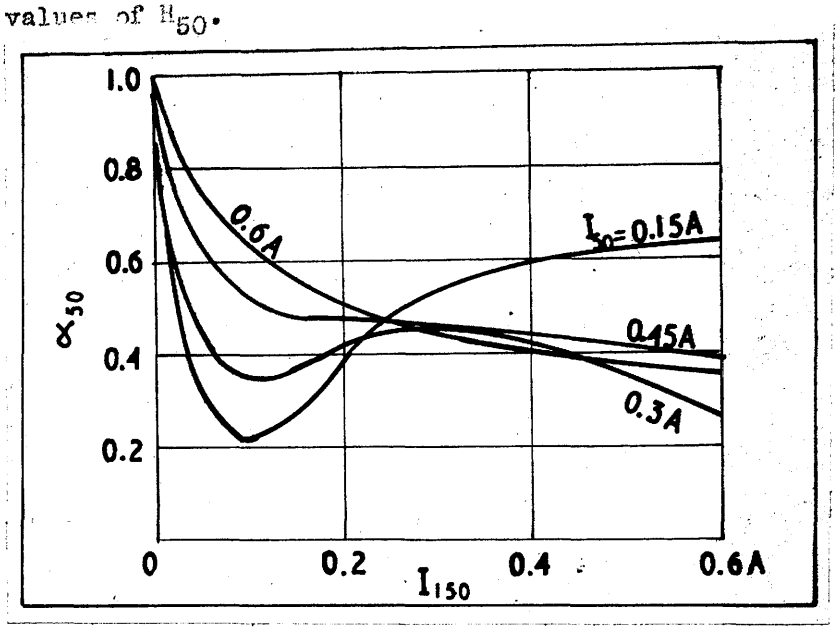

Fig. 11.
Variation of α_{50}.

The variation of α_{50} (Fig. 11) indicates that the effect of phase change for low values of H_{150} is more pronounced when H_{50} is small. When H_{150} is increased, this effect is swamped. As the higher-frequency component is further increased, a large phase effect is obtained, provided the lower-frequency component is large enough to take the core into the saturated region (See Fig. 11. When I_{50} = 0.15A, α = 0.64, while for I_{50} = 0.3A; α = 0.35 for the same value of I_{150}). For large low-frequency core loss variations due to the effect of phase change, there are two possible core conditions

1) Peak magnetizing force H_m just below the knee of the B - H curve. (i.e. μ_{max})

2) $H_{50} > H_m$ in 1) and H_{150} large.

The relative phase angles at which the maximum and minimum core loss values are obtained have been given for all the foregoing tests. This serves as an indication of core conditions, giving a measure of the flux distortion and eddy current loss present in the core. When the core is operating well into the saturated region, the angle changes considerably with an increase in H_{150}:

Variation of maximum and minimum values of 150-c/s component of core loss

I_{150}		0.1	0.2	0.3	0.4	0.5	0.55
	W_{150max}	0.14	0.39	0.65	1.0	1.41	1.61
H_{50} = 109.2	φ	0	-4°	-9°	-17°	-20°	-25°
I_{50} = 0.6A	W_{150min}	-	0.05	0.3	0.6	0.95	1.15
	φ	-	75°	70°	65°	50°	50°
	W_{150max}	0.12	0.32	0.57	0.91	1.33	1.65
H_{50} = 81.9	φ	0	+10°	-8°	-10°	-30°	-30°
I_{50} = 0.45A	W_{150min}	0	0.21	0.46	0.77	1.19	1.44
	φ	100°	90°	85°	80°	40°	30°
	W_{150max}	0.07	0.24	0.5	0.88	1.60	2.04
H_{50} = 54.6	φ	60°	60°	60°	65°	68°	75°
I_{50} = 0.3A	W_{150min}	0.07	0.21	0.46	0.82	1.34	1.62
	φ	8°	8°	10°	10°	0°	0°

(Contd) I_{150} / I_{50}		0.1	0.2	0.3	0.4	0.5	0.55
0.6A	α_{150}	-	0.128	0.462	0.6	0.675	0.715
0.45A	α_{150}	-	0.66	0.81	0.845	0.895	0.872
0.3A	α_{150}	-	0.875	0.92	0.936	0.835	0.795

$$\alpha_{150} = \frac{W_{150}/\text{core min}}{W_{150}/\text{core max.}}$$

From Figs. 12 and 13 it is seen that the minimum values of W_{150} and maximum values, provided the core is not fully saturated, are obtained for the largest value of H_{50}. This would be expected since the available flux change will be large when H_{50} is large. As the core is taken well into the saturated region by an increase in H_{150}, the maximum core loss value is now given by the minimum value of H_{50}. This is due to the core being carried well into saturation by the relatively large 150-c/s component. ($H_{150} > H_{50}$ for this condition to occur). The flux density waveform is now sharply peaked, giving rise to a large 150-c/s loss component.

The variation of α_{150} (Fig. 14) shows that the largest core loss swing, with phase angle, occurs when H_{50} is large and H_{150} is small.

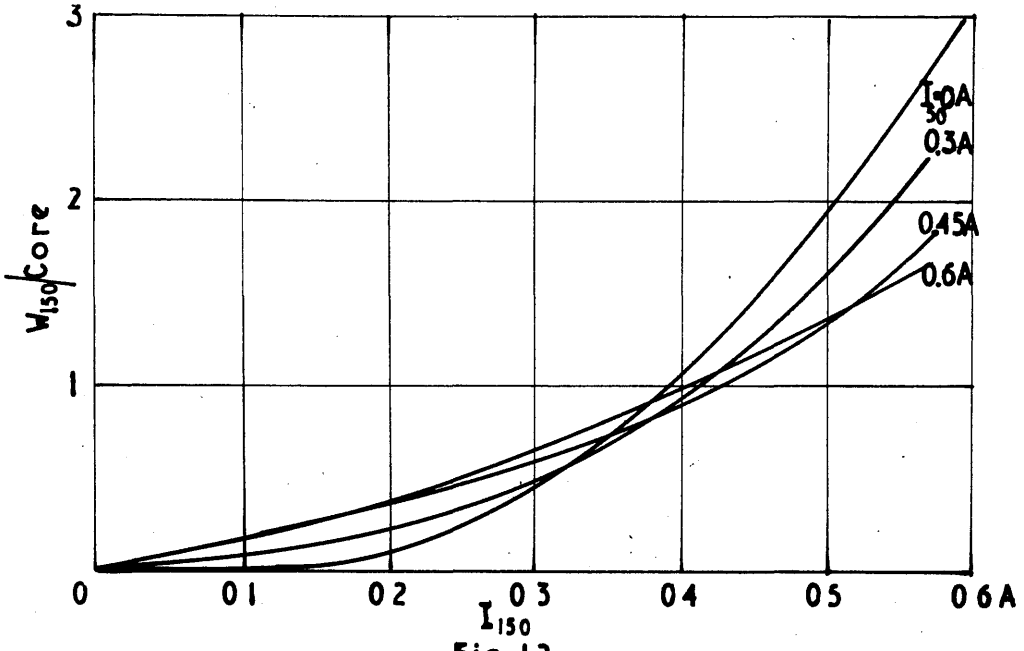

Fig. 12.

Variation of $W_{150\,MAX}$

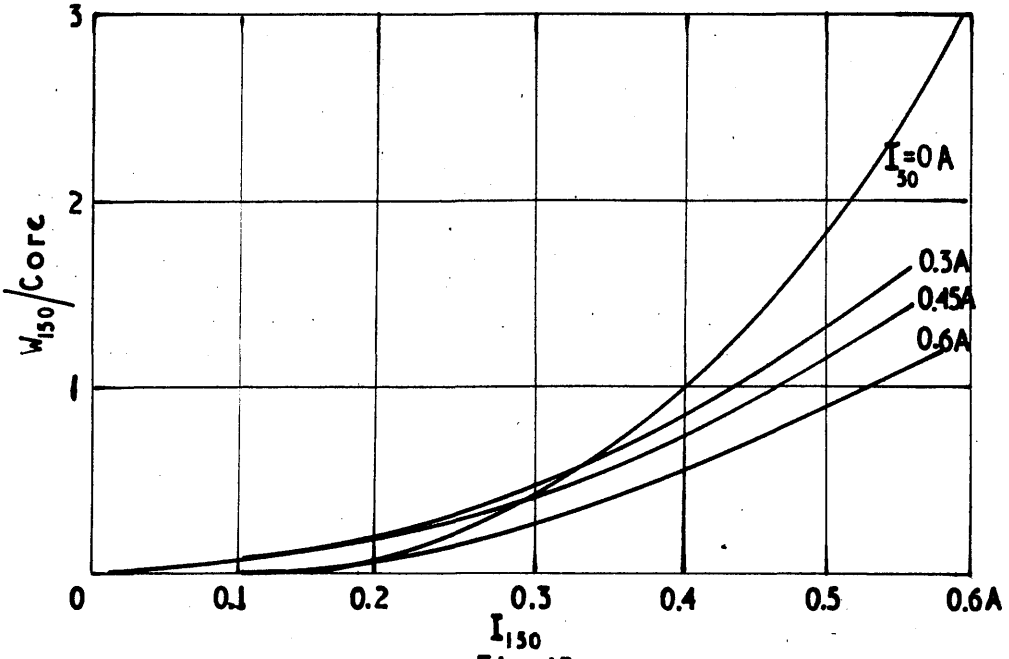

Fig. 13.

Variation of $W_{150\,MIN}$

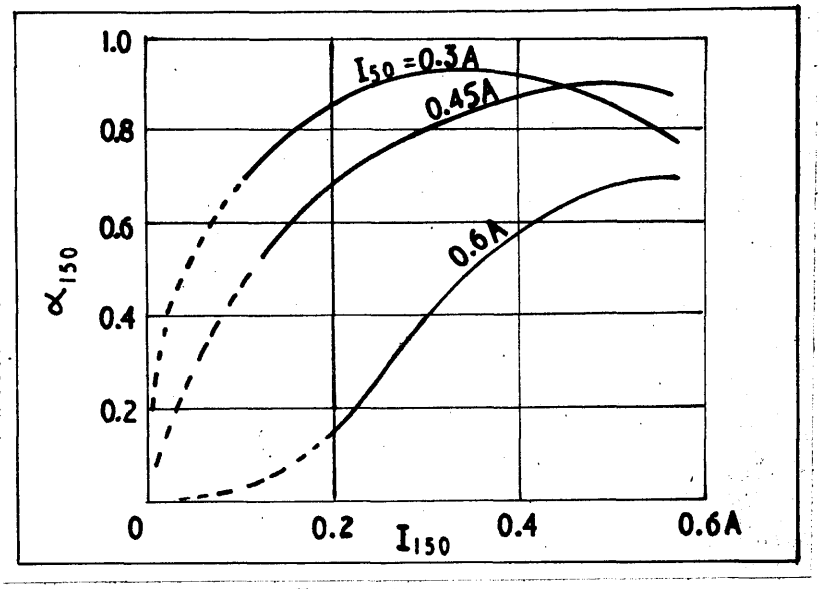

Fig. 14.
Variation of α_{150}.

A similar series of tests was carried out with the cores magnetized at 50 c/s and 100 c/s. The core magnetizing force is defined as $h = h_1 \cos(\omega t + \phi) + h_2 \cos 2\omega t$. The results are summarized in Figs. 15 - 23.

The curves of most interest are those showing the variation of W_{Tmin} and W_{50min} (Figs. 16 and 19). When compared with the corresponding results obtained previously for 150 c/s and 50 c/s, it is seen that the W_T curve has a minimum value for low values of 100-c/s magnetizing force, whereas for 150-c/s excitation the minimum occurs when H_{150} is zero. Thus, under combined magnetization at 50 and 100 c/s, the total core loss is less than the single low frequency loss, over the lower range of H_{100}, when the total core magnetizing force is defined as

$$h = h_1 \cos \omega t + h_2 \cos 2 \omega t$$

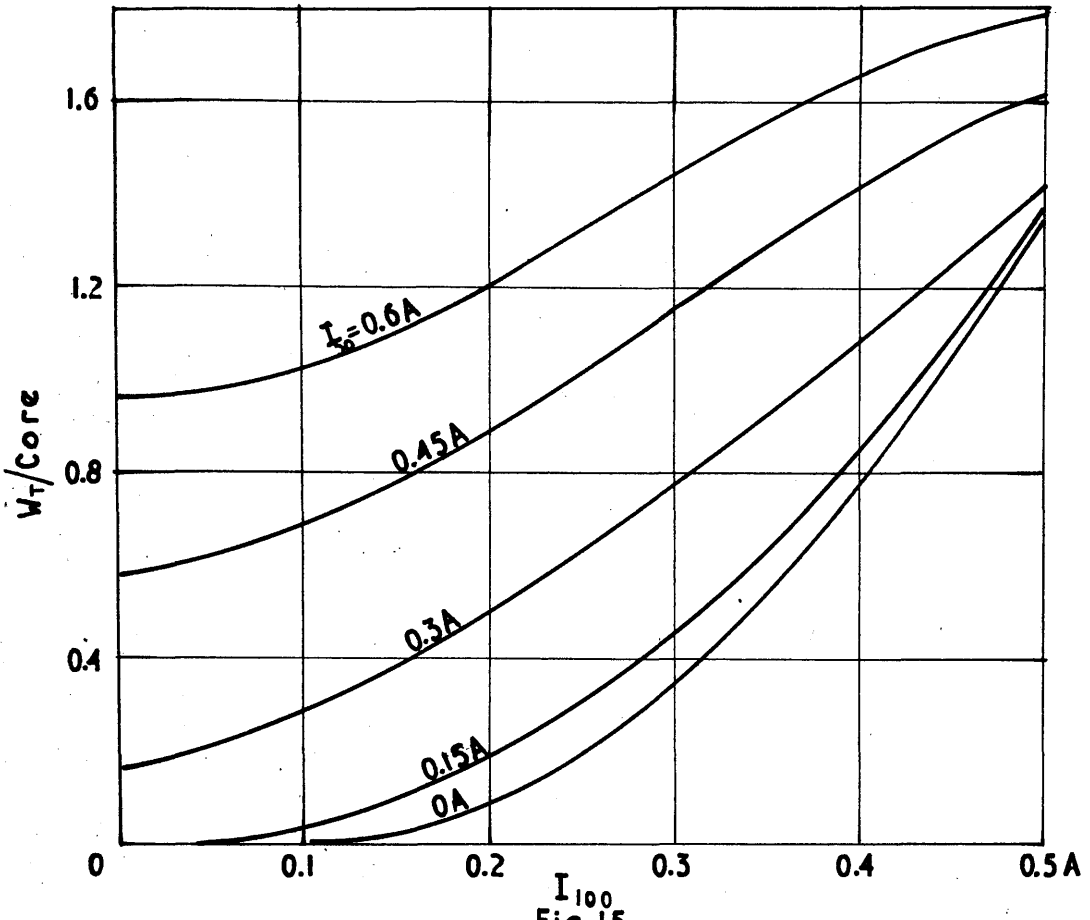

Fig. 15.
Variation of $W_{T.\ MAX.}$

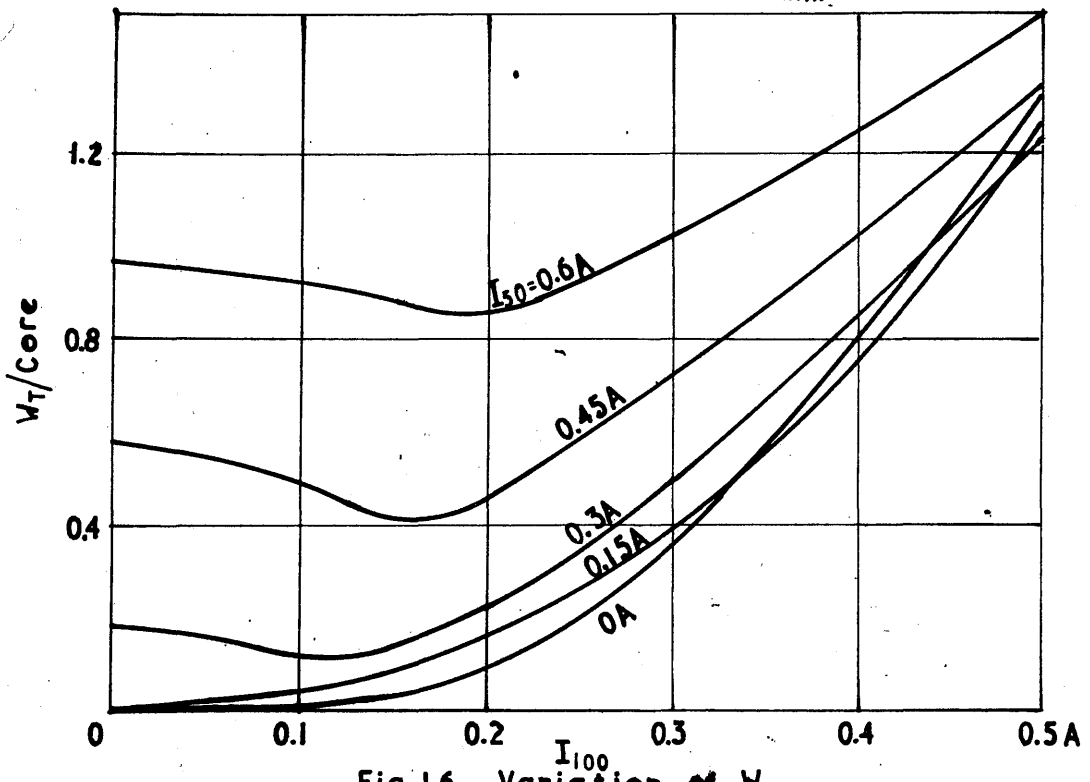

Fig. 16. Variation of $W_{T.\ MIN.}$

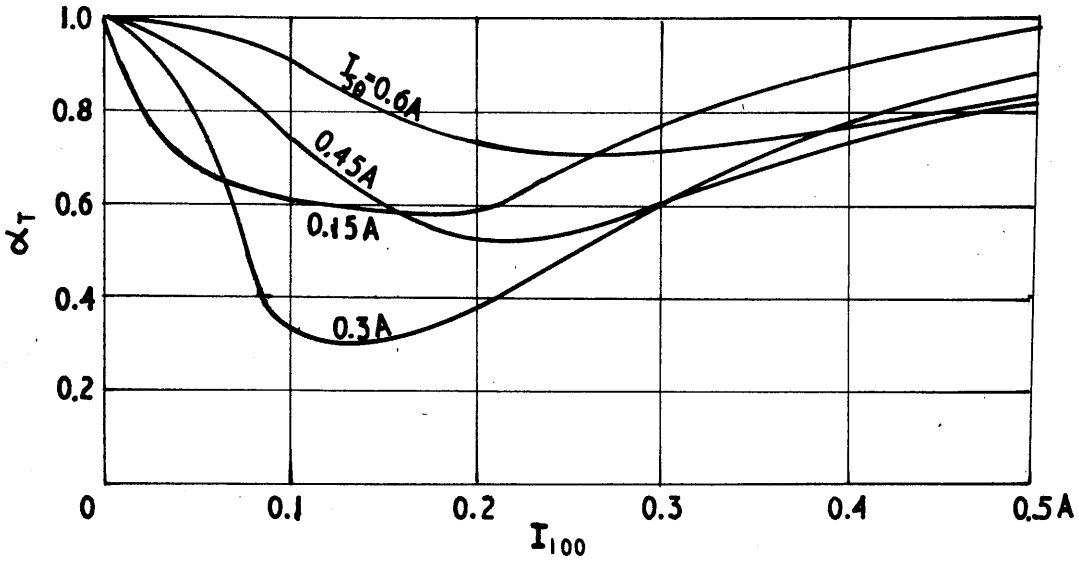

Fig. 17.
Variation of α_T

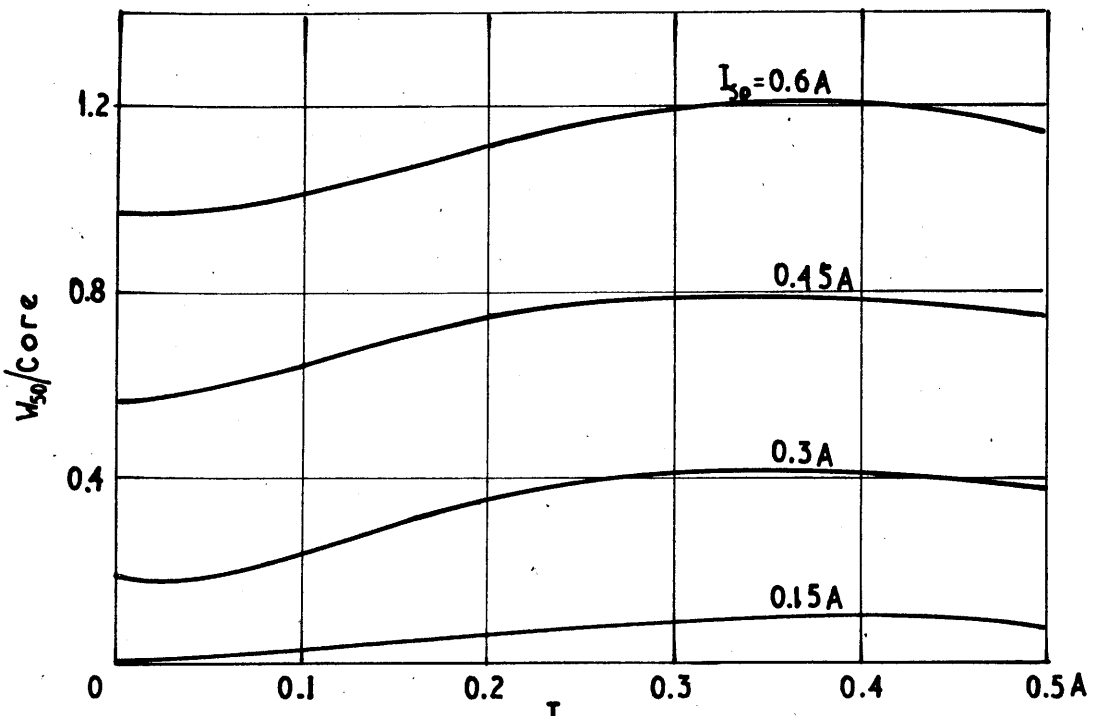

Fig. 18.
Variation of $W_{50.MAX.}$

The reduction occurs, provided the lower frequency loop is formed by a magnetizing force which causes this loop to extend above the "lower bend" region of the magnetization characteristic, i.e. when $I_{50} > 0.2A$ approximately. The percentage reduction is greater in the region when $I_{50} = 0.3A$ corresponding to operation at the maximum core permeability. This position of operation also gives the largest change of core loss with phase angle, as shown by the variation of α_T in Fig. 17. Approximately, for values of H_{50} in the saturated region, the maximum phase effect is obtained for $H_{100} = \frac{1}{2} H_{50}$. This also is the minimum value of H_{100} to cause the magnetizing force wave to be re-entrant for all values of phase angle. (See also Part I, Chapter 3).

The variation of W_{50min} (Fig. 19) is seen to be similar to the values previously obtained for 150-c/s excitation. If the 100-c/s magnetizing force could be increased further, the gradual reduction in W_{50} would be obtained for large values of H_{100}. The reduction at lower values of 150-c/s magnetizing force may be due to the 150-c/s flux component being caused partly by its own magnetizing force and partly from the 3rd harmonic component of the 50-c/s flux wave. In the 100-c/s case, there is no interaction between fluxes since their frequency components are all dissimilar (i.e. odds from 50 c/s; evens from 100 c/s).

The maximum phase effect again occurs for $I_{50} = 0.3A$ when $I_{100} = 0.15A$, i.e. $H_{100} = \frac{1}{2} H_{50}$.

The results for W_{100} (Figs. 21 - 23) show that this component of loss is reduced as the low frequency magnetizing force is increased, the maximum phase effect occuring with the largest value of low frequency magnetizing force.

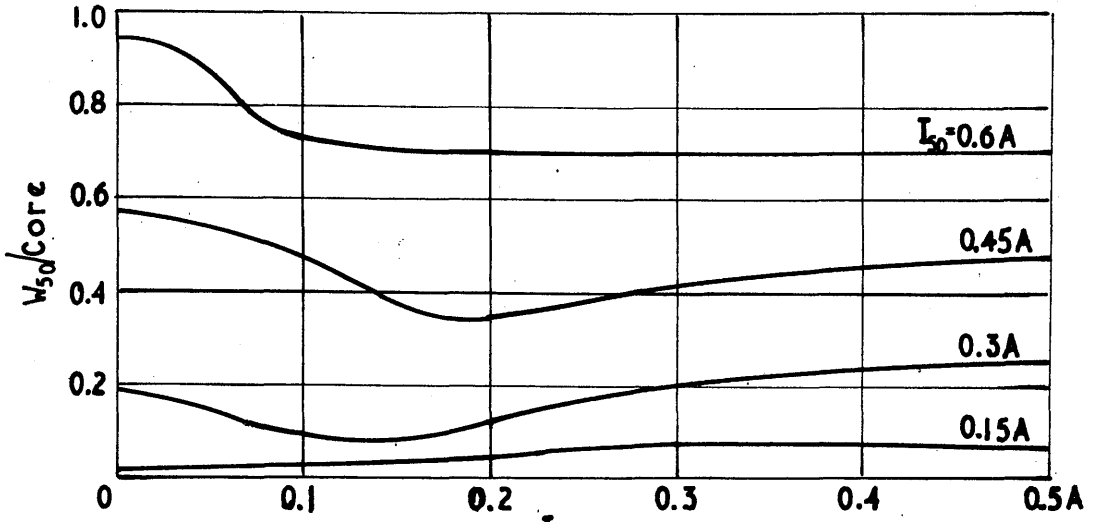

Fig.19.
Variation of $W_{50.\,MIN.}$

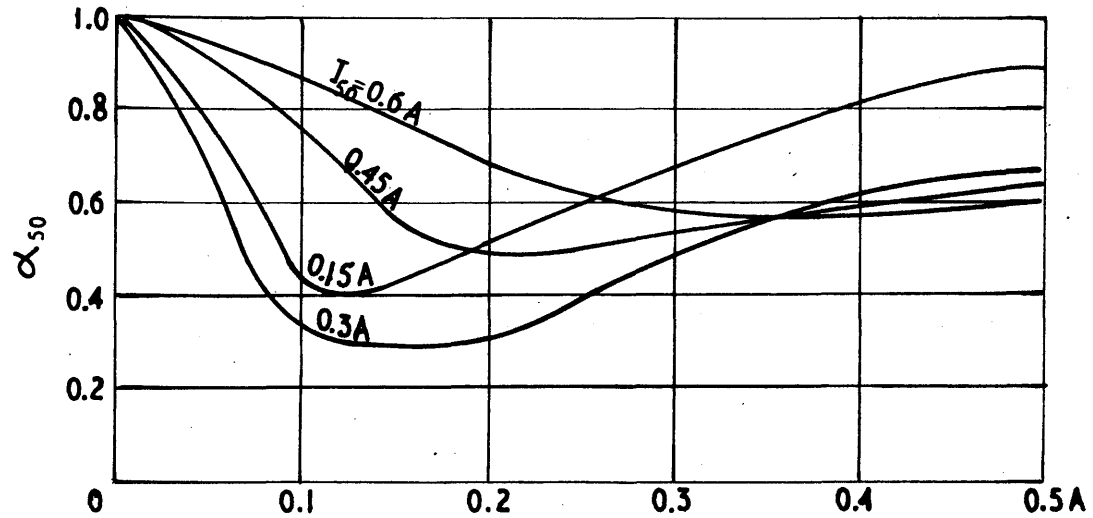

Fig.20.
Variation of α_{50}

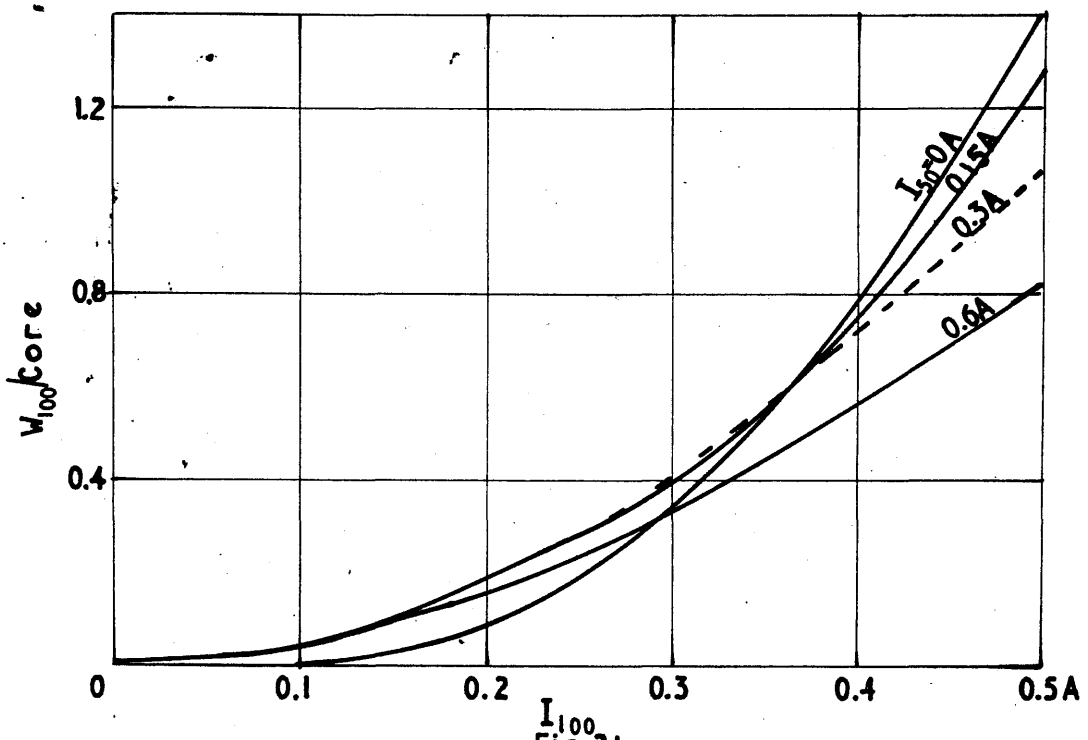

Fig. 21.
Variation of $W_{100.MAX.}$

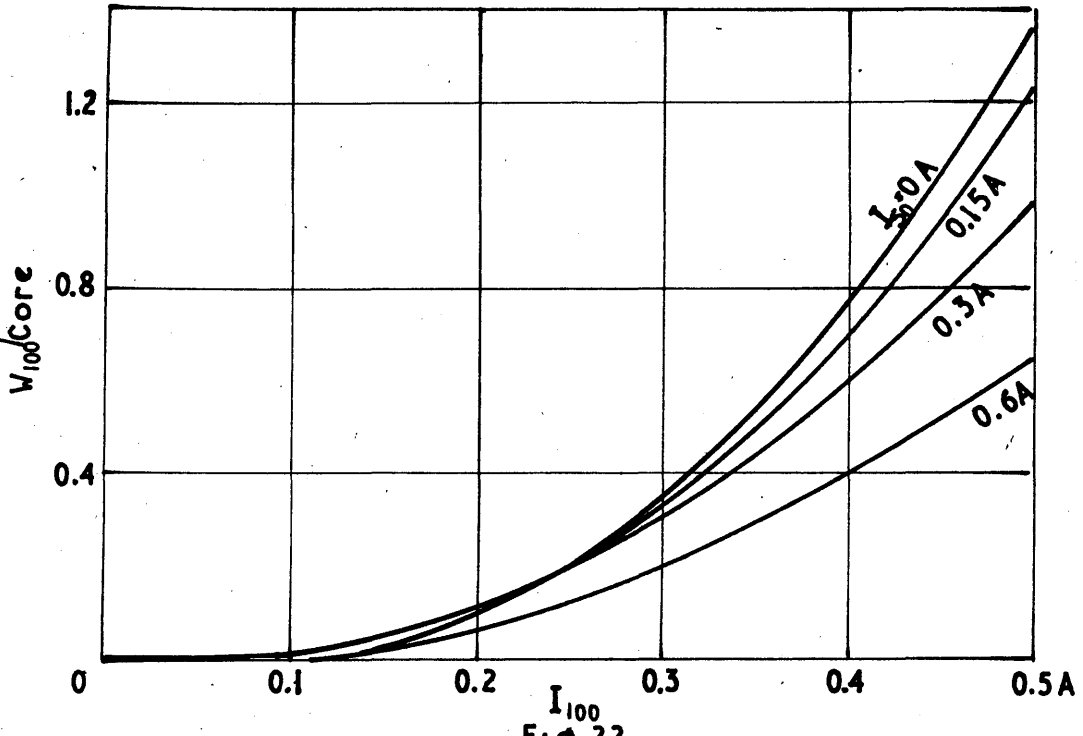

Fig. 22.
Variation of $W_{100.MIN.}$

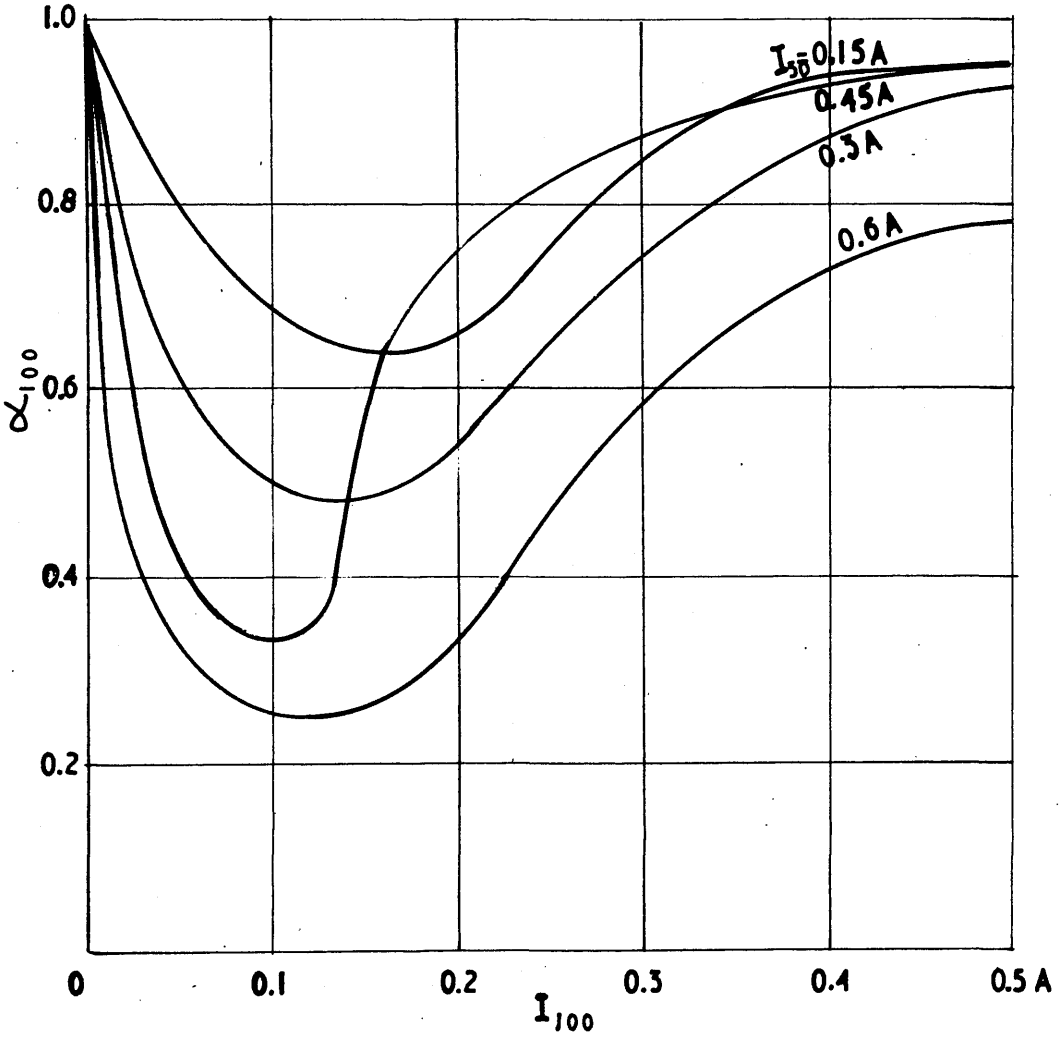

Fig. 23.
Variation of α_{100}

CHAPTER 4

EFFECT OF RELATIVE PHASE ANGLE CHANGE ON LOSS COMPONENTS.

In the preceding section it is seen that there are very large changes in the core loss components due to a change of phase angle. The values obtained only indicate the extreme conditions of loss component and it is considered desirable to investigate how these quantities alter between their extreme limits. Accordingly, locked frequency supplies were used and the relative phase angle altered over a complete range of values. The individual loss components were obtained from a.c. potentiometer measurements. Details of the a.c. potentiometer circuits used to enable two-frequency results to be measured are given in Appendix (a).

The magnetization conditions considered are

$$h' = h_1 \sin (314t + \varphi) + h_2 \sin 628t$$

and $$h'' = h_1 \sin (314t + \varphi) + h_3 \sin 942t$$

The results are obtained for $h_1 = 154.4$ AT/m over a range of values for h_2 and h_3 and additionally for $h_1 = 77.2$ AT/m. The range of phase angle, which is always obtained with respect to the 50-c/s supply, necessary to carry the core through a complete cycle of loss changes depends on the higher frequency component. With 100-c/s excitation the core conditions repeat after 180° as the one minor loop has then returned to its original position. Over the range 0° - 90° the results are repeated again from 90° - 180°, due to the loop symmetry. The core loss conditions when $\varphi = 10°$ say, are identical

with those obtained when φ = 100°. Hence a complete cycle of the phase effects will be obtained if φ is varied from 0° - 90°. Similarly with 150-c/s excitation the core conditions repeat exactly, i.e. each of the two minor loops return to their original position after a change of 240°, but due to loop symmetry the conditions obtained over 0 - 120° are repeated from 120° - 240°. A complete cycle of results is obtained with 120° change of phase. In addition to core loss values the peak core flux-density is obtained for all phase angles. Due to the possibility of the induced voltage wave being re-entrant, the standard method of obtaining B_m by a rectifier voltmeter cannot be applied and the peak flux value was read directly using a valve voltmeter (see Appendix (c)). To enable the eddy-current loss in the core to be approximately obtained an r.m.s. meter was connected across the 400^T search coil. To prevent any current being taken in this circuit a vacuo-junction and unipivot movement were used, full details of which are given in Appendix (c). Using the approximate formula for eddy-loss derived in Appendix (d), the true total core hysteresis loss can be estimated. At the present time, no method has been devised to determine what percentage of the total eddy-current is supplied from source 1 and source 2 since when 50 and 150-c/s supplies are used, there is interaction between the 150-c/s voltage component and the third harmonic of the 50-c/s voltage. This is not a serious matter as it is the variation in <u>total</u> core loss from <u>each</u> source which is being investigated. Additionally, the trend at the present time is not to separate out the hysteresis and eddy-current loss components due to the large discrepancies obtained, but to treat

the core loss as a complete unit. In practical cases, of course, it is the total loss which is of concern. (See also Appendix (d)).

Test A gives results for combined magnetization at 50 and 100 c/s. A series of tests was carried out by variation of the 100-c/s magnetizing force. A specimen set of results obtained from one of these tests is shown.

The variation in individual loss components and total core loss for the above case is shown in Fig. 24. The results from the complete series of tests are summarized in Figs. 25 - 28.

Test A. I_{50} = 0.6A

I_{100} = 0.6A h = 154 sin ($\omega t + \phi$) + 154 sin 2 ωt

ϕ	0	10	20	30	40
$I_{50} + a_1$	0.263	0.353	0.426	0.497	0.547
$+ jb_1$	-0.54	-0.485	-0.416	-0.335	-0.246
$E_{50} + a_2$	0.544	0.532	0.501	0.452	0.370
$+ jb_2$	-0.139	-0.06	0.027	0.178	0.310
Voltage Factor	20	20	20	20	20
$I_{100} + c_1$	0.578	0.578	0.578	0.578	0.578
$+ jd_1$	0.05	0.05	0.05	0.05	0.05
$E_{100} + c_2$	0.123	0.092	0.064	0.188	0.31
$+ jd_2$	0.87	0.877	0.837	0.666	0.495
Voltage Factor	20	20	20	20	20
$a_1a_2 + b_1b_2$	0.218	0.216	0.202	0.166	0.126
W_{50}/core	1.09	1.08	1.01	0.83	0.63
$c_1c_2 + d_1d_2$	0.115	0.097	0.079	0.141	0.205
W_{100}/core	0.144	0.121	0.099	0.176	0.265
$W_{50} + W_{100}$/core	1.234	1.201	1.109	1.006	0.886
$B_{mT} + V_e$	0.709	0.709	0.709	0.768	0.797
$B_{mT} - V_e$	0.945	0.915	0.855	0.680	0.517
B_{mT} peak-peak	1.654	1.624	1.564	1.448	1.314
V_{400}^{T} r.m.s.	16.7	16.0	15.2	13.8	13.7
Eddy Loss/core	0.338	0.308	0.279	0.232	0.227
W_T hyst	0.896	0.893	0.830	0.774	0.659
B_{m50}	0.826	0.790	0.737	0.718	0.715
B_{m100}	0.325	0.325	0.31	0.256	0.216

$h = 154 \sin(\omega t + \phi) + 154 \sin 2\omega t$

ϕ	50	60	70	80	90
$I_{50} + a_1$	0.575	0.594	0.594	0.58	0.55
$+ jb_1$	-0.174	-0.072	0.03	0.138	0.234
$E_{50} + a_2$	0.403	0.367	0.317	0.259	0.173
$+ jb_2$	0.444	0.474	0.498	0.51	0.508
Voltage Factor	20	20	20	20	20
$I_{100} + c_1$	1.120	1.120	1.120	1.120	1.120
$+ jd_1$	0.070	0.070	0.070	0.070	0.070
$E_{100} + c_2$	0.324	0.325	0.291	0.274	0.283
$+ jd_2$	0.464	0.506	0.556	0.561	0.595
Voltage Factor	40	40	40	40	40
$a_1a_2 + b_1b_2$	0.155	0.184	0.203	0.224	0.213
W_{50}/core	0.775	0.920	1.015	1.12	1.065
$c_1c_2 + d_1d_2$	0.395	0.399	0.365	0.345	0.359
W_{100}/core	0.990	1.00	0.910	0.863	0.895
$W_{50} + W_{100}$	1.765	1.920	1.925	1.983	1.960
$B_{mT} + V_e$	1.11	1.17	1.19	1.19	1.14
$B_{mT} - V_e$	0.676	0.73	0.77	0.79	0.83
B_{mT} peak-peak	1.786	1.90	1.96	1.98	1.97
V_{400T} r.m.s.	20.4	21.0	21.7	22.0	22.0
Eddy loss /core	0.50	0.532	0.568	0.585	0.585
W_T hyst	1.265	1.388	1.357	1.398	1.375
B_{m50}	0.886	0.886	0.873	0.845	0.792
B_{m100}	0.416	0.445	0.465	0.475	0.487

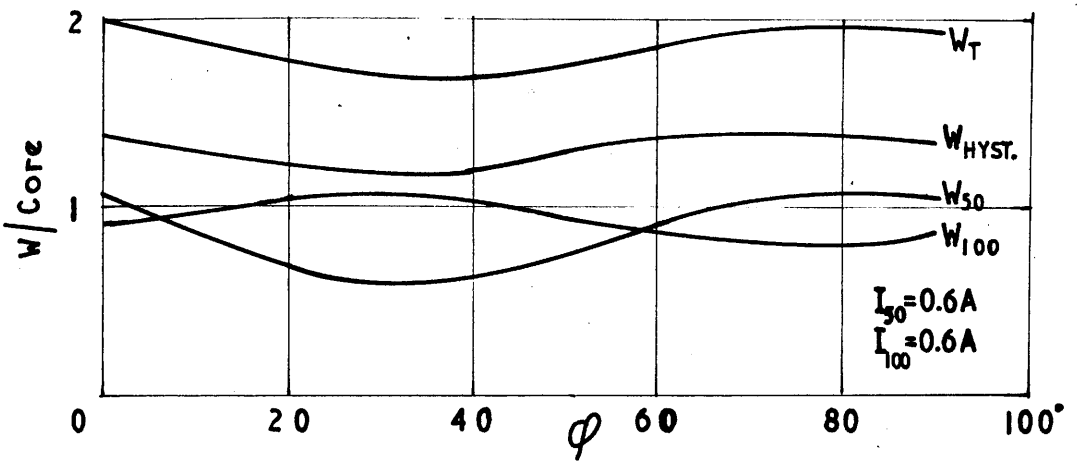

Fig. 24.

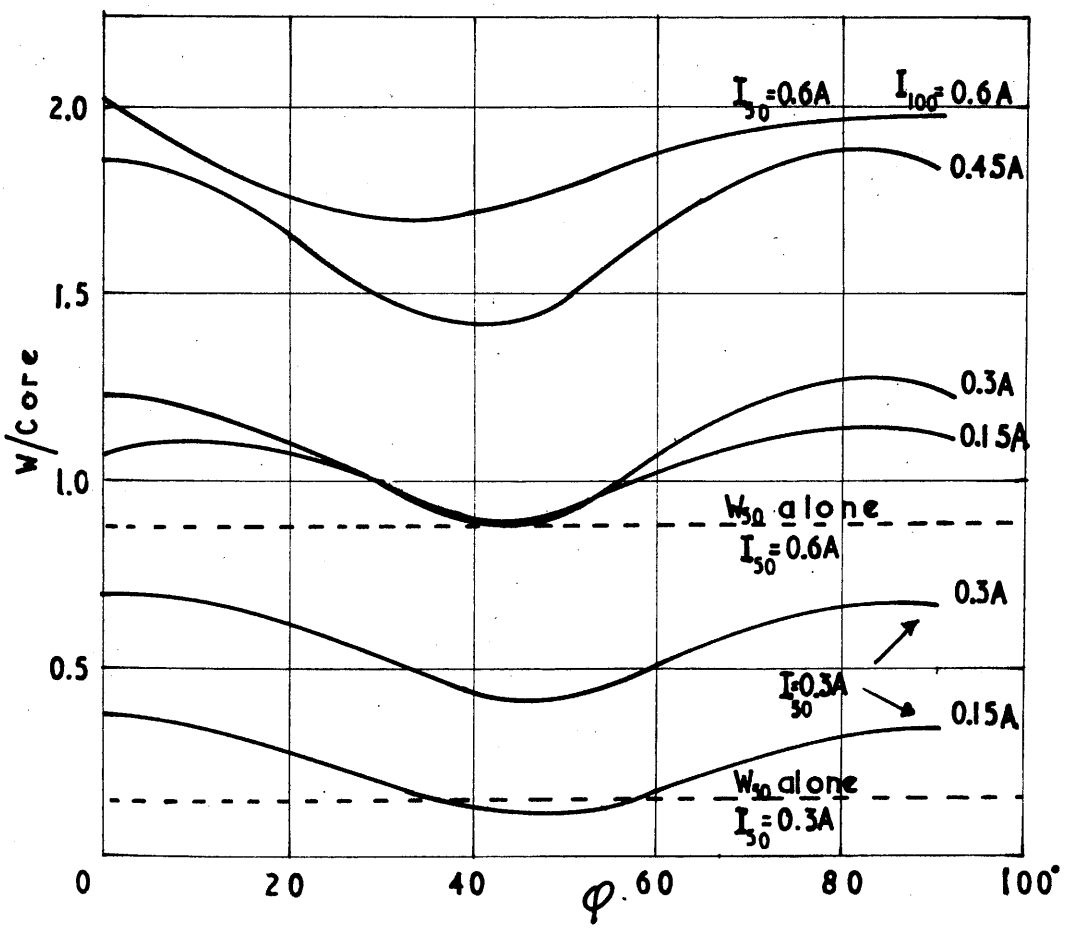

Fig. 25.
Variation of total core loss

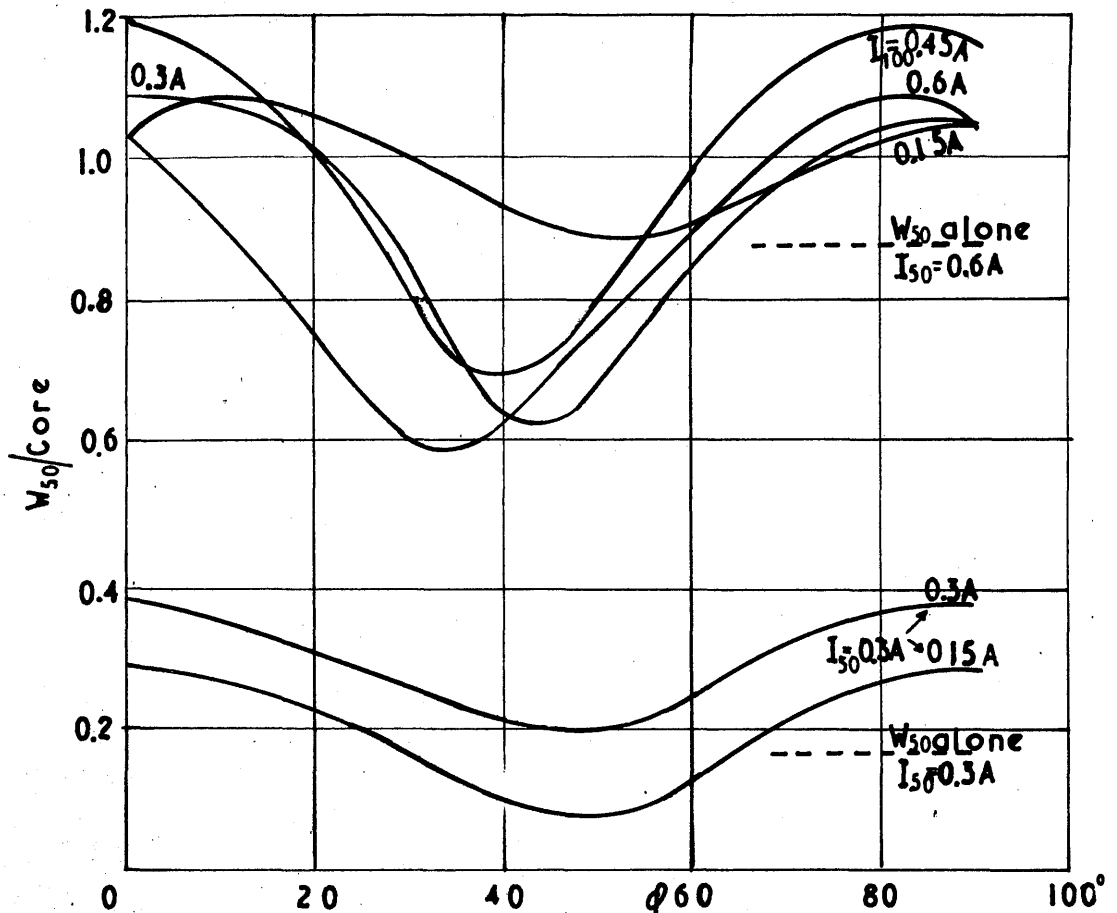

Fig. 26.

Variation of $W_{50}\left[h = h_1 \sin(\omega t + \varphi) + h_2 \sin 2\omega t\right]$

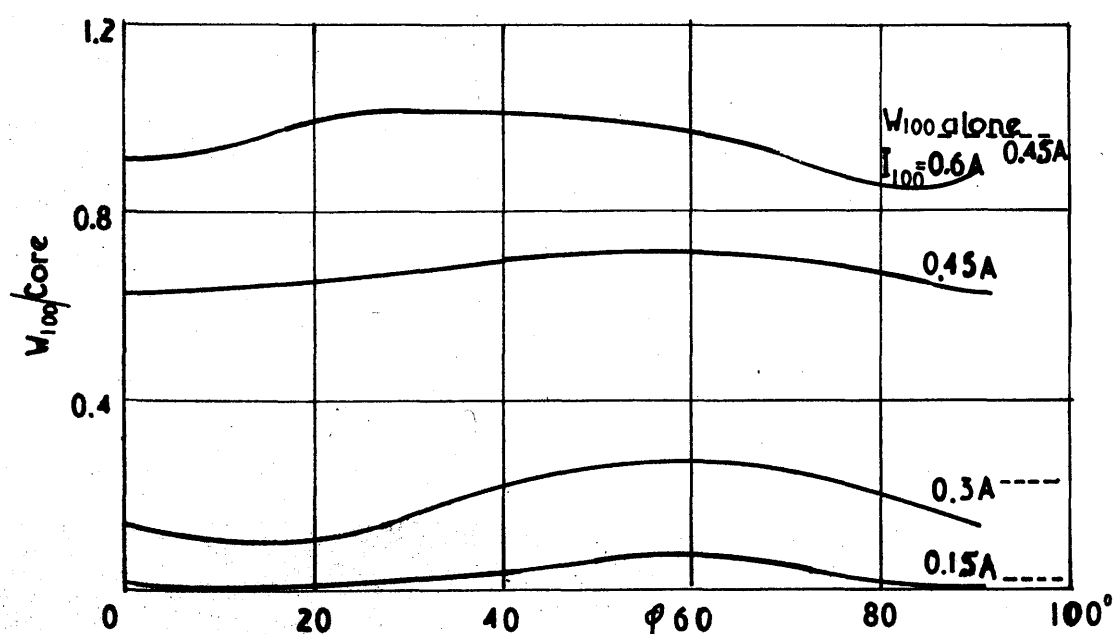

Fig. 27.

Variation of W_{100} when $I_{50}=0.6A$

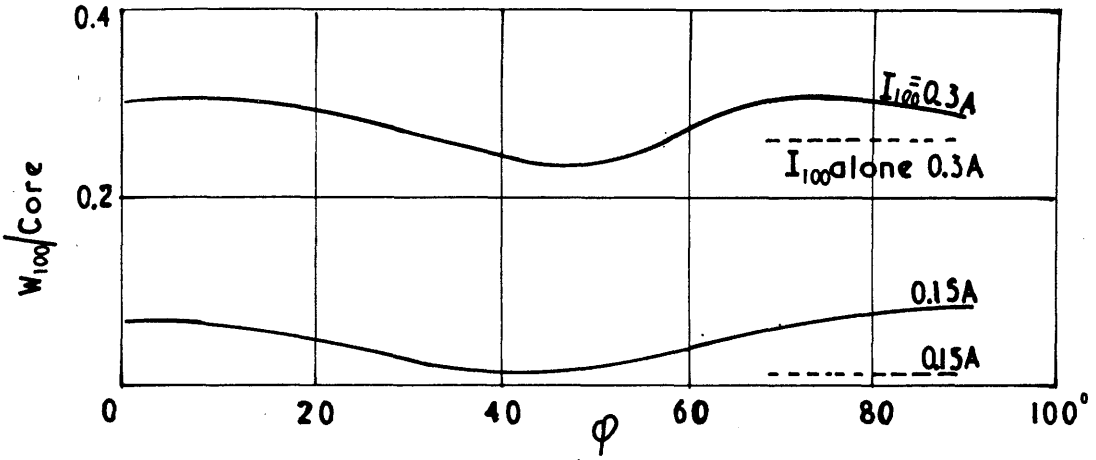

Fig. 28.

Variation of W_{100} when I_{50}=0.3A

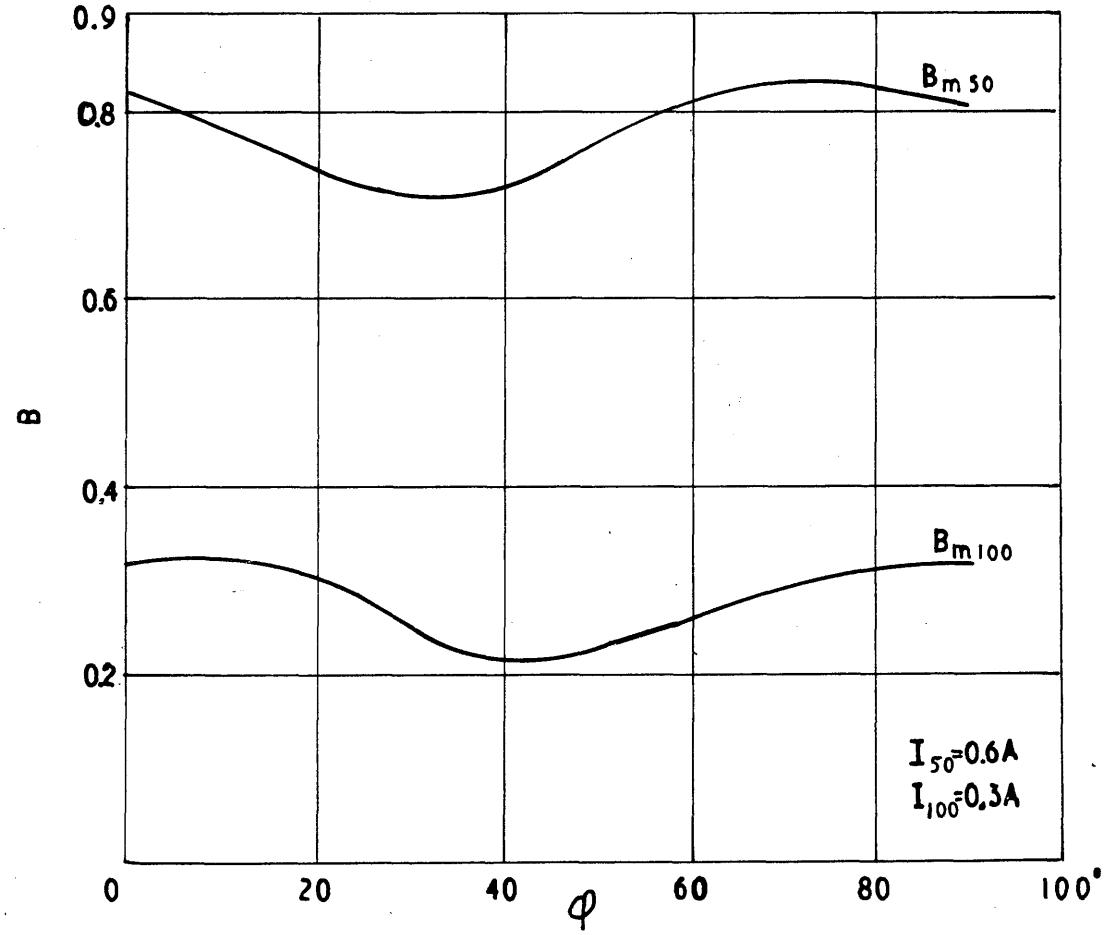

Fig. 29.

Variation of flux density components

For combined magnetization in the range $k > 0 < 1$ ($k = \frac{h_{100}}{h_{50}}$) the total core loss under this condition is greater than the loss obtained when the low frequency term is acting alone. The effect of phase on the total loss causes it to vary between wide limits, as shown in Fig. 25. When the core is magnetized at 50 and 100 c/s the minimum total core loss occurs when $\varphi = 45^{\circ}$ (approximately), which is also the condition for minimum magnetizing force. The variation in total loss is relatively small in comparison with the changes in the individual loss components. The lower frequency term will be considered first since it is usually of most interest.

There are two distinct regions of operation for phase effects, the first applicable when the core is operating below saturation, and the second when it is well into the saturated region. For the first case, the necessary conditions to give a reduction in low-frequency core loss below the value obtained under sine-current single-frequency excitation follow the theory in Part I. These results are shown for the case when $I_{50} = 0.3A$, $I_{100} = 0.15A$ and 0.3A. For the latter case, it is seen from Fig. 26 that no reduction in low-frequency loss occurs over the phase angle range, whereas when the 100-c/s component is reduced to 0.15A, there is a reduction in loss over a range of phase angles from $\varphi = 30 \rightarrow 60^{\circ}$.

It must be borne in mind that in Part I the results were obtained by assuming an expression which of necessity comprised only a few terms to represent a function which would be defined accurately by a very large number of terms. In this way, the theory ceases to be of value when the

cores are operating well into the saturated region. From the experimental results, Fig. 26, it is seen that, provided the 100-c/s component of magnetizing force exceeds 25% of the fundamental term, there will be a reduction in low-frequency core loss. As the 100-c/s component is increased, the minimum value of core loss is further reduced.

The necessary requirement for a reduction of loss in the two regions of core operation are exactly opposite, i.e.

1) Small H_{100} (only limited range of values)

2) Large H_{100} (the larger H_{100}, the smaller W_{50}).

The phase angle values throughout these tests are determined with respect to the current wave and hence due to the angle (not a constant) between $\overline{B}$ and $\overline{H}$ in the core the minimum loss will not always occur at the same phase angle value when the core is in the saturated region, since the flux wave then contains a high percentage of harmonic terms. This is shown in Fig. 26, where the minimum occurs at $\varphi = 45^{\circ}$ for $I_{100} = 0.15A$ and is shifted to $\varphi = 34^{\circ}$ when $I_{100} = 0.6A$. The variation of the actual minimum and maximum values has been considered previously in Part II, Chapter 3, for a large range of 50 and 100-c/s magnetization conditions.

It is of interest to compare the variation of the 50-c/s component of flux density in the core with the loss value obtained as the phase angle is altered over the range. Since the 50-c/s component of magnetizing force is constant in magnitude, the variation in core loss is caused by alteration in the magnitude and phase of this flux component. It is seen that the phase angle for minimum core loss

is not that which gives a minimum value for B_{m50} (Fig. 29). It can thus be stated that the reduction in loss occurs primarily due to a change in the angle of the complex permeability. This change is caused by the action of the higher frequency components acting on the core.

The variation in the 100-c/s loss component with phase angle does not show a large variation when its magnetizing force is large. (Fig. 27). As this value is reduced to $0.5H_{50}$, comparatively large changes in loss are obtained. This is the smallest value of superimposed magnetizing force to give a re-entrant wave for all phase angle values. For this value of H_{100} and all larger values, the loss under single frequency conditions is greater than when the same magnetizing force is acting with a low-frequency value large enough to take the core into the saturated region.

When the low-frequency value is reduced, it is seen from Fig. 28 that the individual loss value for $H_{100} = H_{50}$ is the mean value of the loss under combined magnetization. For smaller values of H_{100} the loss is greater than obtained in the single frequency test.

As previously, the core conditions determine whether the higher-frequency loss term is increased or decreased when the same sinusoidal magnetizing force acts under combined conditions. When the core is operating in the saturated region, there will be a reduction in this loss term. It must be noted that conditions are considered in the range $H_{100} \not> H_{50}$. If $H_{100} \gg H_{50}$ the above conditions no longer apply since in the limit when $H_{50} \rightarrow 0$, there will be no change in the higher-frequency loss term.

When the total core loss is obtained with given values of magnetizing force and the cores are operating under single frequency magnetization, it is seen that the sum of these values is always greater than the minimum loss obtained with the same magnetizing force components under combined magnetization. When the 100-c/s component is small in comparison with H_{50}, there is very little difference between the individual sum of W_{50} and W_{100} and the minimum value for combined conditions.

When the 50-c/s component is large enough to take the core to the saturated region, the loss under combined conditions is less for all phase angle values than the sum of the single frequency values. For the case when H_{50} is small, the minimum loss under combined conditions is less than the sum of the individual loss values, but as the relative phase of the components is altered the combined loss becomes greater than the sum of the individual losses. This would be expected since, if the core is operating below the saturation region, an increase in magnetizing force will also cause a large increase in flux density with a corresponding increase in loss.

The corresponding results from single and combined tests are given below.

I_{50}	0.6	0.6	0.6	0.6	0.3	0.3
I_{100}	0.6	0.45	0.3	0.15	0.3	0.15
Single frequency tests. W_{50}	0.872	0.872	0.872	0.872	0.169	0.169
W_{100}	1.92	1.04	0.275	0.0113	0.275	0.0113
$W_{50} + W_{100}$	2.792	1.912	1.147	0.883	0.444	0.180
Combined conditions W_{Tmax}	2.0	1.86	1.24	1.15	0.70	0.40
W_{Tmin}	1.7	1.42	0.90	0.87	0.42	0.12

Core Impedance.

The large power changes which are associated with the variation of relative phase angle imply that under sine current conditions the core impedance is varying. Due to the two-frequency excitation, the impedance terms will be considered with reference to each supply circuit, i.e. Z_{50} , Z_{100}. These terms are obtained from the voltage and current values measured on the a.c. potentiometer. For the case when I_{50} = 0.6A, I_{100} = 0.6A, the variation of the impedance Z_{50} is shown in Fig. 30. While the change in this term is not very large, its phase varies 20°, giving larger variations in the R and X components. The effect of a phase angle change causes a 35% change in the reactance term and an 88% change in the resistance term. These values being obtained with respect to the minimum values of R_{50} and X_{50}. The corresponding changes in the 100-c/s terms are shown in Fig. 31. They are not so large as the variations in the lower frequency terms, as would be expected.

From these results it is seen that a change of relative phase angle can also be used to alter the core impedance, which is presented to either supply, i.e. a variable impedance is obtained, whose value is dependent on the relative angle between the two magnetizing forces.

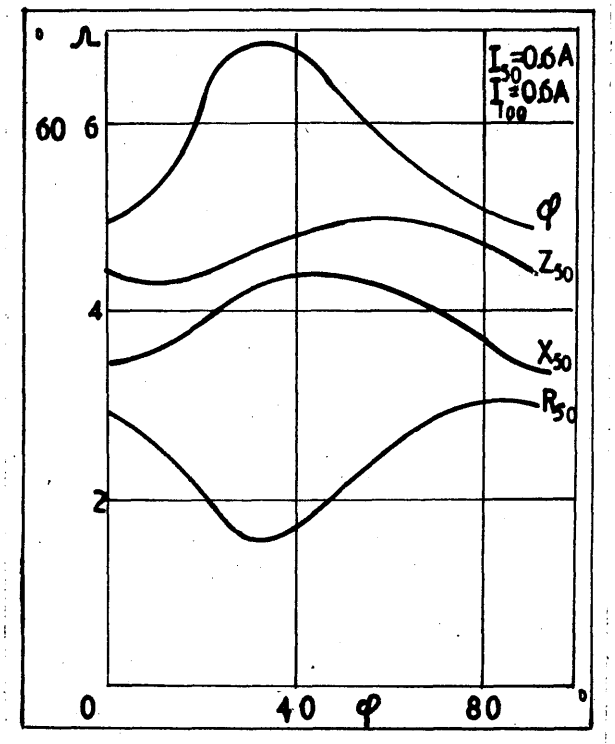

Fig. 30.
Variation of Z_{50} and its components.

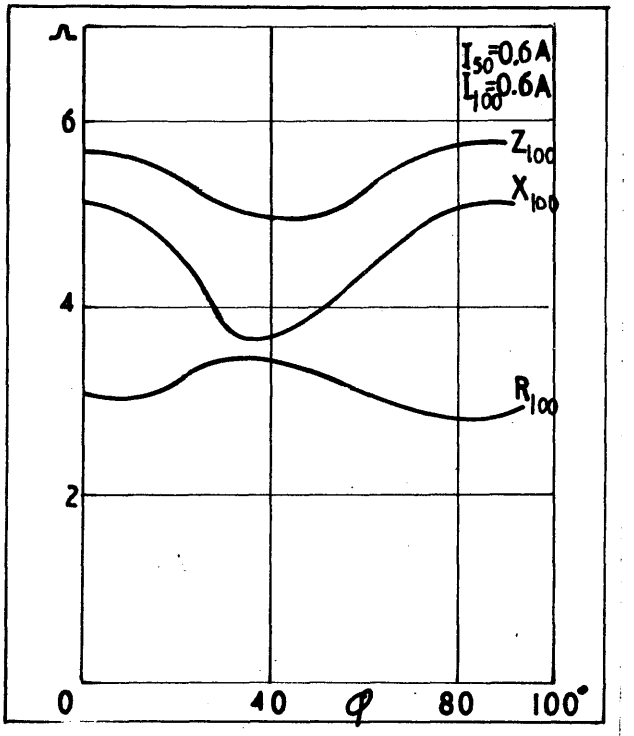

Fig. 31.
Variation of Z_{100} and its components.

Variation of impedance terms I_{50} = 0.6A I_{100} = 0.6A

φ	0	10	20	30	40
E_{50} (100^T)	2.7	2.6	2.64	2.81	2.92
Z_{50}	4.5	4.34	4.4	4.68	4.86
R_{50}	2.92	2.6	2.02	1.67	1.78
X_{50}	3.42	3.48	3.90	4.36	4.52
φ_{50}	49°30'	53°20'	62°36'	69°12'	68°30'
E_{100} (100^T)	3.2	3.75	3.07	2.82	2.27
Z_{100}	5.70	5.8	5.5	5.05	4.95
R_{100}	3.03	3.0	3.3	3.49	3.40
X_{100}	4.82	4.97	4.41	3.64	3.59

φ	50	60	70	80	90
E_{50} (100^T)	3.0	3.0	2.95	2.87	2.68
Z_{50}	5.0	5.0	4.92	4.88	4.46
R_{50}	2.12	2.56	2.85	3.12	2.96
X_{50}	4.50	4.31	3.98	3.75	3.32
φ_{50}	64°54'	59°12'	54°30'	50°	48°12'
E_{100} (100^T)	2.82	3.0	3.13	3.25	3.3
Z_{100}	5.05	5.35	5.6	5.8	5.88
R_{100}	3.14	3.17	2.88	2.74	2.84
X_{100}	3.94	4.32	4.80	5.11	5.16

Flux distortion with change of phase angle.

The flux distortion which occurs when a core is subjected to sine current conditions may be expressed in a variety of forms, but it is important that whichever method is chosen should be most sensitive to deviations from the sinusoidal condition. The usual measurement of distortion in circuits is expressed by the form factor but, as is well known, this term is very insensitive to harmonic content. In fact, a 50% second harmonic term only causes an 11% change in the form factor from the sinusoidal value. Additionally, of course, the effect of the phase of the second harmonic term can alter the form factor value, since it is obtained from the mean value of the wave.

Another possible measure of distortion can be expressed as $\frac{\text{Total harmonic content of voltage}}{\text{mean rectified voltage}}$. This is a very useful ratio when harmonic power conditions are being investigated, since it gives the ratio of the error in the core loss (as measured on a.c. potentiometer) to the true loss. In practice, these quantities cannot be measured easily or accurately, due to the difficulty of measuring the mean value and since the harmonic voltage is normally small, additional amplifiers are required.

The standard definition for Distortion Factor is

$$\frac{\text{R.m.s. total harmonic content}}{\text{Total r.m.s. of the wave.}}$$

Since it is relatively easy to obtain these quantities accurately, this ratio is considered suitable to express the distortion occurring under combined magnetization as the phase is altered.

The induced voltage wave across T turns on one core is given by

$$e = e_1 \sin\theta + e_2 \sin(2\theta + \alpha_2) + \ldots\ldots + e_n \sin(n\theta + \alpha_n)$$

then the distortion factor is given by

$$D\% = \frac{\sqrt{\sum_{n=2}^{n=\infty} e_n^2}}{\sqrt{\sum_{n=1}^{n=\infty} e_n^2}} \times 100$$

The total r.m.s. value of the induced voltage wave was obtained throughout by the use of a vacuo junction and unipivot meter (see Appendix (c)).

The r.m.s. value of the fundamental voltage component E_1 was obtained from the a.c. potentiometer results and hence the numerator of the above expression is given by

$$E_{r.m.s.}^2 - E_1^2$$

A typical set of results are shown below.

I_{50} = 0.6A

I_{100} = 0.6A

Values obtained from test A. (Pages 86 and 87)

φ	0	10	20	30	40	50	60	70	80	90
$E_{r.m.s.}$	5.75	5.5	5.17	5.0	5.0	5.1	5.25	5.44	5.5	5.5
E_{50}	2.7	2.6	2.64	2.81	2.92	3.0	3.0	2.96	2.87	2.26
E_H	5.04	4.85	4.43	4.14	4.06	4.13	4.3	4.57	4.70	5.02
D%	87.6	88.2	85.6	82.6	81.1	81.1	82	84.2	85.5	91.4

The voltage values are obtained w.r.t. a 100 turn winding. The minimum distortion occurs in the region where the total loss is a minimum, i.e. $\varphi = 40^{\circ}$. This corresponds to the minimum value of total core flux density (see Figs. 32 and 33). The change in distortion factor as the phase angle is varied, is comperatively small.

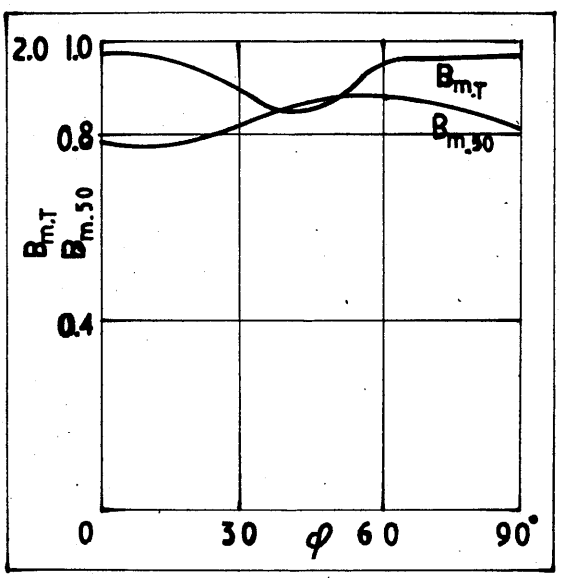

Fig. 32.
Variation of flux density components.

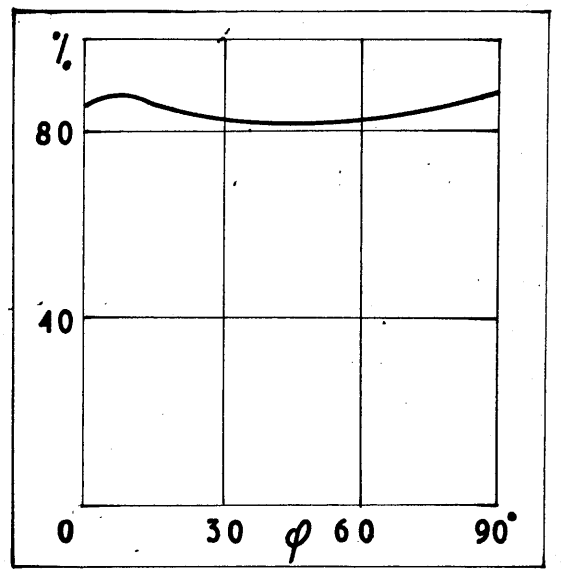

Fig. 33.
Variation of distortion factor

Test B.

A corresponding series of results were obtained for combined magnetization at 50 and 150 c/s. A specimen set of results from one of these tests is shown overleaf. The variation in the individual loss components for the above case is shown in Fig. 34. The results from the complete series of tests are summarized in Figs. 35 - 37.

Test B.

I_{50} = 0.6A

I_{100} = 0.6A

$h = 154 \sin(\omega t + \phi) + 154 \sin 3\omega t$

ϕ	0	10	20	30	40	50	60
$I_{50} + a_1$	-0.271	-0.385	-0.44	-0.498	-0.545	-0.575	-0.595
$+ jb_1$	0.519	0.46	0.40	0.32	0.224	0.134	0.025
$E_{50} + a_2$	0.677	0.669	0.651	0.611	0.56	0.491	0.359
$+ jb_2$	0.081	0.134	0.179	0.22	0.264	0.308	0.367
Voltage Factor	20	20	20	20	20	20	20
$I_{150} + c_1$	0.606	0.606	0.606	0.606	0.606	0.606	0.606
$+ jd_1$	0.067	0.067	0.067	0.067	0.067	0.067	0.067
$E_{150} + c_2$	0.556	0.508	0.491	0.481	0.395	0.406	0.388
$+ jd_2$	0.645	0.688	0.766	0.813	0.905	0.934	0.933
Voltage Factor	20	20	20	20	20	20	20
$a_1a_2 + b_1b_2$	0.142	0.197	0.214	0.234	0.246	0.242	0.205
W_{50}/core	0.71	0.985	1.07	1.17	1.23	1.21	1.03
$c_1c_2 + d_1d_2$	0.379	0.354	0.348	0.345	0.299	0.309	0.298
W_{150}/core	1.89	1.77	1.74	1.72	1.49	1.54	1.49
$W_{50} + W_{150}$	2.6	2.75	2.81	2.89	2.72	2.75	2.52
B_{m50}	0.995	1.00	0.989	0.95	0.91	0.846	0.75
B_{m100}	0.415	0.415	0.443	0.457	0.49	0.494	0.491
B_{mT}	0.93	0.956	0.98	0.99	1.0	0.996	0.98
V_{400T} r.m.s.	24.3	25.4	25.4	25.4	25	24.7	23.3
Eddy loss/core	0.71	0.787	0.787	0.787	0.755	0.739	0.653
W_T (hyst)	1.89	1.963	2.024	2.103	1.965	2.011	1.867

$h = 154 \sin(\omega t + \phi) + 154 \sin 3\omega t$

ϕ	70	80	90	100	110	120
$I_{50} + a_1$	-0.588	-0.54	-0.52	-0.46	-0.384	-0.29
$+ jb_1$	-0.104	-0.205	-0.3	-0.384	-0.46	-0.50
$E_{50} + a_2$	0.146	-0.041	-0.193	-0.292	-0.363	-0.41
$+ jb_2$	0.476	0.547	0.58	0.577	0.557	0.53
Voltage Factor	20	20	20	20	20	20
$I_{150} + c_1$	0.606	0.606	0.606	0.606	0.606	0.606
$+ jd_1$	0.067	0.067	0.067	0.067	0.067	0.067
$E_{150} + c_2$	0.431	0.46	0.535	0.623	0.60	0.55
$+ jd_2$	0.765	0.541	0.48	0.545	0.58	0.632
Voltage Factor	20	20	20	20	20	20
$a_1a_2 + b_1b_2$	0.1355	0.0904	0.074	0.070	0.118	0.145
W_{50}/core	0.675	0.451	0.37	0.35	0.59	0.725
$c_1c_2 + d_1d_2$	0.312	0.315	0.356	0.414	0.403	0.376
W_{150}/core	1.56	1.57	1.78	2.07	2.02	1.88
$W_{50} + W_{150}$	2.235	2.02	2.15	2.42	2.61	2.60
B_{m50}	0.726	0.80	0.895	0.946	0.974	0.978
B_{m150}	0.426	0.346	0.349	0.40	0.405	0.406
B_{mT}	0.95	0.92	0.9	0.86	0.88	0.93
V_{400T} r.m.s.	20.7	20.5	21.3	22.7	23.3	24
Eddy Loss/core	0.517	0.510	0.548	0.624	0.660	0.702
W_T (hyst)	1.718	1.51	1.602	1.796	1.95	1.898

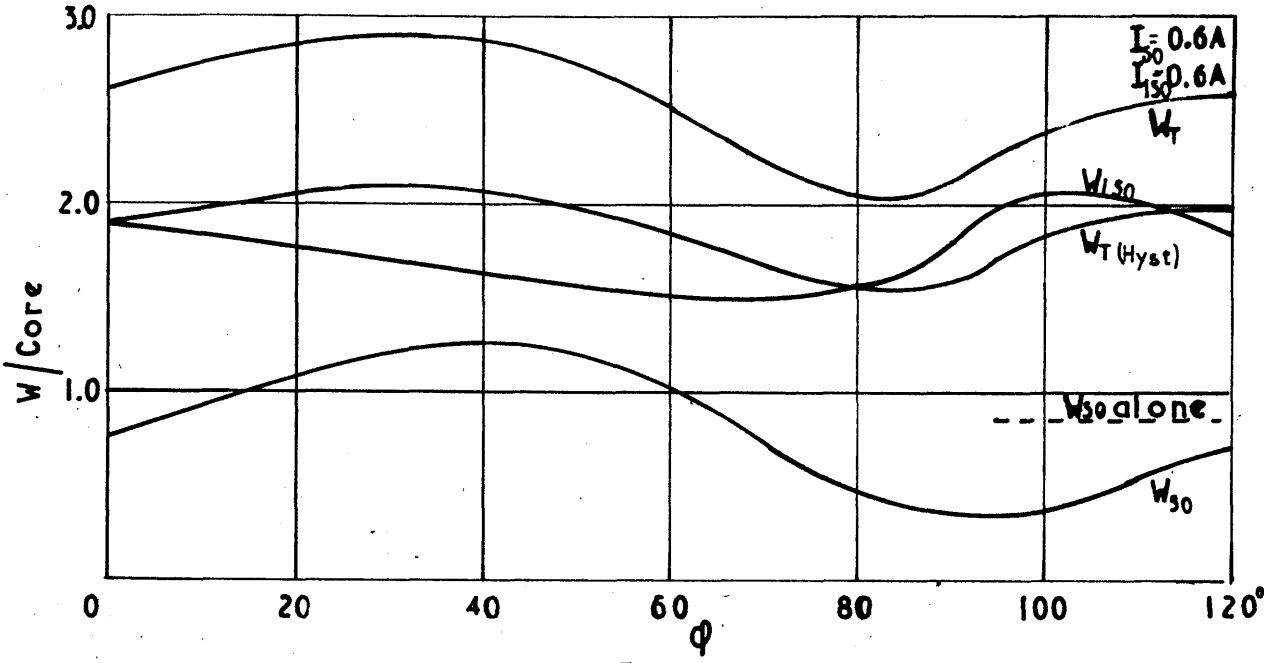

Fig. 34.
Variation of core loss components

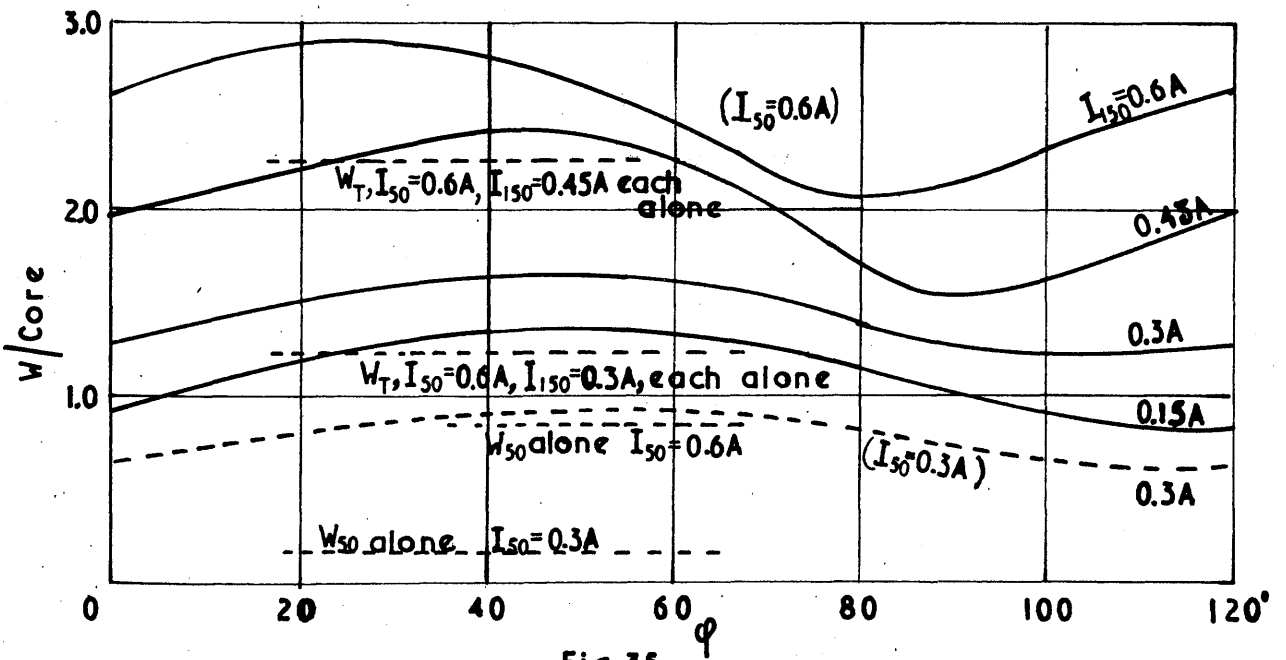

Fig. 35.
Variation of total loss

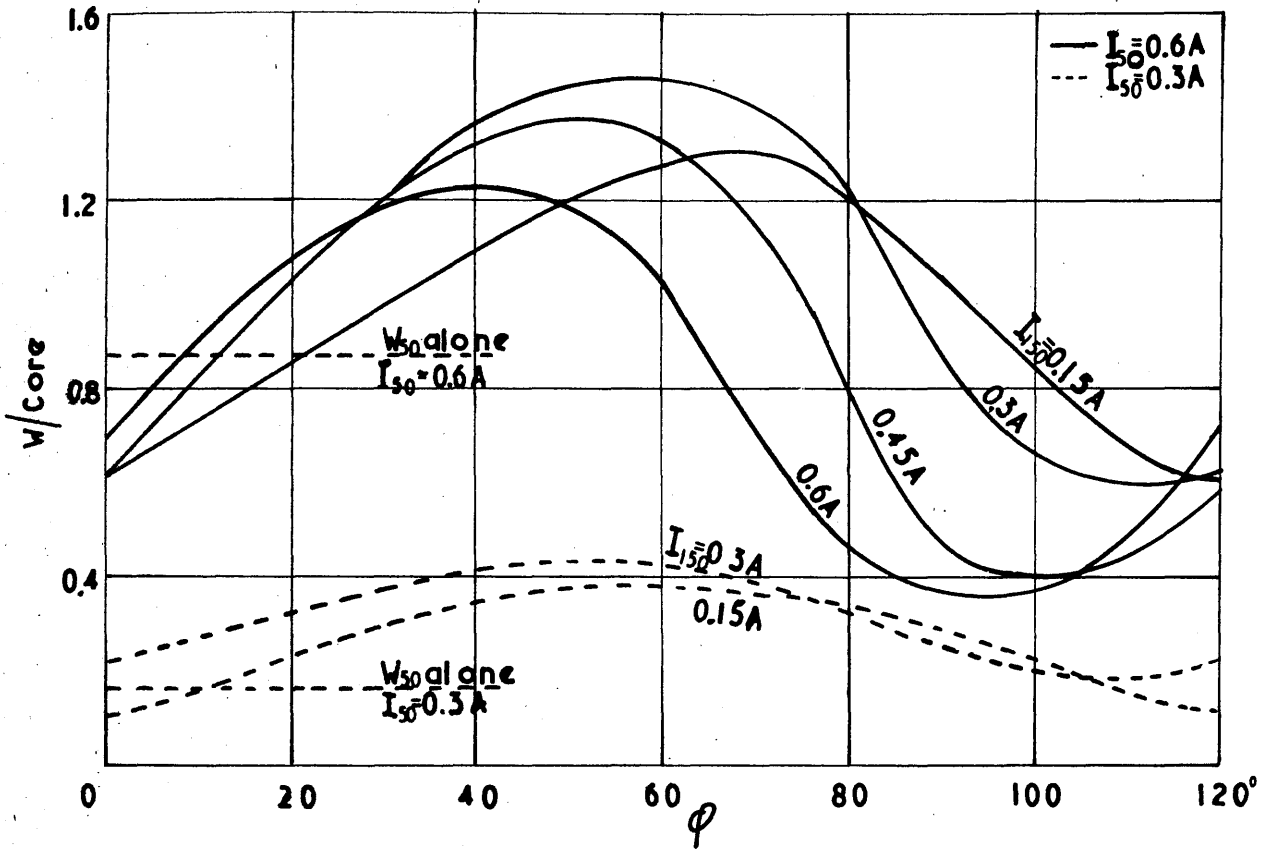

Fig. 36
Variation of W_{50}

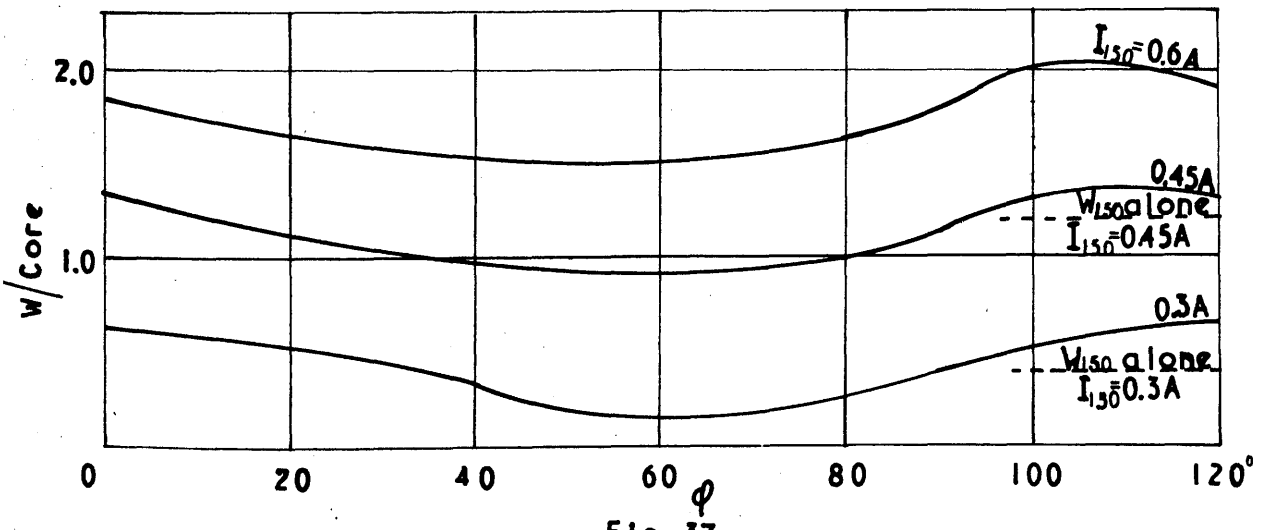

Fig. 37.
Variation of W_{150}

When the cores are subjected to sine current combined magnetization at 50 and 150 c/s, similar results are obtained due to the variation of the relative phase angle. For the same magnetizing force values larger variations are noted in the values of total loss and its two components. (Figs. 35 - 37). As previously, the minimum value of the 50-c/s loss component occurs for the largest value of H_{150}. The maximum value is obtained with a smaller value of 150-c/s magnetizing than in the previous case. This is attributed to a variation in the core impedance to the third harmonic of the 50-c/s flux wave, due to interaction in the core with the fundamental component of the 150-c/s component.

The total core loss is greater for all values of φ than the loss obtained under single low-frequency magnetization. The low-frequency loss component reaches its maximum value in the region $\varphi = 60^{\circ}$, which corresponds to the maximum value of the total magnetizing force. The minimum value of low frequency loss obtained when the core is operating in the saturated region is considerably less than the single frequency value. When the core is not operating in the saturated region, the conditions for a reduction in loss are as given in Part I.

It is seen that the core conditions with phase angle change are practically identical for the two cases considered, i.e. 50 c/s, 100 c/s and 50 c/s, 150 c/s. Similar changes in core impedance occur as shown in Fig. 38.

It is usually stated that the effects of the eddy-current component of core loss upon the hysteresis loop is to cause it to increase

in area, retaining its same general shape. The resulting loop obtained being a measure of the total core loss. No methods are available to obtain directly the hysteresis loop only, when the core is cyclically magnetized at power frequencies unless a core material is used which has a negligibly small eddy loss (i.e. powder cores, Ferrite, Gecallo r etc.). From core data the eddy-current loss may be approximately obtained by the expression in appendix (d). If this quantity is subtracted from the total core loss, the resulting core hysteresis loss is obtained. When this is plotted to a base of phase angle (see Fig. 34) it is seen that the true hysteresis loss varies in the same manner as the total loss but with different numerical quantities. The loop expressions developed in Part I (on the assumption of no eddy current effects) will, therefore, give an indication of total core loss conditions. The numerical values obtained will obviously be low but maximum and minimum values will be indicated at the phase angle values obtained when eddy currents are present. If the core constants used in Part I are obtained from an actual total loss test on the cores, then the expressions will give results which approximate to the total core loss.

The variation in the impedance terms presented to the supply currents are shown in Figs. 38 and 39. The variations in the components are very large (similar to the 50 and 100-c/s case, see Figs. 30 and 31). When the core is dissipating maximum total power, it is presenting maximum R_{50} component ($\varphi = 40^{o}$). The maximum value of Z_{50} occurs at the same phase angle as W_{50} minimum and the maximum X_{50} occurs at the same angle as the maximum value of the total power loss in the core. Similarly for

the 150-c/s components, maximum Z_{150} and X_{150} occur between maximum W_{50} ($\varphi = 60^{\circ}$) and maximum W_T ($\varphi = 40^{\circ}$). Conditions for the 150-c/s case are practically the exact opposite to the 50-c/s case, minimum X_{150} being obtained at the same phase angle as X_{50} maximum, etc. The 150-c/s components of X and Z change very rapidly for a small phase angle change in the range φ = 60 →80°. Over the 20° the core impedance varies from maximum to minimum and this gives a circuit which is extremely sensitive to phase angle changes. It could be utilized in the form of a controlled variable impedance.

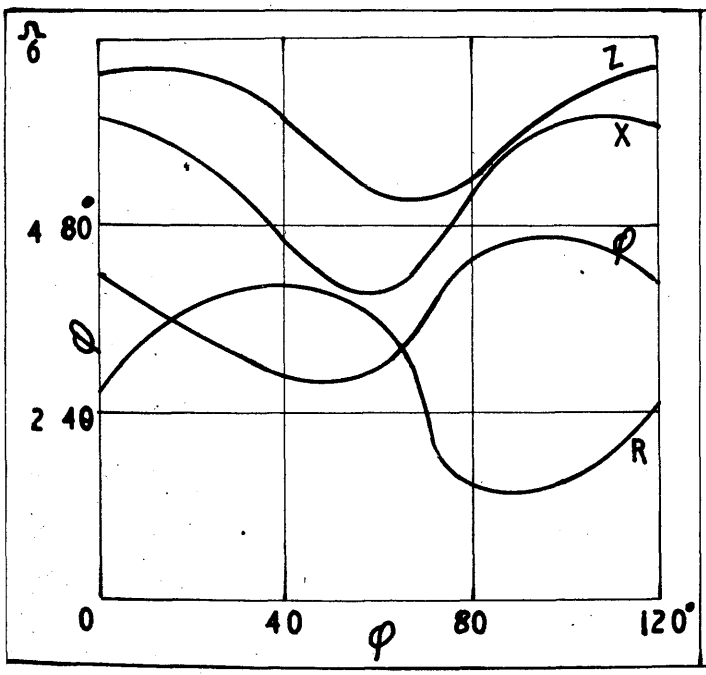

Fig. 38.
Variation of Z_{50} and its components.

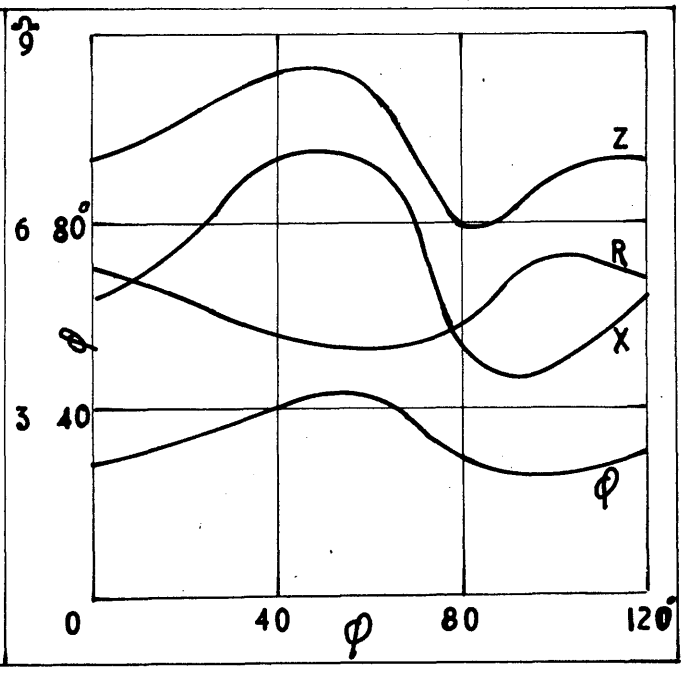

Fig. 39
Variation of Z_{150} and its components.

Throughout all the tests, the cores are magnetized under sine current conditions, giving rise to a distorted flux wave. Since the core loss is dependent primarily on the values of the fundamental frequency terms of B and H, the same core loss will be obtained if the cores are subjected to sine flux conditions, the value of the flux component being the same as the fundamental frequency term in the distorted flux wave. The effects due to eddy currents will not cause much variation in the loss term, as the difference between the r.m.s. value of voltage induced in a core winding under sine flux conditions to that under sine current, for the same fundamental flux component is

$$E_1 - \sqrt{E_1^2 + \sum_2^\infty E_n^2}$$

If it is assumed that the eddy current loss is constant for given fundamental flux density components then, under sine current conditions, the same core loss will be obtained if the fundamental flux components are identical. It is also assumed that there is no difference in the time effect of the core magnetization, when conditions are altered from sine current to sine flux.

From the previous test for various values of phase angle and $k \left(= \frac{H_{100}}{H_{50}} \right)$ the factor $k' = \frac{B_{100}}{B_{50}}$ is obtained from the a.c. potentiometer readings. These results are given on Page 104 and shown in Fig. 40. It is seen that, when the lower-frequency magnetizing force is large ($I_{50} = 0.6A$) the same loss would be obtained with a lower value of k' than k, i.e. when

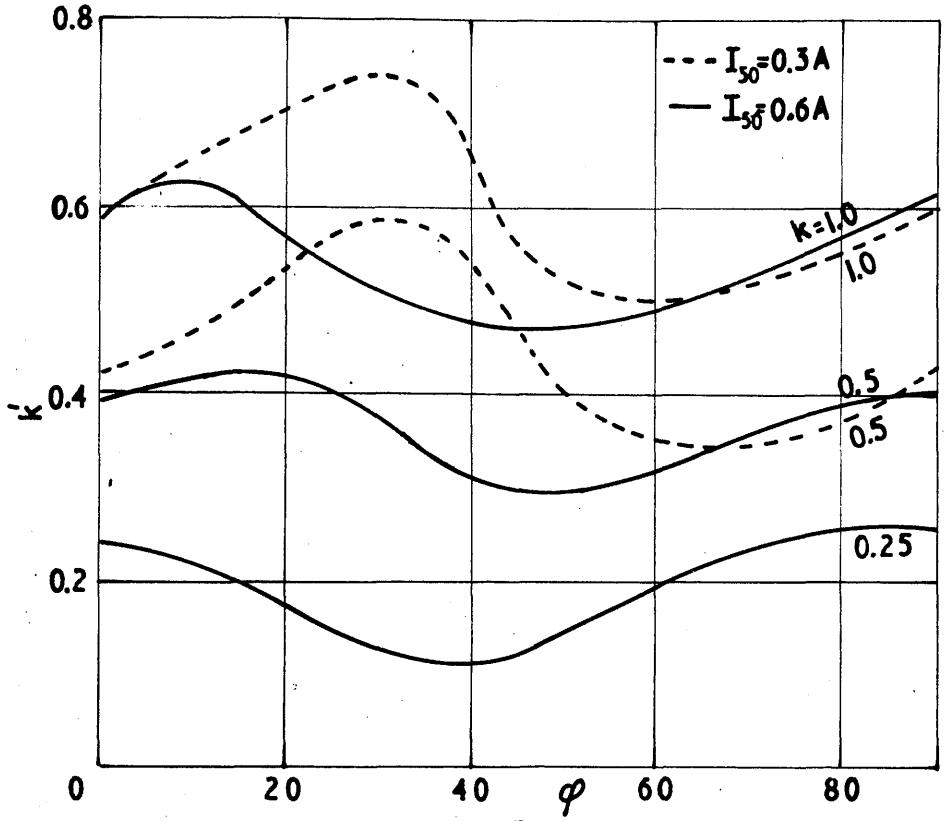

Fig. 40.
Variation of k' for various values of k_{50}
(50,100 c/s)

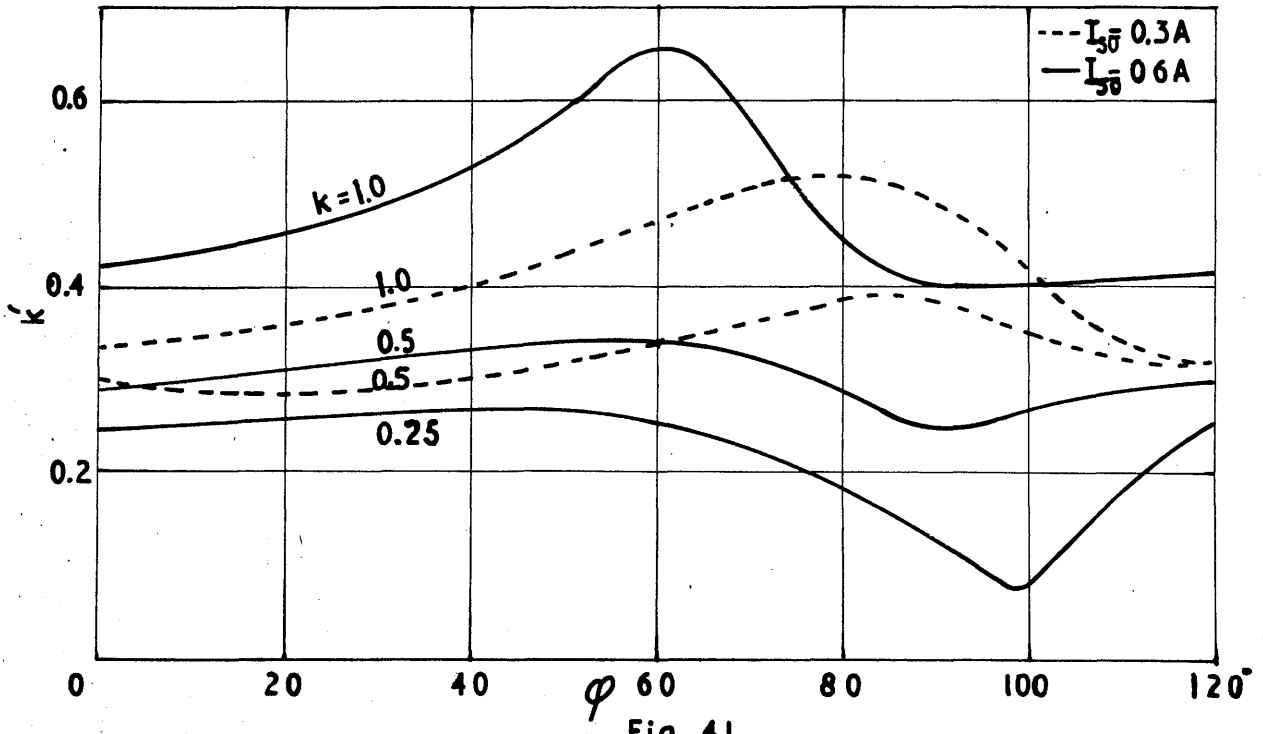

Fig. 41.
Variation of k' for various values of k_{50}
(50,150 c/s)

the core is operating in the saturated region, the flux density ratio $\frac{B_{100}}{B_{50}}$ is smaller than the corresponding magnetizing force ratio $\frac{H_{100}}{H_{50}}$ for the same core loss at the same phase angle. The reduction in the ratio is even larger in the 150-c/s case, as shown in Fig. 41. Consequently under sine flux combined magnetization, relatively small percentage modulations will cause appreciable changes in core loss. When the core is operating below the saturation region, the range of "k'" values are much closer to the corresponding "k" values for the 50 and 100-c/s case. Since most iron-cored circuits are designed to operate in the "knee" region of the magnetization characteristic, it can be seen that even small harmonic voltage components in the applied voltage wave, can cause appreciable changes in the core loss.

Variation of k' for fundamental componerrts of flux density wave for given values of k, where $B_{100} = k' B_{50}$ and $H_{100} = k H_{50}$

I_{50} = 0.6A	k'				
			φ		
k	0	10	20	30	40
1.0	0.590	0.631	0.575	0.502	0.475
0.75	0.495	0.556	0.542	0.479	0.421
0.5	0.393	0.411	0.42	0.357	0.302
0.25	0.24	0.211	0.171	0.136	0.110
I_{50} = 0.3A					
1.0	0.590	0.647	0.700	0.751	0.643
0.5	0.422	0.471	0.535	0.596	0.55

$B_{150} = k' B_{50}$

$H_{150} = k H_{50}$

I_{50} = 0.6A	k'						
k	φ 0	10	20	30	40	50	60
1.0	0.417	0.415	0.450	0.482	0.537	0.583	0.657
0.75	0.371	0.362	0.340	0.356	0.403	0.436	0.453
0.5	0.292	0.305	0.321	0.316	0.332	0.345	0.349
0.25	0.251	0.257	0.257	0.274	0.260	0.266	0.248
I_{50} = 0.3A							
1.0	0.356	0.358	0.368	0.391	0.402	0.422	0.468
0.5	0.311	0.315	0.279	0.297	0.324	0.316	0.338

I_{50} = 0.6A	k'				
k	φ 50	60	70	80	90
1.0	0.471	0.502	0.532	0.562	0.615
0.75	0.413	0.418	0.450	0.488	0.538
0.5	0.289	0.315	0.354	0.385	0.406
0.25	0.180	0.192	0.233	0.232	0.255
I_{50} = 0.3A					
1.0	0.520	0.504	0.520	0.546	0.618
0.5	0.391	0.362	0.366	0.377	0.423

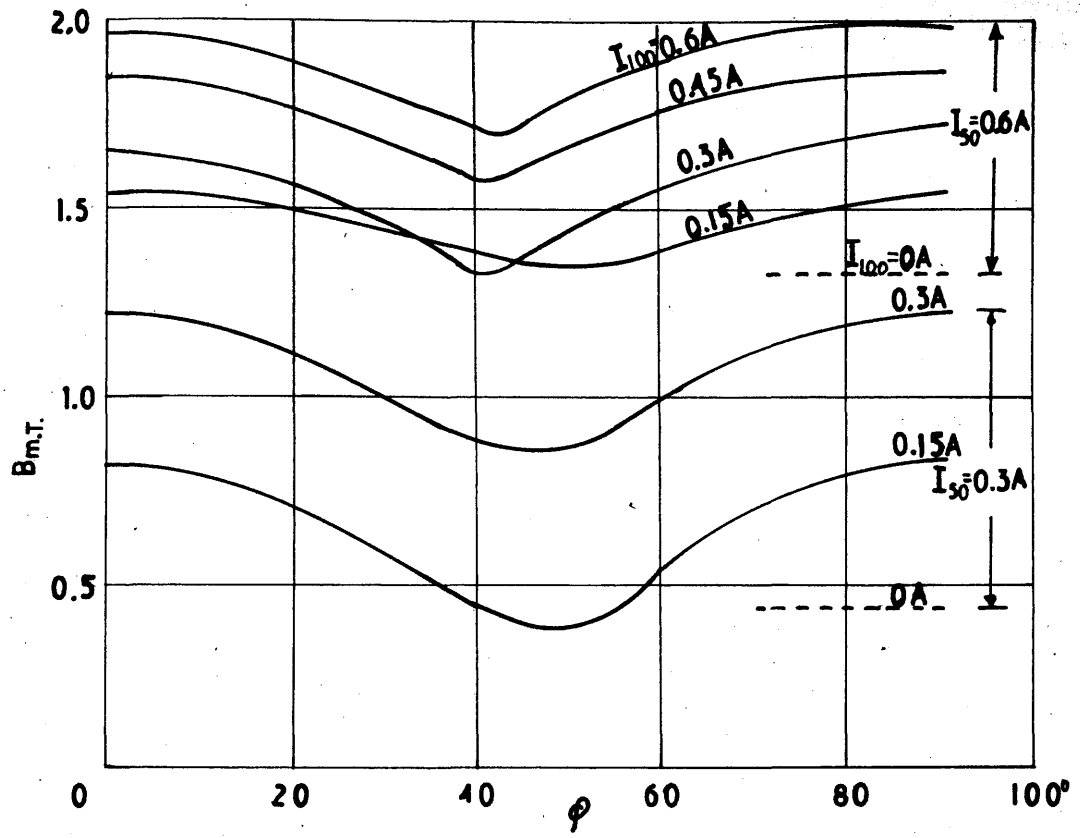

Fig. 42.
Variation of peak-peak flux density

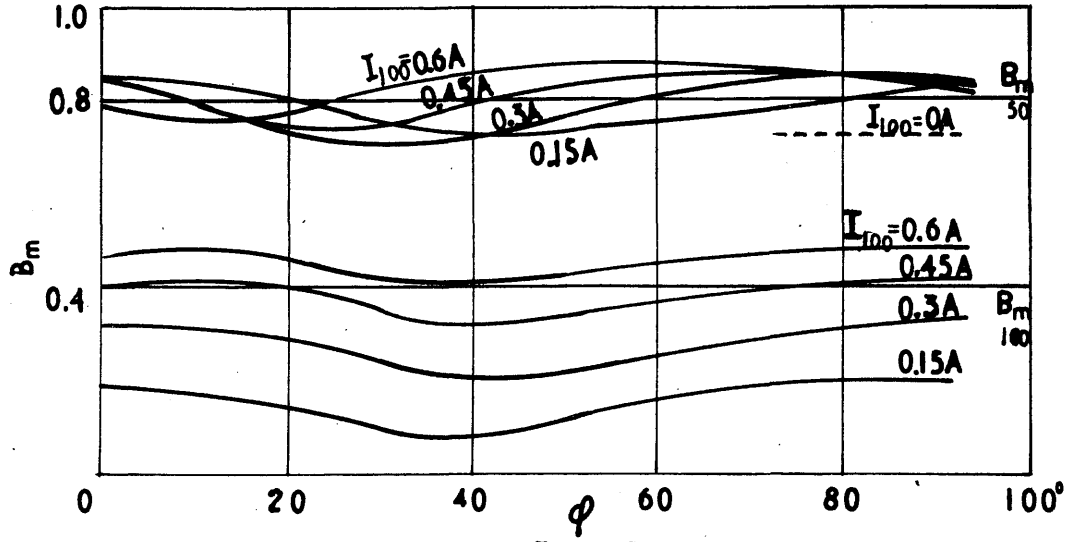

Fig. 43.
Variation of flux density

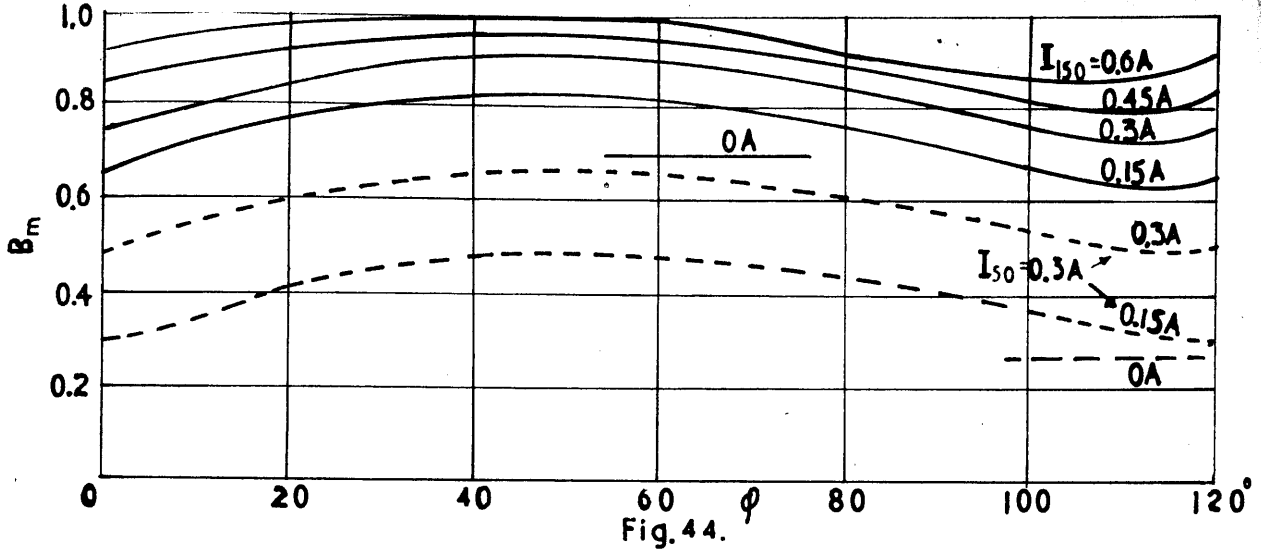

Fig. 44.
Variation of total flux density

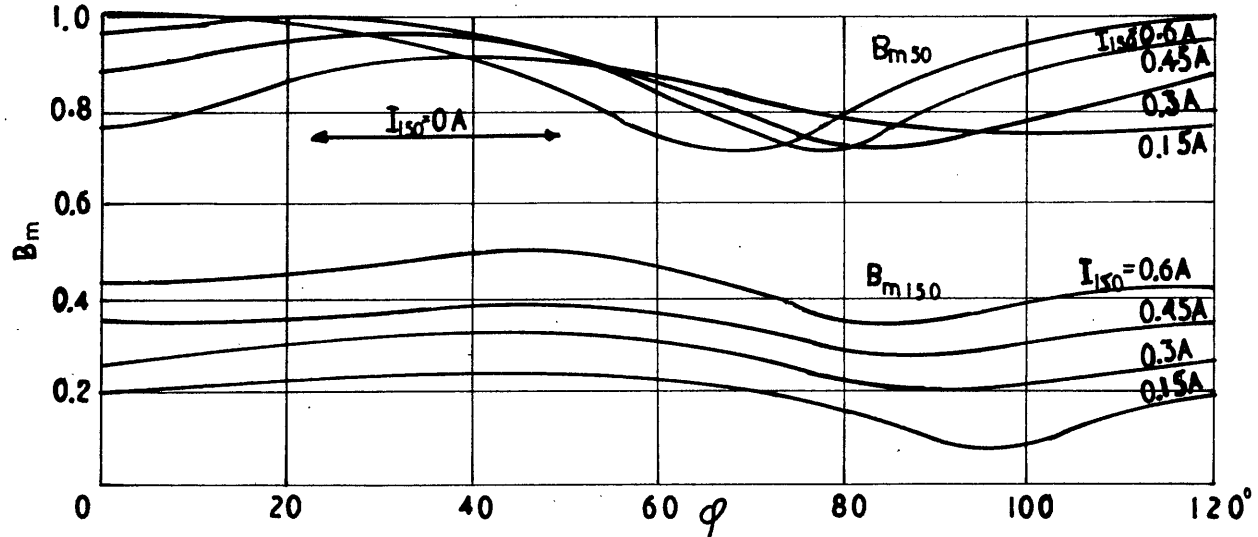

Fig. 45.
Variation of flux density components

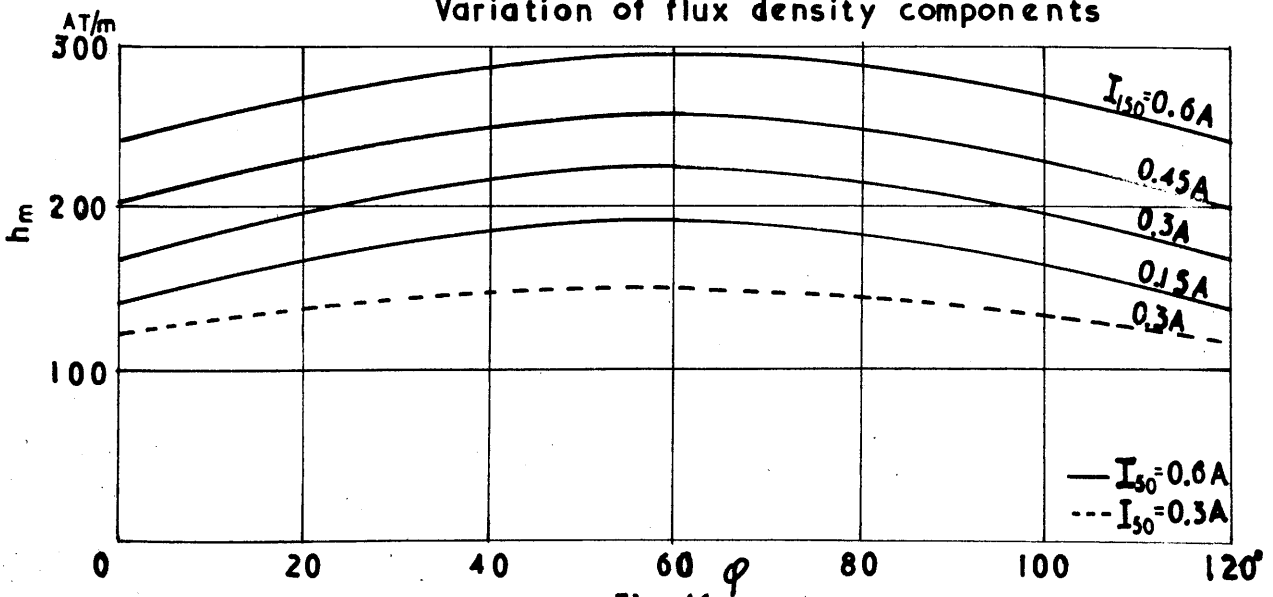

Fig. 46.
Variation of peak magnetizing force

I_{50} = 0.6A	k'					
k	70	80	φ 90	100	110	120
1.0	0.587	0.432	0.390	0.423	0.416	0.415
0.75	0.456	0.382	0.327	0.350	0.352	0.356
0.5	0.341	0.275	0.248	0.264	0.289	0.304
0.25	0.244	0.189	-	0.081	0.194	0.255
I_{50} = 0.3A						
1.0	0.508	0.519	0.493	0.405	0.347	0.322
0.5	0.348	0.391	0.391	0.354	0.320	

The variation of the flux density components at 50, 100 c/s and 50, 150 c/s are shown in Figs. 43 and 45.

The corresponding peak values of total core flux density for the latter case are shown in Fig. 44. Due to the unsymmetrical loop obtained under combined magnetization at 50 and 100 c/s, the peak to peak values of flux density are plotted in Fig. 42. The positive and negative peak values were individually obtained during the tests on the cores and are tabulated for each core condition in the tables of results. The corresponding values for single frequency excitation are also shown on these graphs.

It is noted that the total flux density at 50 and 150 c/s reaches its maximum value in the region $\varphi = 40 \rightarrow 60^{\circ}$. For the largest value of I_{150} the angle is 40°. Since the maximum value of the magnetizing force (see Fig. 46) occurs when $\varphi = 60^{\circ}$ the angle of lag between the peak values of B and H is clearly demonstrated. This is similarly shown

by the shift in the position of the minimum value of total flux density from $\varphi = 0^\circ = 120^\circ$ to $\varphi = 100^\circ$ as the superimposed component is increased. For the 100-c/s case the minimum value of magnetizing force occurs at $\varphi = 45^\circ$ and it is seen that the minimum value of peak-to-peak flux density occurs at a slightly smaller angle.

The minimum value of B_{m50} over the range of I_{150} is equal to the corresponding flux density value obtained under single frequency conditions. The higher the value of I_{150} the smaller is the value of φ for minimum 50-c/s flux density; this is also the condition for minimum 50-c/s core loss.

For both 150 and 100-c/s conditions the maximum 50-c/s flux density component is obtained with the largest value of superimposed magnetizing force.

In both tests the graphs for the higher frequency flux density terms follow the same pattern as the total flux density. The effect of any increase in the higher frequency magnetizing force merely altering the magnitude of the components, their graphs keeping the same general shape. This is especially true for the case at 100 c/s.

CHAPTER 5

PHOTOGRAPHIC RECORDS OF CORE CONDITIONS.

To illustrate the change in magnetizing force, flux density and core loss loop shape when the phase angle is altered, a series of oscillographic records* was obtained for the typical case of core magnetizing force $h = 154.4 \sin(\omega t + \varphi) + 154.4 \sin 3\omega t$. ($I_{50} = 0.6A$, $I_{150} = 0.6A$).

This gives rise to minor loops for all values of φ since the magnetizing force wave is always re-entrant. It can be seen that the shape of the minor loop formed depends on its position w.r.t. the major loop. In the saturated region (e.g. $\varphi = 0, \rightarrow 30^{\circ}$) the minor loop has naturally a very small change of flux density with change of magnetizing force, but this does not imply that the 150-c/s core loss will be a minimum (see Fig. 37). Over this region, the flux density waveform is almost flat-topped and practically constant due to the small flux-density change.

When the phase angle is increased further, the minor loops enlarge since they are now formed on the unsaturated portion of the major loop. The flux density waveform becomes peaky (over the region $\varphi = 40^{\circ} \rightarrow 80^{\circ}$) and it is noted that when $\varphi = 70^{\circ} \rightarrow 80^{\circ}$ the flux density and magnetizing force waveforms are practically identical, indicating that the flux-density wave under these conditions is predominantly 50 and 150-c/s

---

* For circuit details see Appendix (c).

components. This suggests that the core is operating in a region of minimum flux distortion. A further increase of phase angle carries the minor loop up the steep portion of the major loop, where the flux density change is quite considerable ($\varphi = 80^{\circ} \rightarrow 110^{\circ}$). The flux density waveform is similar to that obtained when ($\varphi = 0 \rightarrow 40^{\circ}$) and is almost flat-topped.

The total enclosed area of each complete loop is proportional to the core-loss obtained for that value of φ. To enable the loop area to be converted directly to core loss in watts, a trace of the single frequency (50 c/s) loop was obtained for h = 154.4 sin 314t. The loop area scale is 0.157 W/cm^2.

The core loss values obtained by wattmeter measurements are compared with those from a measurement of the loop areas over the range of phase angles from $0 \rightarrow 110^{\circ}$. The following results are obtained.

φ	0	10	20	30	40	50	
W_T from loop	2.12	2.12	2.25	2.3	2.68	2.26	W
W_T wattmeter	2.17	2.3	2.4	2.46	2.46	2.46	W

φ	60	70	80	90	100	110	
W_T from loop	2.3	2.2	1.84	2.19	2.38	2.1	W
W_T from wattmeter.	2.4	2.22	2.06	2.08	2.13	2.16	W

It must be remembered that the accuracy of the loop areas depends on a number of factors:-

1) Integrating circuit to give flux density values from voltage wave.

2) Amplifier used for vertical deflection.

3) Optical system in camera

4) Developing and printing of the film.

It is usual to assume an overall error of 5% due to these items. Hence from the above results it is seen that the loops truly represent core conditions under combined magnetization and do give an indication of the total core loss.

The oscillographic records show loop, flux density wave and magnetizing force wave for the range of phase angle values 0° - 110° at 10° intervals.

From the total loss loops it is seen that the minor loop area varies considerably over the range of phase angle values. It might be assumed that, when the minor loop area was a minimum, the 150-c/s component of core loss would also be a minimum. That this is not the case may be shown by considering the components which make up the total loop at the two extreme cases of peak magnetizing force,

$$h = h_1 \sin \omega t + h_3 \sin 3\omega t$$

and $$h = h_1 \sin (\omega t + 60^{\circ}) + h_3 \sin 3\omega t$$

for the case when $h_1 = h_3 = 154.4$ AT/m.

$h = 154.4 \sin (\omega t + \varphi) + 154.4 \sin 3\omega t$

$\varphi = 0°$

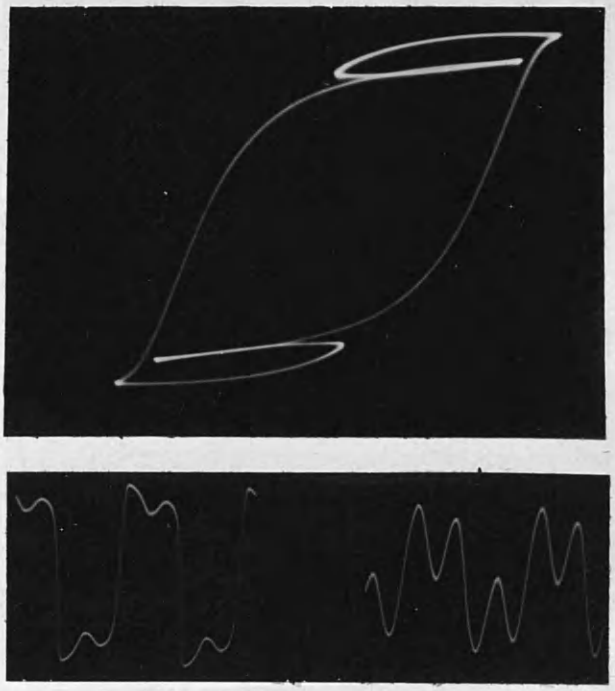

$\varphi = 10°$

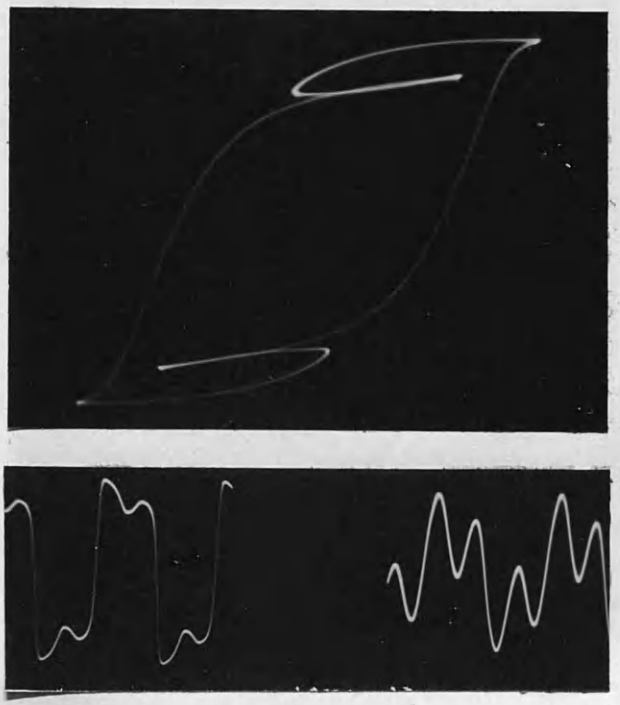

$\varphi = 20°$

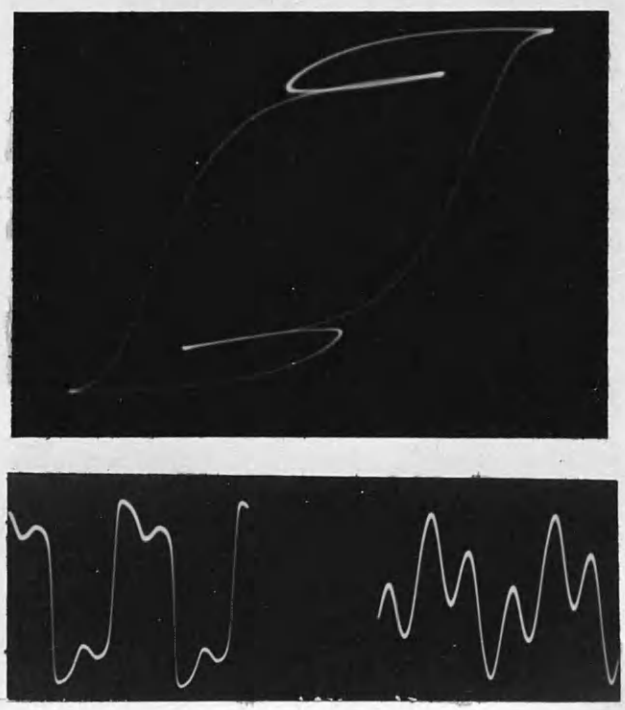

$\varphi = 30°$

$h = 154.4 \sin (\omega t + \varphi) + 154.4 \sin 3\omega t$

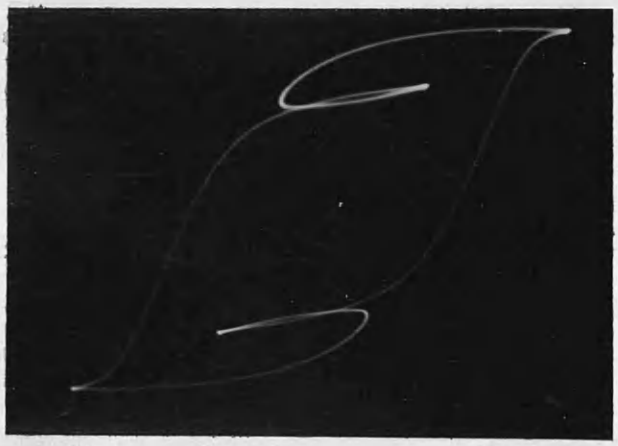

$\varphi = 40^\circ$

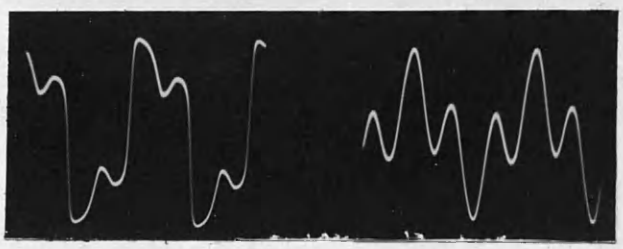

$\varphi = 50^\circ$

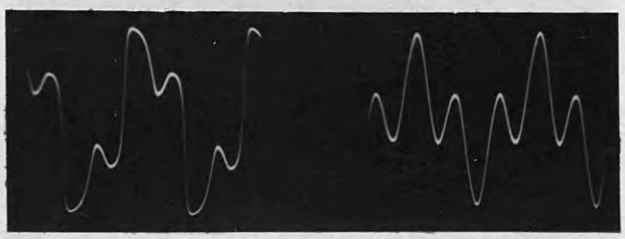

$\varphi = 60^\circ$

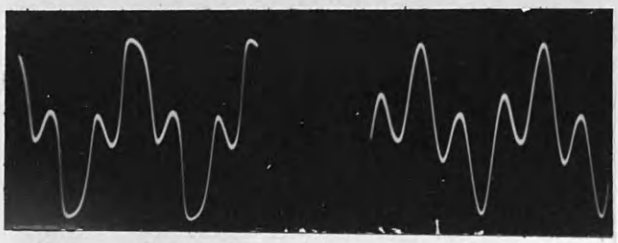

$\varphi = 70^\circ$

$h = 154.4 \sin (\omega t + \varphi) + 154.4 \sin 3\omega t$

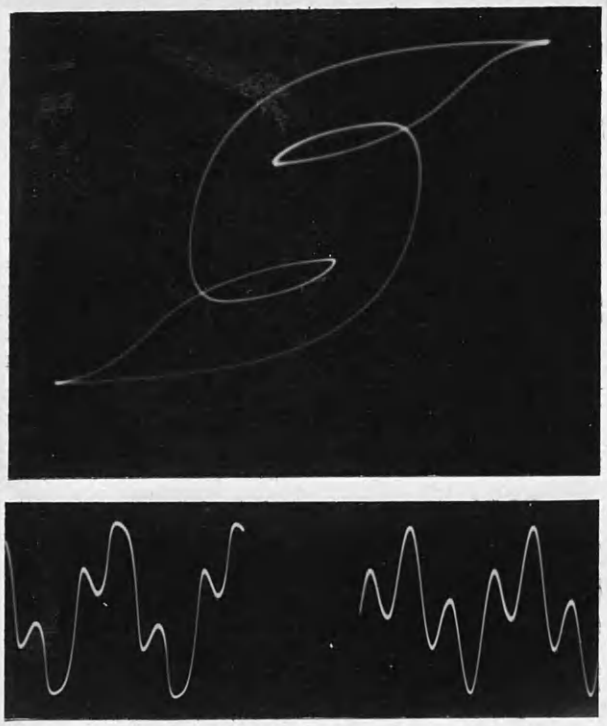

$\varphi = 80°$

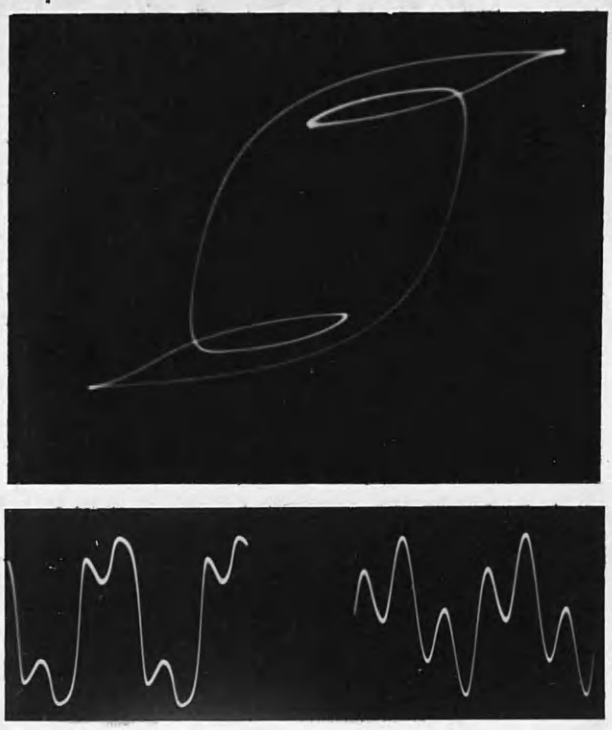

$\varphi = 90°$

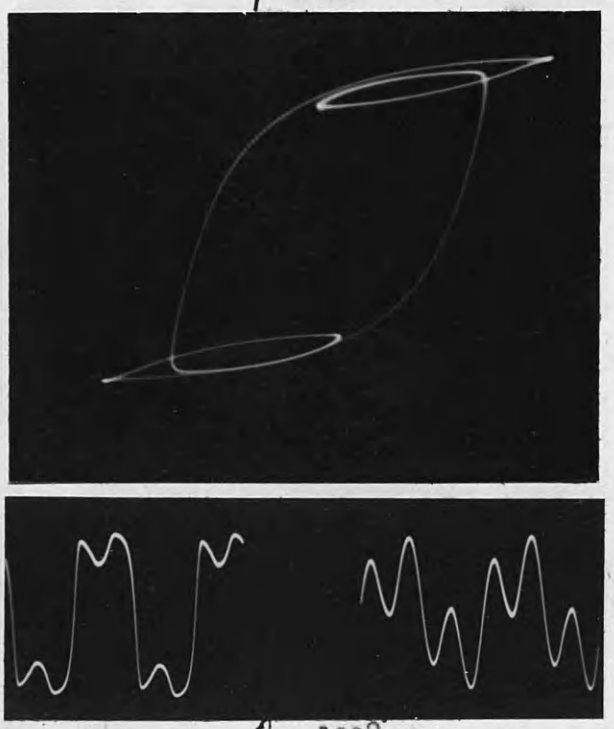

$\varphi = 100°$

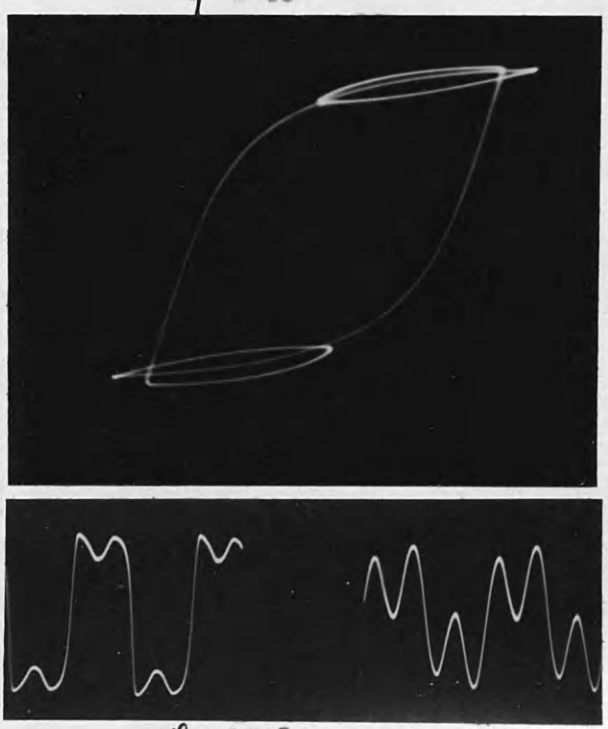

$\varphi = 110°$

For the simple case of a loop obtained when a magnetic core is subjected to a single-frequency sinusoidal magnetizing force, it has been shown by Thompson[5] that the hysteresis loop can always be analysed into a harmonic series of closed curves, corresponding to the various terms in the analysis of the flux-density wave. The series of closed curves takes the form of a harmonic series of Lissajous' figures whose enclosed areas are all zero except the fundamental sine-term. The effect of the fundamental cosine-term causes the fundamental ellipse to be non-orthogonally placed but to possess the same area as the orthogonally placed ellipse, due to the sine term only.

Under conditions of combined magnetization, the loop obtained from the 50-c/s component of the magnetizing force and the total core flux density will comprise a series of Lissajous' figures as above. All these figures have zero area except the fundamental sine terms, whose area is proportional to the 50-c/s core loss. Similarly, when the loop is obtained from the 150-c/s component of magnetizing force, the loop area is proportional to the 150-c/s core loss.

The sum of these two loop areas must equal the total loss loop since it is built up from these two components only.

Typical loop components are shown for $h' = 154.4 \sin \omega t + 154.4 \sin 3\omega t$ and $h'' = 154.4 \sin (\omega t + 60) + 154.4 \sin 3\omega t$ and the corresponding areas obtained by planimeter. It is seen that, as would be expected, $W_T = W_{50} + W_{150}$ since there is no flow of harmonic power in the supply

circuits. The corresponding single frequency loop obtained when $h = 154.4 \sin \omega t$ is also shown for comparison.

Loop areas

	W_{50}	W_{150}	$W_{50} + W_{150}$	W_T	
(i)	6.2	20.3	26.5	27.0	cm^2
(ii)	16.5	16.5	33.0	32	cm^2

From the above, it is seen that the minor loop area itself is no indication of the 150-c/s core loss, since when $\varphi = 0$ the minor loops are smaller than when $\varphi = 60$, while the corresponding 150-c/s core loss value is greater when $\varphi = 0$.

Single frequency magnetization

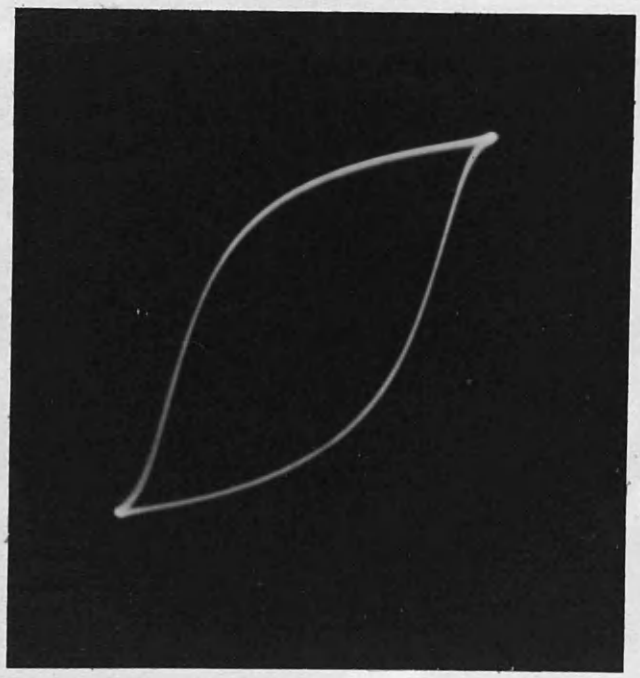

$h = 154.4 \sin 314t.$

CORE LOSS LOOPS

$h = 154.4 \sin \omega t + 154.4 \sin 3\omega t$

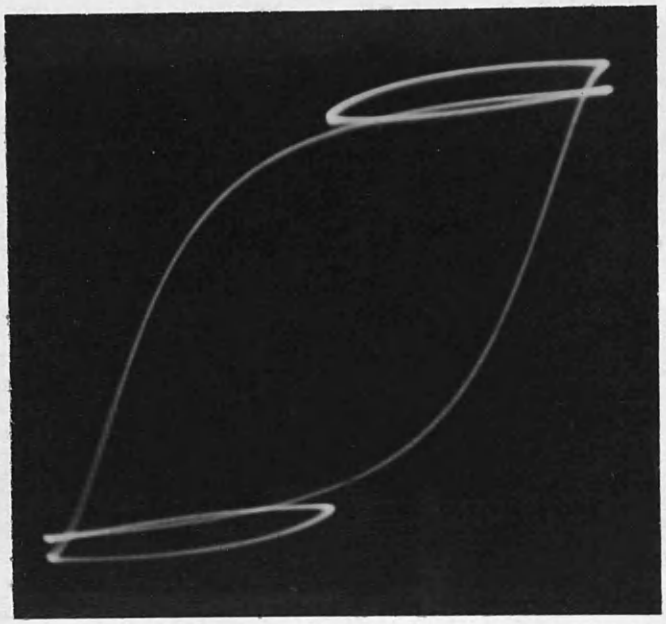

H_T, B_T; Area $\propto W_T$

H_{50}, B_T; Area $\propto W_{50}$

H_{150}, B_T; Area $\propto W_{150}$

CORE LOSS LOOPS

$h = 154.4 \sin(\omega t + 60) + 154 \sin 3\omega t$

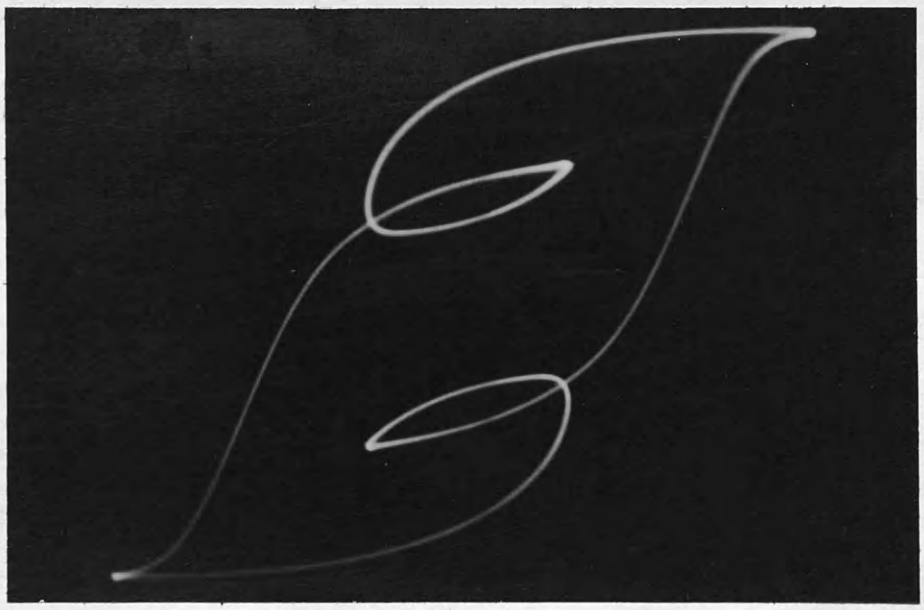

H_T, B_T; Area $\propto W_T$

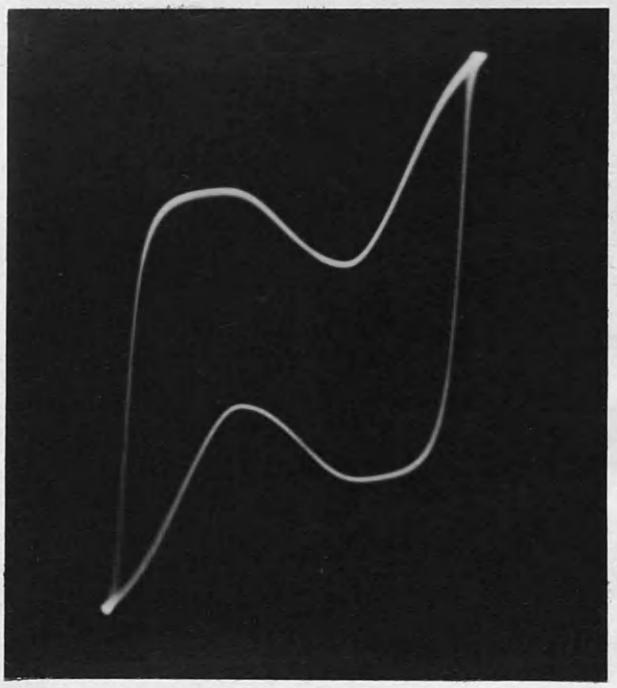

H_{50}, B_T; Area $\propto W_{50}$.

H_{150}, B_T, Area $\propto W_{150}$

A similar series of core loss loops are shown for the case of a core magnetizing force defined by

$$h = h_1 \sin(\omega t + \varphi) + h_2 \sin 2\omega t$$

Due to the presence of an even term in the magnetizing force, the loop will be unsymmetrical about the origin, and have one minor loop formed. The phase angle φ must be altered 180° to repeat identical core conditions, but the form of the loops obtained over the range $0 \rightarrow 90°$ are the same as $90° \rightarrow 180°$ in area. The loop for $\varphi = 100°$ is the same as $\varphi = 10°$ when viewed after 180° rotation. Accordingly, all core conditions can be visualized from B, H and loop traces over the range $0° \rightarrow 90°$. It is seen that the flux density waveform follows the same general shape as the magnetizing force wave, and contains a large percentage of even harmonics.

It is seen from the loop traces that the minor loops are well formed near the tip of the major loop, while for intermediate values the minor loop is only just formed in some cases. Since k = 1 for this condition of core magnetization, the magnetizing force wave is re-entrant for all values of φ, (see also Part I, Chapter 3) and the flux-density waveform is also seen to be re-entrant throughout the range of phase angle. For $\varphi = 0$, 75° and 90° the flux density wave is only just re-entrant due to the formation of the minor loop on the portion of the major loop which is almost horizontal, giving a resultant small change in flux from a large magnetizing force change.

The core loss loops, flux density and magnetizing force waves are shown on Pages 120 and 121 for the case

$h = 116 \sin (\omega t + \varphi) + 116 \sin 2 \omega t$ for the phase angle range $0 \rightarrow 90^{\circ}$ at 15° intervals. The corresponding single frequency core conditions are shown below for the same magnetizing forces,

i.e. $h = 116 \sin 314t$

and $h = 116 \sin 628t$.

Single frequency magnetization conditions.

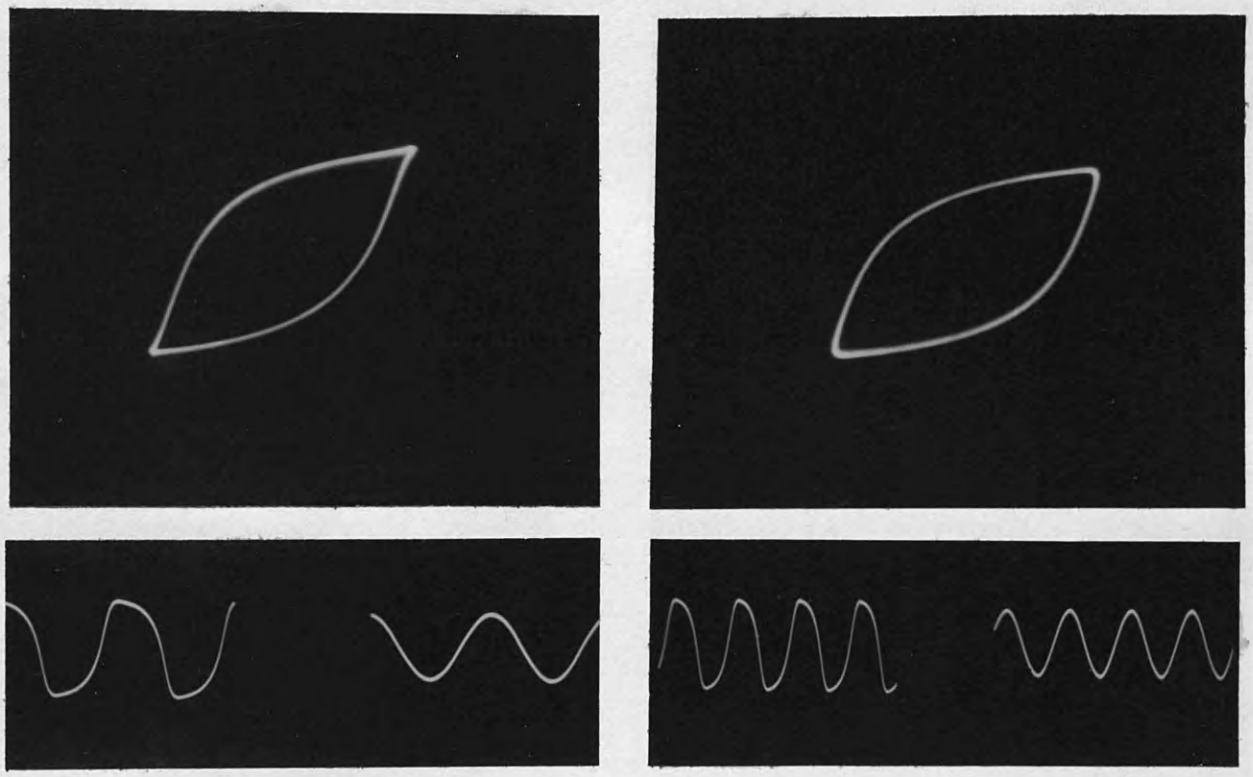

50 c/s alone.

100 c/s alone.

$h = 116 \sin(\omega t + \varphi) + 116 \sin 2\omega t$

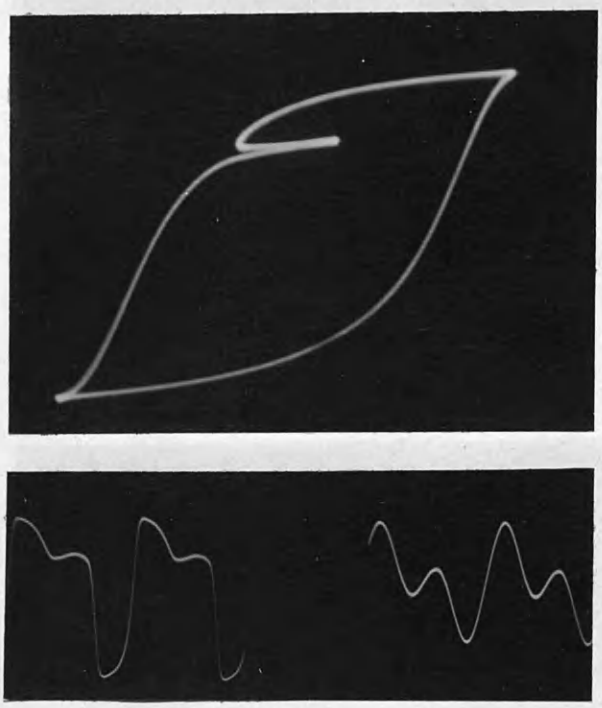

$\varphi = 0^\circ$

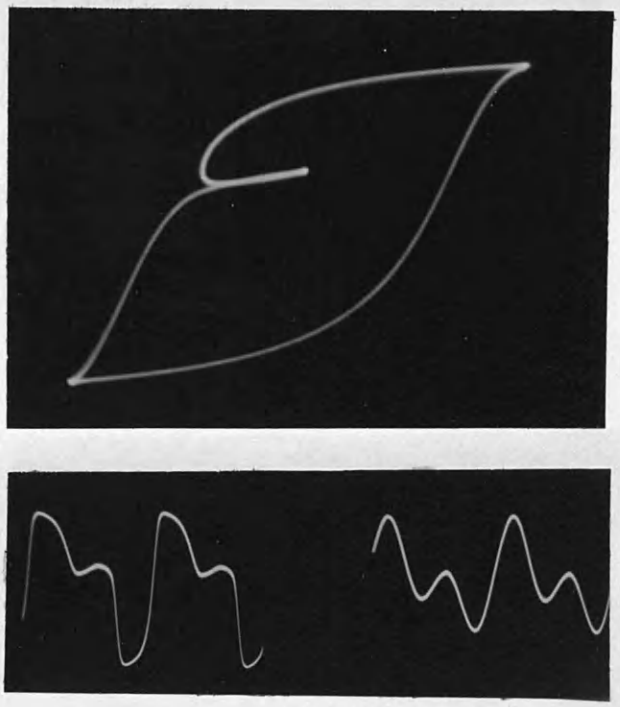

$\varphi = 15^\circ$

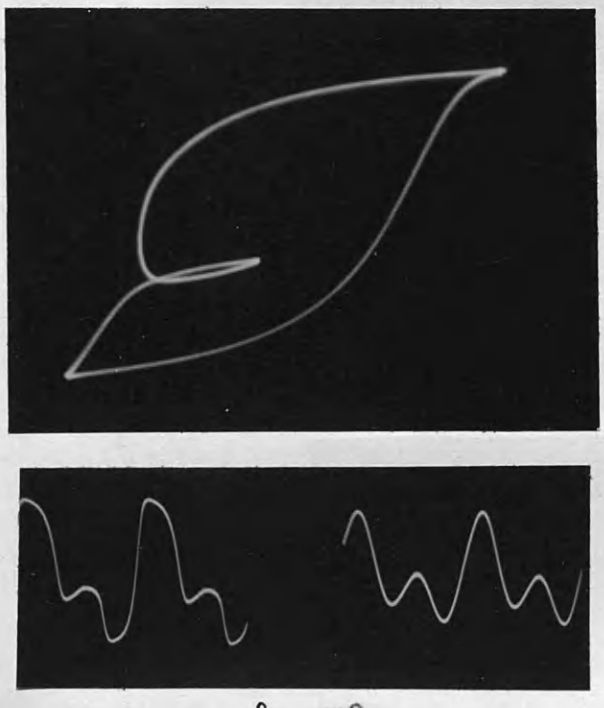

$\varphi = 30^\circ$

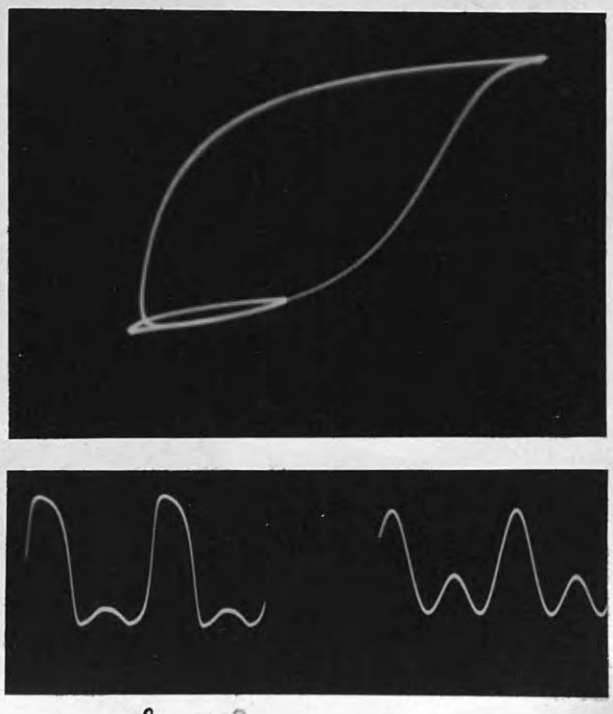

$\varphi = 45^\circ$

$h = 116 \sin (\omega t + \varphi) + 116 \sin 2\omega t$

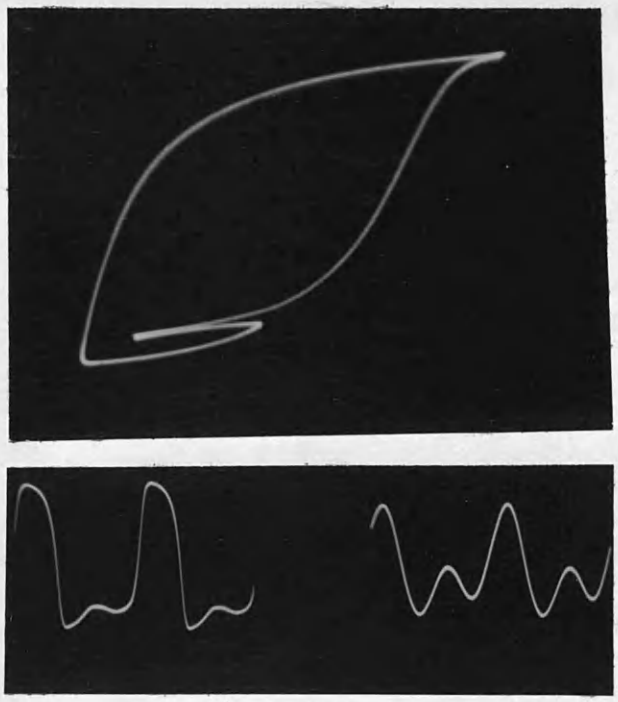

$\varphi = 60^\circ$

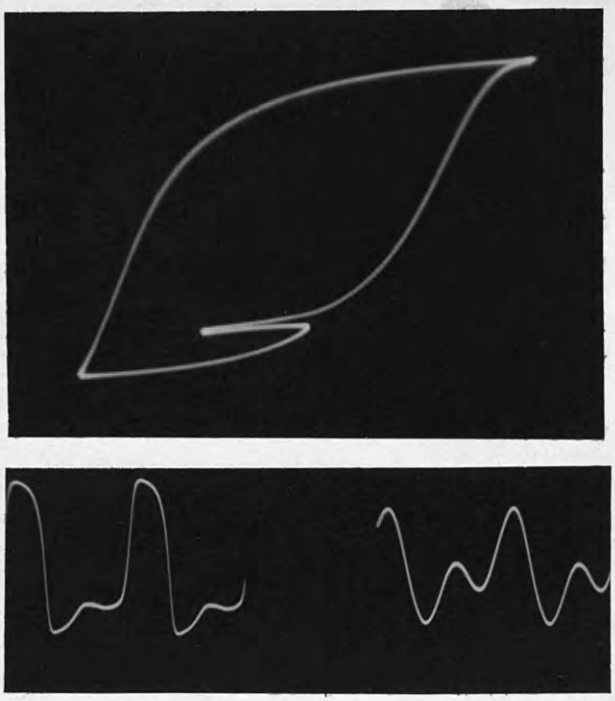

$\varphi = 75^\circ$

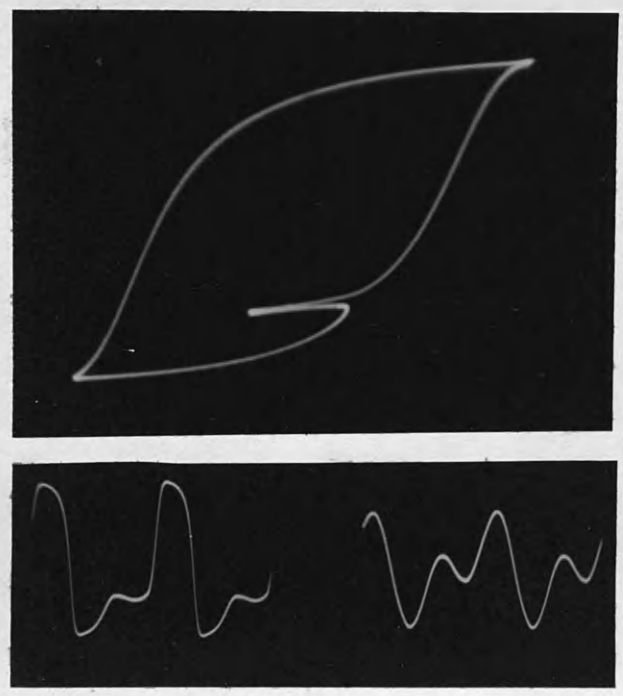

$\varphi = 90^\circ$

The components of the total loop in the two extreme cases, i.e.

$h' = h_1 \sin \omega t + h_2 \sin 2\omega t$

and $h'' = h_1 \sin (\omega t + 45) + h_2 \sin 2\omega t$

corresponding to the maximum and minimum value of peak to peak magnetizing force are shown on Page 123 and 124.

The relative areas of the loops (which were all obtained to the same scale) are tabulated below.

Loop Areas

	W_{50}	W_{100}	$W_{50} + W_{100}$	W_T
(i) cm^2	13.6	10.4	24.0	23.8
(ii) cm^2	6.3	12.4	18.7	19.0

CORE LOSS LOOPS

$h = 116 \sin \omega t + 116 \sin 2\omega t$

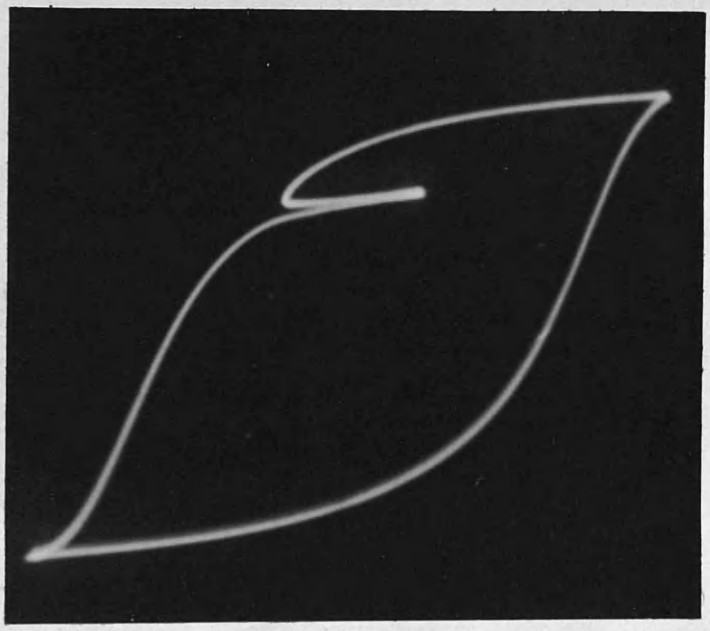

H_T, B_T; Area $\propto W_T$

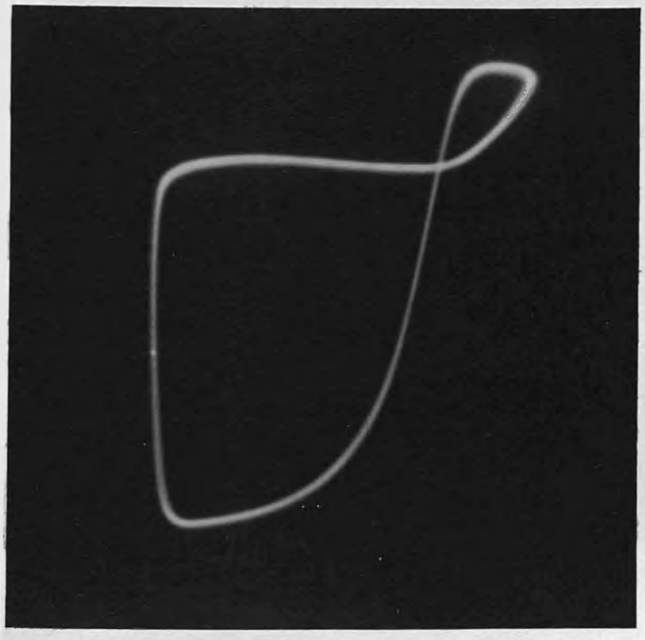

H_{50}, B_T; Area $\propto W_{50}$

H_{100}, B_T; Area $\propto W_{100}$

CORE LOSS LOOPS

$h = 116 \sin(\omega t + 45^\circ) + 116 \sin 2\omega t$

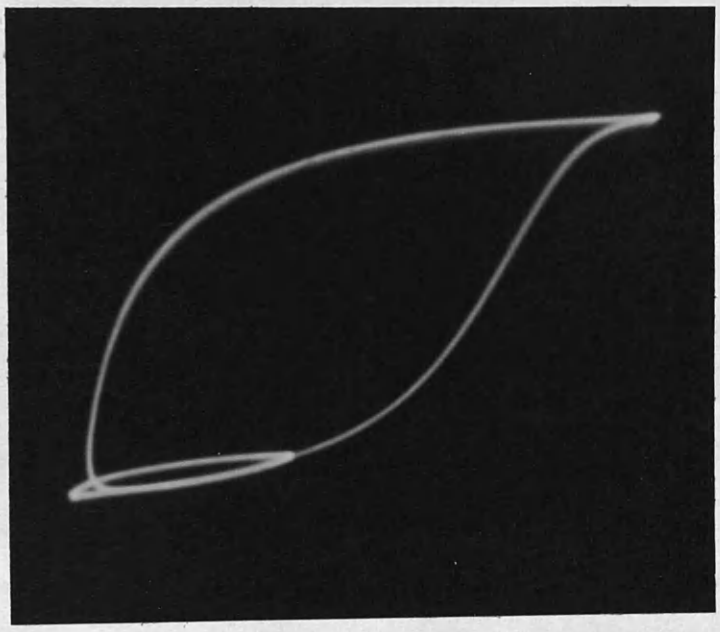

H_T, B_T; Area $\propto W_T$

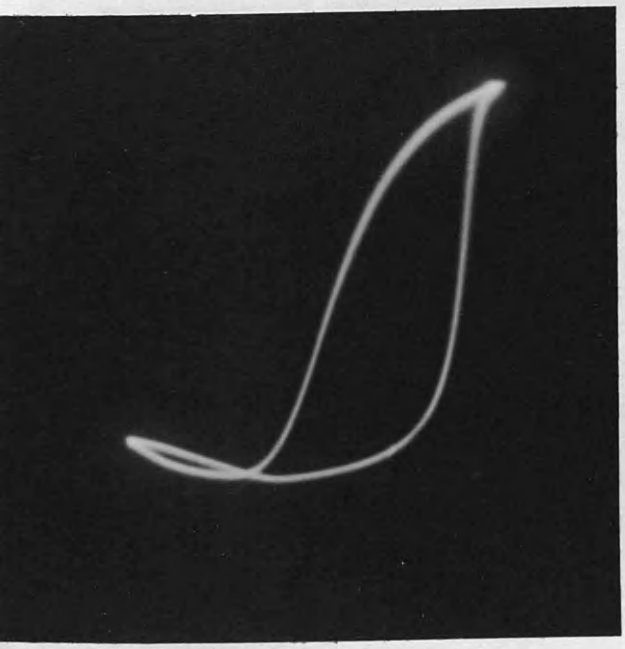

H_{50}, B_{50}; Area $\propto W_{50}$.

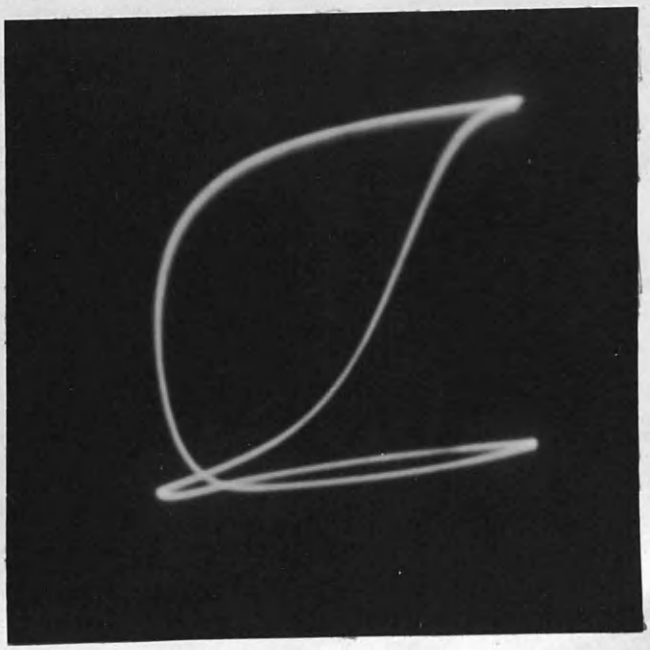

H_{100}, B_T; Area $\propto W_{100}$.

CHAPTER 6

HIGH FREQUENCY TESTS.

Effects of the variation in frequency of the superimposed magnetizing force upon core loss and flux density values of the low frequency component.

This series of tests was carried out at high frequency values which eliminated the effects of the phase of each component. In addition, since the two sources used, the 50-c/s supply and a high frequency source, were not locked together in any way, the actual position of the minor loops formed would not necessarily be stationary w.r.t. the major loop. If the high frequency value is not quite an exact multiple of the low frequency component, the minor loops will drift slowly round the major loop. When the drift is arranged to be very slow (0.5 c/s), an inspection of the meters in the circuit will show if there is any appreciable phase effect. Above a ratio of $\frac{10}{1}$ for the frequencies of the applied magnetizing forces, the effects of phase change are no longer significant.

The 50-c/s and the high frequency magnetizing forces were maintained constant as the frequency was varied.

Test I.

I_{50} = 0.6A, I_{hf} = 0.2A, i.e. H_{50} = 109.2, H_{hf} = 36.4

High frequency c/s	500	750	1000	1500	2000	3000	5000
I_{50} a_1	0.585	0.587	0.588	0.587	0.584	0.591	0.587
$+ jb_1$	0.005	0.01	0.00	0.00	0.00	0.00	0.00
V_{50} a_2	0.661	0.660	0.666	0.664	0.660	0.655	0.638
(400^T) $+ jb_2$	0.897	0.902	0.907	0.90	0.902	0.913	0.894
Voltage Factor	10	10	10	10	10	10	10
V_{50} (400^T)	11.14	11.14	11.21	11.18	11.18	11.25	11.0
B_{m50}	0.825	0.825	0.83	0.826	0.826	0.834	0.814
V_T (400^T)	11.05	11.05	11.05	11.05	11.05	10.8	10.8
B_{mT}	0.816	0.816	0.816	0.816	0.816	0.80	0.80
$a_1a_2 + b_1b_2$	0.390	0.395	0.391	0.392	0.386	0.397	0.376
W_{50}/core	0.975	0.988	0.977	0.978	0.965	0.97	0.940
I_{50} exact	0.585	0.587	0.588	0.587	0.584	0.591	0.587

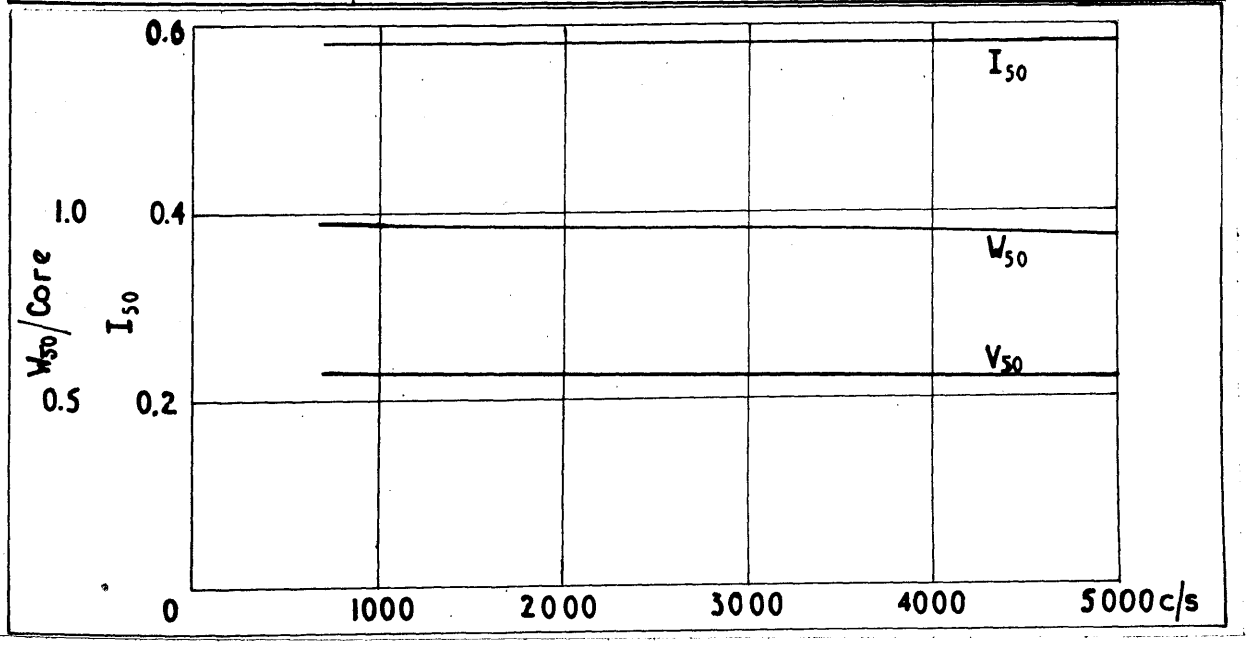

Fig. 47.
Variation of W_{50} with frequency.

Fig. 47 shows the variation of these components with frequency. Over the frequency range 500 - 3000 c/s the results are practically constant. Hence it may be assumed that under the above conditions, frequency variation of the high frequency component does not cause any variation in the low frequency components.

It is, therefore, sufficient to carry out a further series of tests, at one value of high frequency component only. The value chosen is 1450 c/s, which was obtained from a high-frequency alternator.

The low frequency magnetizing force was maintained constant and the high frequency value varied over the range, 4.55 - 127.5 AT/m. (i.e. I_{hf} = 0.025A $\rightarrow$ 0.7A). Readings were obtained for the l.f. core loss, B_{m50} and B_{mf}. A series of results was obtained for different values of H_{50} in the range 27.3 $\rightarrow$ 127.5 AT/m. (I_{50}, 0.15A $\rightarrow$ 0.7A).

A set of results for one of these tests is shown overleaf. The complete results are shown graphically in Figs. 48 and 49.

Core magnetization at 50 c/s and 1450 c/s

I_{50} = 0.7A 50-c/s circuit 1130Ω

H_{50} = 127 AT/m 1450-c/s circuit 360Ω, 0.25μF

	I_{hf}	0	0.05	0.1	0.2	0.3	0.4	0.5	0.6	0.7
	H_{hf}	0	9.1	18.2	36.4	54.6	72.8	91	109	127
I_{50}	$+ a_1$	0.691	0.694	0.693	0.694	0.693	0.693	0.691	0.691	0.692
	$+ jb_1$	0.018	0.018	0.017	0.017	0.016	0.016	0.015	0.015	0.015
V_{50}	$+ a_2$	0.30	0.311	0.318	0.310	0.294	0.274	0.256	0.236	0.216
	$+ jb_2$	0.491	0.50	0.511	0.546	0.575	0.599	0.618	0.633	0.640
Voltage Factor		20	20	20	20	20	20	20	20	20
$a_1a_2 + b_1b_2$		0.216	0.225	0.229	0.226	0.213	0.20	0.186	0.173	0.159
W_{50}/core		1.08	1.125	1.145	1.13	1.065	1.0	0.93	0.865	0.795
V_{50} (400T)		11.7	11.8	12.06	12.6	12.9	13.16	13.4	13.50	13.5
B_{m50}		0.864	0.871	0.89	0.93	0.953	0.97	0.99	0.995	0.995
V_T (400T)		10.5	10.7	11.1	11.9	12.45	12.75	13.2	13.34	13.85
B_{mT}		0.775	0.79	0.82	0.818	0.92	0.94	0.975	0.985	1.02

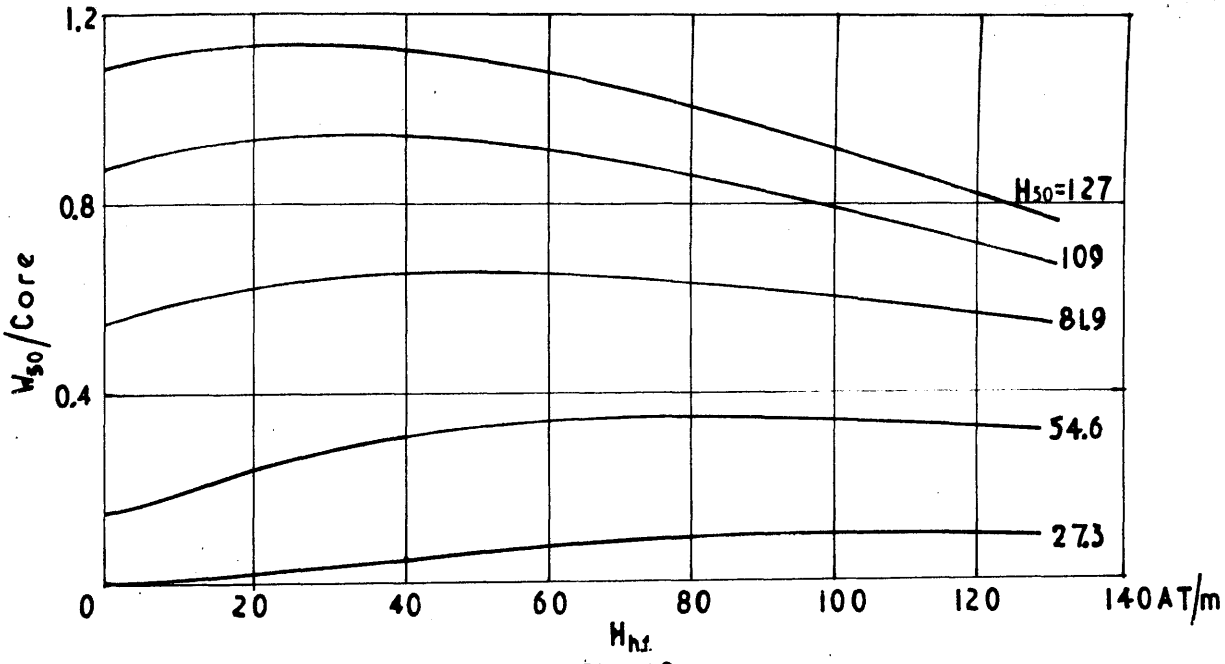

Fig. 48.

Variation of W_{50} with $H_{h.f.}$ for values of H_{50}

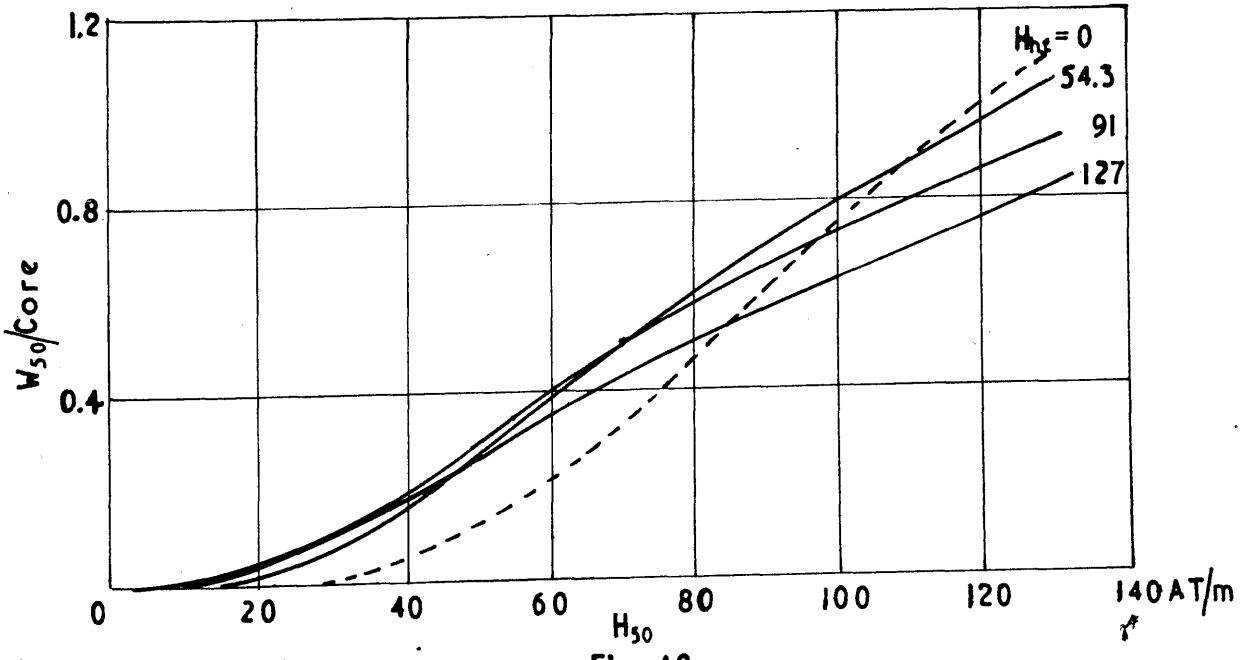

Fig. 49.

Variation of W_{50} with H_{50} for values of $H_{h.f.}$

From Fig. 48 it can be seen that the 50-c/s core loss for a constant value of H_{50} varies considerably as the value of $H_{h.f.}$ is increased. The extent of the variation increases with the value of H_{50} and from the graphs, it is observed that when H_{50} = 127 AT/m the 50-c/s core loss increases to a maximum when $H_{h.f.}$ = 22 AT/m, and thereafter decreases as the high frequency magnetizing force is increased. It should be noted that the core-loss value decreases below the value obtained when $H_{h.f.}$ = 0 for the case considered. As the l.f. component is reduced, the maximum loss value occurs at higher value of $H_{h.f.}$, indicating that the phenomena is dependent on the shape of the hysteresis loop for the material. It is, therefore, seen that the total peak magnetizing force must be sufficient to carry the core material beyond the knee of the magnetization characteristic, to enable the reduction to occur. It must be borne in mind that the total core loss does not show any reduction, since the high frequency source supplies power to the core, which increases as $H_{h.f.}$ is increased.

The effect involved is a phase change of the fundamental component of the flux wave, with respect to the applied magnetizing force. From Fig. 50 it is seen that B_{50} continues to increase in magnitude when $H_{h.f.}$ is increased, but the in-phase component of it decreases when the core reaches the saturated region. The quadrature one continues to increase as shown in the results.

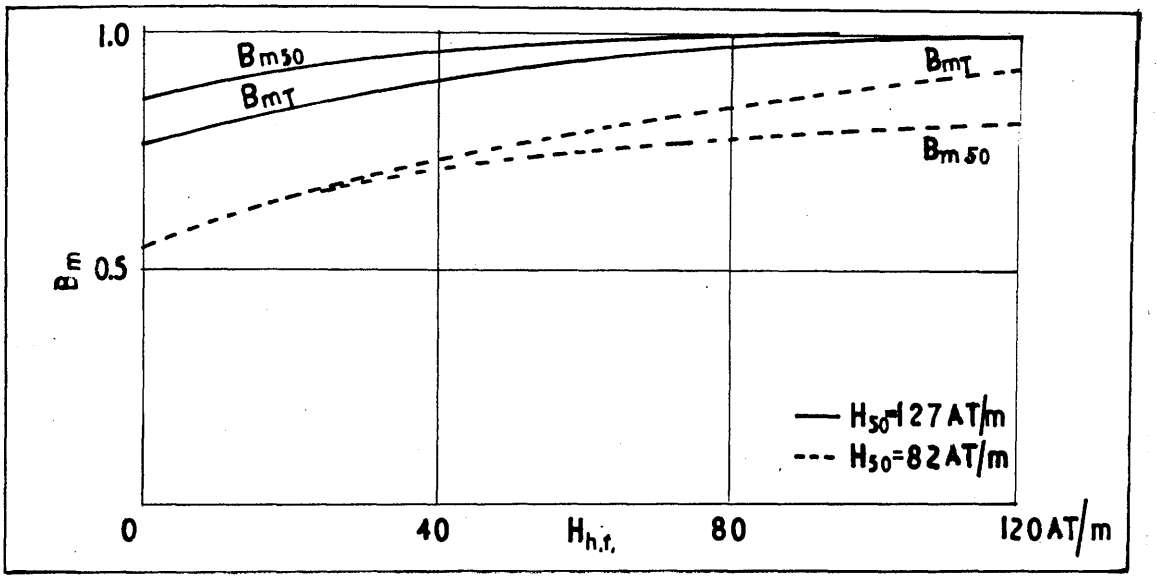

Fig. 50.
Variation of flux-density components.

If the fundamental components of B and H are related by the complex operator μ' (the complex permeability) where

$$\mu' = |\mu'| (\cos\theta - j \sin\theta)$$

$$\therefore \frac{\bar{B}}{\bar{H}} = \frac{j\omega\bar{B}}{\bar{H}} = j\omega\mu\mu_o$$

(where $\mu' = \mu\mu_o$)

$\bar{V} = R\bar{I} + NA\dot{\bar{B}}$ for a coil of N turns and resistance R and $\bar{I} = \frac{l}{N}\bar{H}$

$$\therefore \bar{V} = \bar{I}\left(R + \frac{N^2A}{l}\frac{\bar{B}}{\bar{H}}\right)$$

$$= \bar{I}\left(R + \frac{N^2A}{l} j\omega\mu\mu_o\right)$$

$\therefore$ The impedance of the winding may be written as

$$Z = \frac{\bar{V}}{\bar{I}} = \left(R + \omega\mu\mu_o\frac{N^2A}{l}\sin\theta\right) + j\,\omega\mu\mu_o\frac{N^2A}{l}\cos\theta.$$

As the measurements are obtained from a secondary winding then

$$Z = \omega\mu\mu_o\frac{N^2A}{l}\sin\theta + j\,\omega\mu\mu_o\frac{N^2A}{l}\cos\theta.$$

The "effective resistance", due to hysteresis and eddy current losses will be reduced by a reduction in $\sin\theta$, i.e. θ decreasing. This implies that the core-inductance should increase under these conditions. From the test results, when the low-frequency core-loss is decreasing the core impedance is still increasing, since V_{50} is increasing.

It is suggested that the permeability angle may be altered in the saturated region due to the action of the high frequency components of magnetizing force acting on the magnetic domains.

CHAPTER 7.

HARMONIC POWER.

The results obtained for the high-frequency tests were taken on the assumption that the magnetizing forces were sinusoidal, i.e.

$$h = h_1 \sin \omega t + h_n \sin n\omega t$$

To obtain this condition, it is usual to insert in the circuit a large value of resistance to give sine current conditions. For the circuit under test, care is required to prevent errors arising due to the flow of harmonic power.[6] In any non-linear element energized from a source which has a finite resistance, the following relationship is true for the practical condition of sine current or sine voltage excitation.

Power supplied to element at fundamental frequency = Power dissipated in element + power dissipated in circuit by harmonic components generated in the element.

The alternating current potentiometer gives a measure of the power at fundamental frequency. This will not be a true indication of the core-loss if any harmonic power is flowing. For the case of sine-current excitation, the voltage across the windings on the core will contain harmonics and, if the circuit impedance is small, they will cause corresponding harmonic currents to flow. When this occurs, the magnetizing force waveform is no longer sinusoidal and hence the assumed conditions of magnetization are not satisfied.

If the magnetizing force applied to the core is maintained constant and the exciting impedance altered, the change in the input power to the core will be a measure of the magnitude of the harmonic power flowing. If no change occurs in the input power as the impedance is altered through wide limits, it may be assumed that the input power to the specimen does not contain any component associated with harmonic power flow.

Two tests were carried out on the circuit as shown in Fig. 51.

Test I. The cores were energized from the 50-c/s circuit only. The current was kept constant throughout and the circuit components were altered as below.

To enable a large value of series resistance to be used, a high voltage is required. This was obtained from a 5-kVA, 2000/100-V, 1-ph transformer (T.6), which was energized from a variable voltage supply, as shown in Fig. 51.

The high-frequency circuit which was not energized, was closed through 0.25μF and 360Ω in series. (These were the values used in the second test).

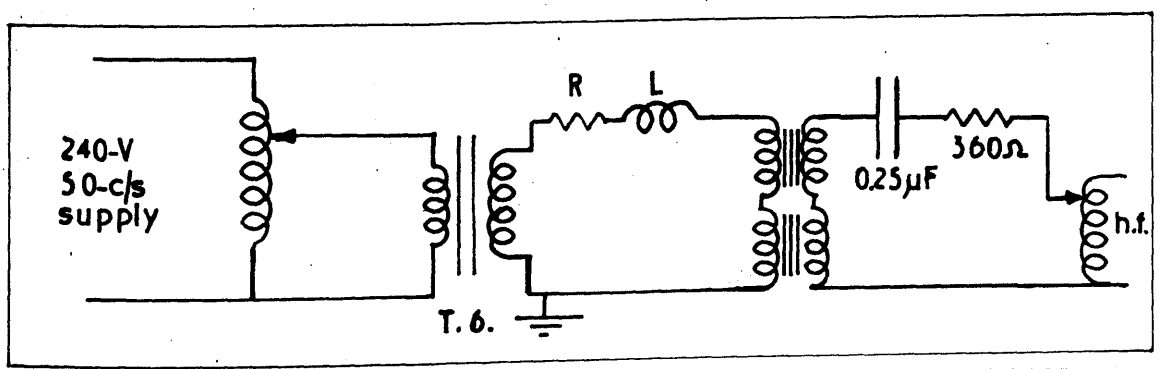

Fig. 51.

Test 1.

	R_{50}	500	1150	2000	1150	2000Ω
	L_{50}	0.66	0	0	0.66	0.66 H
I_{50}	$+ a_1$	0.561	0.595	0.595	0.587	0.60
	$+ jb_1$	-0.206	-0.02	-0.002	-0.105	-0.052
V_{50}	$+ a_2$	0.43	0.521	0.305	0.376	0.342
	$+ jb_2$	.273	0.396	0.408	0.345	0.384
Voltage Factor		20	20	20	20	20
$a_1a_2 + b_1b_2$		0.185	0.183	0.180	0.185	0.186
I_{50}		0.598	0.595	0.595	0.596	0.601
B_{50}		0.754	0.754	0.754	0.755	0.76

The high-frequency circuit was open-circuited to ensure that no current was flowing in it due to slight magnetic unbalance between the two cores: the results obtained when R = 500Ω, L = 0.66H were

$V_{50} = 0.43 + j\ 0.273 = 0.509V$

$I_{50} = 0.561 - j\ 0.206 = 0.596A$

Voltage Factor 20

$\therefore\ a_1a_2 + b_1b_2 = 0.1849$

This compares with 0.185 obtained above, showing that the h.f. circuit impedance is large enough to prevent any l.f. current flow.

From the results of Test 1, it is seen that when the 50-c/s circuit comprises an air-cored inductance of 0.66H and a resistance of 500Ω, the core loss value does not alter when the resistance is more than doubled, and shows a change of 0.54% when it is increased fourfold.

It should be noted that the current value obtained from the a.c. potentiometer results for R = 2000Ω is 0.8% greater than the value for R = 1150Ω. This would tend to increase the core loss in the former case. Hence the 0.54% increase noted above is due in part to the slight change of circuit current. From these results it is seen that, when the 50-c/s circuit has an air-cored inductance of 0.66H in series with a resistance greater than 500Ω, the effects of harmonic power flow are so small as to be considered negligible.

Test 2.

The circuit was connected as for Test 1 with the high frequency supply obtained from the alternator, the current being maintained constant throughout at 0.3A. The 50-c/s current was kept constant at 0.6A and the following results were obtained as the 50-c/s circuit components were altered.

R. Ω	500	500	1100	2000	2000
L. H.	0	0.66	0.66	0.66	0
I_{50} + a_1	0.592	0.559	0.587	0.601	0.597
+ jb_1	-0.055	-0.209	-0.107	-0.06	0
V_{50} + a_2	0.36	0.476	0.405	0.366	0.315
+ jb_2	0.479	0.368	0.444	0.481	0.513
Voltage Factor	20	20	20	20	20
$a_1a_2 + b_1b_2$	0.1866	0.191	0.190	0.1911	0.188
W_{50}	0.932	0.954	0.950	0.955	0.94
I_{50}	0.594	0.596	0.596	0.604	0.597
B_{50}	0.887	0.888	0.888	0.891	0.89

The results of Test 2 show that, when the core is subjected to combined magnetization, the effect of harmonic power in the source impedances may be neglected when circuit components as detailed in Fig. 51 are used.

As a further check, the superimposed test was repeated with a large value of resistance in series. The 50-c/s core loss was measured and compared with the results previously obtained. This showed that, over the range of high-frequency current, the results of the two tests did not differ by more than 1%.

From the foregoing tests it is seen that errors due to harmonic power flow are so small that they may be neglected.

CHAPTER 8

INTERMODULATION PRODUCTS

As shown in Part I, Chapter 7, the induced voltage wave contains harmonics of the supply frequencies f_1 and nf_1 and, additionally, certain intermodulation products. To determine the magnitude of all these components, the cores were energized in the normal manner from 50-c/s and 150-c/s supplies. The wattmeter current coil was disconnected from the core circuit and energized from a variable frequency oscillator. The voltage coil was connected across a 400-turn winding on one core. When the oscillator frequency is just below or just above a harmonic component in the voltage wave, the wattmeter pointer will oscillate. By adjustment of the oscillator frequency the maximum pointer deflection can be easily read; this value is proportional to the harmonic component.

The cores were energised under the condition

$$I_{50} = 0.6A, \qquad I_{150} = 0.45A \qquad (\varphi = 60^\circ)$$

The wattmeter current coil was supplied throughout this test at a constant current (0.1A) from the oscillator. The following were measured:-

1) Voltage components across one core, i.e. w attmeter voltage coil across 400^T winding.
2) Components across 50-c/s supply terminals, (voltage coil across 800^T).
3) Components across 150-c/s supply terminals, (voltage coil across 800^T).

Resul s obtained: (These readings are proportional to the voltage compone ts).

f	50	150	250	350	450	550	650	c/s
$V_{core\ 1}$	0.23	0.27	0.16	0.15	0.11	0.07	0.01	
V_{50}	0.49	0.08	0.11	0.25	0.15	0.05	0.06	
V_{150}	0.13	0.5	0.24	0.08	0.07	0.08	-	

Since the two cores are not subjected to the same conditions of magnetization (Core 1; $h = h_1 \sin(\omega t + 60) + h_3 \sin 3\omega t$, Core 2; $h = h_1 \sin(\omega t + 60) - h_3 \sin 3\omega t$), the results of 1) cannot be directly compared with 2) and 3). It must also be noted that there is a factor of 2 in results 2) and 3), due to the voltage coil being across two 400^T windings in series.

f c/s	Core 1 (A)		V_{50}		V_{150}		$V_{50} + V_{150}$		(B)
50	A-E-F	0.23	2A	0.49	-2(E+F)	0.13	2A-2(E+F)	0.62	0.31
150	-3(C+J-G)	0.27	-6(C+J)	0.08	6G	0.5	-6(C+J-G)	0.58	0.29
250	5(D+K-F)	0.16	10(D+K)	0.11	-10F	0.24	10(D+K-F)	0.35	0.175
350	-7(K-E-L)	0.15	-14K	0.25	14(E+L)	0.08	-14(K-E-L)	0.33	0.165
450	9(J-M)	0.11	18J	0.15	-18M	0.07	18(J-M)	0.22	0.11
550	11(L-N)	0.07	-22N	0.05	22L	0.08	22(L-N)	0.13	0.065
650	13N	0.01	26N	0.06	26N	-	52N	0.06	0.015
750	15P	-	-	-	30P	-	-	-	

Referring to equations 69, 70 and 71 (Part I, Chapter 7), the numerical values may be identified proportionally with the coefficient values obtained under the assumption of single-line magnetization characteristic. The numerical values of the coefficients for Core 1 are given in column A of the table. The corresponding values obtained from the summation of coefficient values for V_{50} and V_{150} are given in column B. It is seen that, due to the effects of hysteresis and eddy currents, the 50-c/s coefficients differ by 22%, the 150 c/s by 7% and the higher orders by less than this figure. This would be expected since the B - H relationship is now a double-valued function of H, and consequently the operating points for given magnetizing force values in each core will give in one case a larger and in the other a smaller flux density value than obtained from a single line characteristic. Due to the non-linearity of the B - H relationship, the flux changes in the two cases for the same magnetizing force are not equal. Additionally, due to the loss term, the flux change will be greater in the practical case. This is borne out by the results on Page 139. Since the basic harmonic terms due to each component of magnetizing force have practically vanished by the 5th, the coefficients at 350, 550 and 650 c/s are caused principally by the intermodulation terms.

The corresponding harmonic components obtained under single-frequency magnetization for the same magnetizing force values are given overleaf.

Values obtained across 400^T winding.

f	I	50	150	250	350	450	750
50 c/s	0.6A	0.2	0.1	0.03	0.005	-	-
150 c/s	0.45A	-	0.34	-	-	0.07	0.005

Comparing these results with those on Page 139 for the same individual magnetizing force values, it is seen that the coefficients are increased under combined magnetization, except for the 150-c/s value which is reduced, due to the presence of the intermodulation terms J and G. The variation is shown when coefficients A', C' and D' for single frequency magnetization (Part I, Chapter 7) are compared with the corresponding ones in the table on Page 139, i.e. (A-F-F); (C+J-G) and (D+K-F). The actual numerical variation depends on the core constants a, b and c and the values of h_1 and h_3.

It should also be noted that under combined conditions, the magnitude of the 150-c/s voltage component appearing across the 50-c/s supply (3C + 3J) is 16% of the 50-c/s value (A) in this test. Similarly, the 50-c/s voltage (E + F) across the 150-c/s supply is 26% of the 150-c/s value (3G). Without the back-back connection of units, the corresponding values (obtained from Page 139 ($V_{core\ 1}$ results) are 110% and 85% respectively. Due to the relatively large percentage of 50-c/s and 150-c/s voltage components appearing across the 150-c/s and 50-c/s supply units with the back-back connection, it is necessary to ensure that the supply current waveforms are sinusoidal.

The preceding method of test can be used to obtain the harmonic components in the current waveform supplied to the cores. If the wattmeter voltage coil is now energized from the oscillator and the current coil inserted in the supply circuit, the peak wattmeter readings obtained as the oscillator frequency is varied will be proportional to the current harmonics.

The following results are obtained when the voltage coil is supplied at 5V and the core energized at $I_{50} = 0.6A$ and $I_{150} = 0.6A$, $\varphi = 0$.

Frequency	I_{50} components	I_{150} components
50	0.560	0.001
150	0.001	0.60
250	-	-
300	-	-

From the above results it is seen that the core is supplied under practically perfect conditions of sine current excitation since the individual harmonic components in the 50-c/s and 150-c/s current waves are less than 0.2%. The same result was obtained with $\varphi = 60^{\circ}$.

As the exciting current values are reduced below 0.6A by the insertion of circuit resistance, the harmonic components are further reduced. Hence it can be stated that under all test conditions, variation of I_{50} and I_{150} in the range $0 \rightarrow 0.6A$, and change of relative phase angles, the cores are subjected to sine current magnetization. The harmonic content being less than 0.2% can be neglected.

CHAPTER 9

CONCLUSIONS

When an iron circuit is subjected to combined magnetization at two frequencies which are integrally related, the core loss which is obtained cannot be directly estimated from single frequency test results. In addition to the variation in loss from single to combined magnetization conditions, the relative phase of the two magnetizing forces affects the magnitude of the core loss obtained. If the ratio of the frequencies is greater than 5:1, then this further complication due to phase becomes so small that it may be neglected.

The cases which have been considered in greatest detail are those where the phase effect is of significance. For two frequency magnetization, this occurs when the frequencies are related in the ratio 1:2. While this case is of greatest interest theoretically, its occurrence in practice would be restricted to iron cores used in rectifier or other circuits where the fundamental and even harmonic components of magnetization are present. Combined magnetization occurring due to the frequency ratio 1:3 is very common and hence the results for this test are really of greater interest. In both cases, the general conclusions are the same; the total core loss under combined conditions is greater than either of the components when acting alone. The variation of the total core loss is not so great as the variation in the lower frequency term. An increase of 200% on the

minimum value of the low frequency core loss is not uncommon as the phase angle is varied. The individual loss terms under combined conditions do attain values less than those obtained under single frequency conditions over a range of phase angle values. For other phase angles they are greater than the single frequency values. The minimum of the lower frequency loss components occur in the region of minimum peak-peak magnetizing force. This same region coincides with the maximum value of the higher frequency loss term. Similarly, for the maximum value of the low frequency term the applied magnetizing force reaches its peak value, giving rise to the minimum value of higher frequency core loss. It is seen that this causes the overall variation in total core loss to be reduced.

The variation of the higher frequency loss term is small when compared with the lower frequency one, when $H_{hf} = H_{lf}$, but as the high frequency term is reduced with respect of H_{lf}, the high frequency loss variation increases slightly till $H_{hf} = \frac{1}{2} H_{lf}$, thereafter decreasing to zero as H_{lf} is reduced. These general conclusions are obtained when the core is being operated at or beyond the "knee" of the magnetization characteristic. This, of course, is the usual region of operation for iron-cored circuits.

When the core is operating below the "knee" region, slightly different conditions are obtained. Under combined magnetization the low frequency loss is now always greater than the single frequency value for the same low frequency magnetizing component. The total loss

for all phase angle values is greater than the sum of both the loss components obtained from single frequency tests. A reduction in the low frequency loss is obtained only over a very limited phase angle change and with small values of the higher frequency term.

Since it is the lower frequency loss term variation which is of greatest interest, the general requirements to obtain this loss value under combined conditions to be less than the single frequency value are: i) For small low frequency terms (below the "knee" of the characteristic), the higher frequency term should be small ($< 50\% H_{lf}$). ii) For operation at or above the knee region, the larger the high frequency term the greater is the possible reduction in low frequency loss term (with correct relative phase angle).

When the frequency of the superimposed component is increased so that the phase effect is no longer of significance, it is seen that, provided the core is operating beyond the "knee" region, the low frequency loss term is reduced. As the high frequency magnetizing force is increased, the low frequency loss continues to be reduced. Of course, the <u>total</u> loss continues increasing due to the relatively large increase in the higher frequency term.

The use of the back-back method of core connection has been justified in theory and practice to give the desired core magnetization conditions and, when used in conjunction with the special supply circuits, errors due to harmonic power flow are kept to a minimum.

The work considered in this Thesis has dealt entirely with single-phase core magnetization conditions. It is, of course, obvious that a further wide field of work is available to investigate multi-phase connections under conditions of variable phase combined magnetization.

Since the completion of this experimental work, the author has started to consider the most practical case of the above, namely three-phase combined magnetization. This is of importance in practice, since in general the supply voltage applied to transformers etc. does contain various percentages of harmonic components, causing a change in core loss from the calculated values obtained on the assumption of sinusoidal flux conditions. The same general conditions are again observed as the relative phase angle between the two components of magnetization is altered. It is seen that, if it is possible to control the relative phase angle between the components, an appreciable reduction in core loss is obtained. It is hoped in the very near future to publish the results of these three-phase tests.

Up to this point, the magnetic material has only been considered to be subjected to two-frequency magnetization. It is obvious that this could be extended to three- and perhaps four-frequency conditions. The back-back method can still be used, but the number of identical cores must be increased. A typical practical case, which could then be fully investigated, is the core loss occurring in a smoothing choke in a rectifier circuit. The magnetizing force would comprise a d.c. term and the appropriate even harmonic terms.

From the foregoing, it is seen that the subject matter of this Thesis deals only with a very restricted field of the general case of a magnetic material subjected to combined magnetization, but is hoped in the future that other approaches may be investigated.

BIBLIOGRAPHY.

1. PETERSON, E. "Harmonic production in ferromagnetic materials at low frequencies and low flux densities". Bell System Technical Journal, 1928, 7, Page 762.

2. BALL, J.D. "The unsymmetrical hysteresis loop". Transactions of the American I.E.E., 1915, 34, Page 2693.

3. FINZI, G. and GEROSA, G. Rendiconte del R. Istituto Lombardo, 1891, 24.

4. EWING, J.A. "Magnetic induction in iron and other metals". ("The Electrician", 1893). Page 320.

5. THOMPSON, S.P. "On hysteresis loops and Lissajous' figures". Philosophical Magazine 1910, 20, Page 417.

6. GREIG, J. and PARTON, J.E. "Harmonic power in iron testing". Engineering, 1938, 146, Page 431.

7. SPINELLI, F. "Electric lighting and the conversion of 3-ph to 1-ph currents of triplen frequency". Electrician, 1912, 70, Page 97.

8. TAYLOR, A.M. "Static transformers for simultaneous changing of frequency and pressure of alternating currents". Journal I.E.E., 1914, 52, Page 700.

9. BRAILSFORD, F. "Frequency-changing at supply frequencies by static means". Journal I.E.E., 1933, 73, Page 309.

Appendix (a)

Measuring Circuits

1) Alternating current potentiometer

The a.c. potentiometer was used to measure voltage and current quantities throughout the tests and from these values the power loss was readily obtained.

Under combined magnetization conditions it was necessary to measure, for a given magnetizing force, the voltage and current quantities at two different frequencies. These measurements were all required as nearly simultaneously as practicable. Since the a.c. potentiometer normally available consists basically of one in-phase and quadrature wire supplied at one frequency, say f_1, it was necessary to assemble a switching system which would change over the supplies to the measuring wires from f_1 to nf_1. Due to the change of frequency, the circuit components in series with the quadrature wire also require to be altered.

The circuits which require switching are -

1) Input to supply transformer
2) Detector circuit
3) Quadrature wire components
4) Test input.

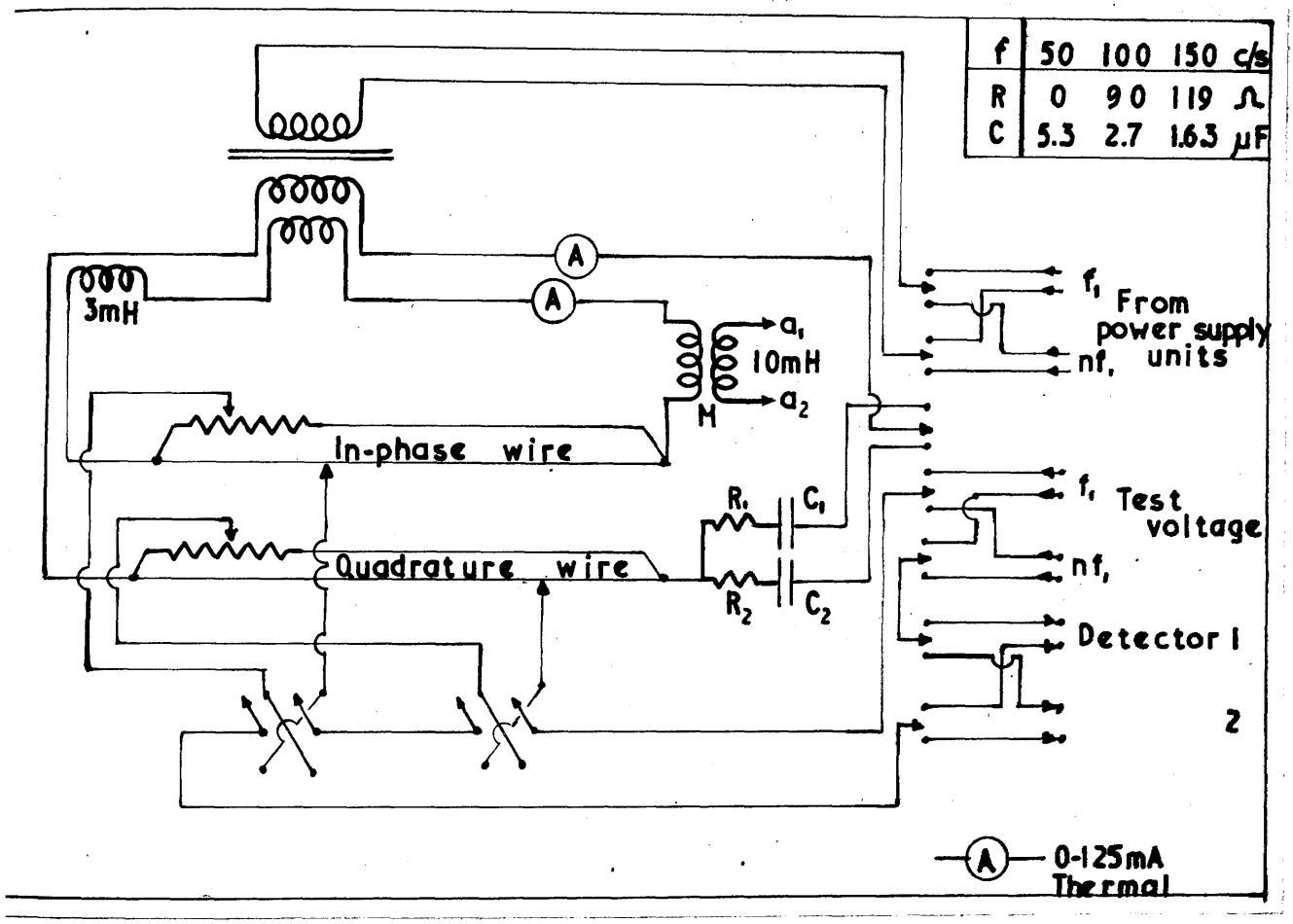

Fig. 52.
Alternating Current Potentiometer Circuit.

The complete circuit diagram for the potentiometer circuit is shown in Fig. 52. The supply voltages to this unit were obtained from Variac transformers, which enabled the wire currents to be adjusted to the standard value. A mutual inductance was inserted in the in-phase wire to check that there was a 90° shift between the two wire voltages. Any discrepancies were adjusted by variation of the R - C components in the quadrature wire. When this check was being carried out, the terminals a_1 a_2 were connected to the test voltage terminals f_1 or f_2.

For the 50-c/s tests the potentiometer was standardized to give 1V/wire, while for the 150-c/s tests it was 0.5V/wire or 1V/wire, depending on the voltage available from the 150-c/s source. Throughout the experimental results the wire voltage is stated where it differs from 1V.

The wire current values for each case were obtained by the normal method of d.c. calibration against a Standard Cell.

The detector used for the 50-c/s case was a standard vibration galvanometer which could be tuned over the frequency range 20 - 60 c/s. Great care was taken to ensure that it was sharply tuned when in use. As no suitable vibration galvanometer was available for the other test frequencies, a Baldwin electronically operated null indicator was used. This unit could be tuned by suitable external capacitance but even under these conditions was not sufficiently frequency sensitive. To increase this, a selective amplifier was inserted between the potentiometer and the detector, thereby increasing the overall accuracy of the potentiometer results. The detector circuit under these conditions is shown schematically in Fig. 53.

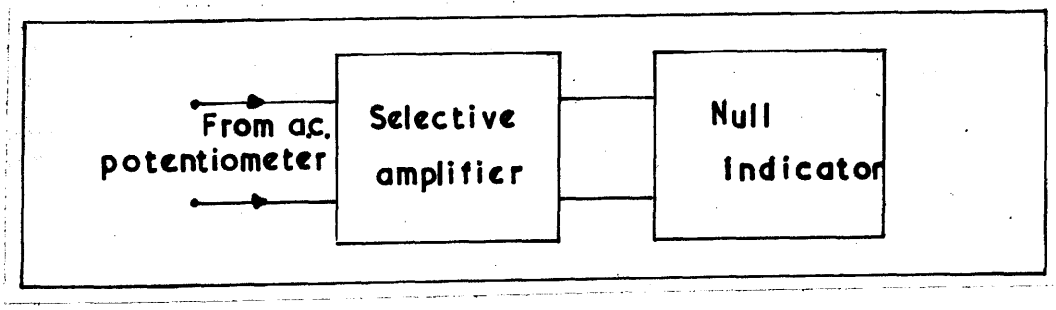

Fig. 53.

Theory of measurements from potentiometer results.

1. Amplitude of magnetizing force components.

The potentiometer is used to measure the r.m.s. value of the alternating voltage developed across a standard resistance in the energizing circuit. In this way, the two current values I_1 and I_n are obtained.

$$I_1' = a_1 + jb_1 \text{ and } I_1 = \sqrt{a^2 + b^2}$$

$$I_n' = c_1 + jd_1 \qquad I_n = \sqrt{c^2 + d^2}$$

The amplitudes of the components of the core magnetizing force are then,

$$h_1 = \frac{\sqrt{2} I_1 N_1}{\pi D} \quad \text{and} \quad h_n = \frac{\sqrt{2} I_n N_n}{\pi D}$$

where D is the mean core diameter.

2. Amplitude of fundamental component of flux density.

The components of the induced voltage E_1 and E_n in a winding of N_2 turns on the specimen are obtained from the potentiometer results. It is usually necessary to insert a potential divider between the specimen terminals and the potentiometer. The voltage factor K (<1) introduced by it must be taken into account as below.

Let measured voltage at f_1 be

$$E_2' = a_2 + jb_2$$

$$\therefore \quad E_2 = \sqrt{a^2 + b^2}$$

$$\therefore \quad \text{Voltage at specimen terminals} = \frac{E_2}{K}$$

$$\therefore \quad B_1 = \frac{E_2}{4.44\, f_1\, N_2 A} \text{ weber/m}^2$$

and similarly for B_n.

3. Iron Loss in specimen.

The losses in hysteresis and eddy currents can be readily obtained from the current and voltage readings.

$$W_1 = \frac{N_1}{KN_2} (a_1a_2 + b_1b_2)$$

and $W_n = \frac{N_n}{K'N_2} (c_1c_2 + d_1d_2)$

In the test results $N_1 = N_n = 100$ and $N_2 = 400$, except where stated otherwise.

$\therefore$ Total iron loss in specimen under combined magnetization =

$$\frac{N_1}{N_2} \left[\frac{a_1a_2 + b_1b_2}{K} + \frac{c_1c_2 + d_1d_2}{K'} \right]$$

From the core weight (0.639 kg) the iron loss in W/kg can be readily obtained.

Appendix (b)

Supply Units

From the theoretical and experimental work in the previous Chapters, it is evident that the supply units required are of a rather special nature. The essential requirement that the supply frequencies must be synchronized to one another suggests that mechanically coupled alternators would be suitable. The ideal set would comprise a synchronous motor driving alternators with various numbers of pole-pairs depending on the frequencies required. The requirement of relative phase change between the supplies could then be obtained by rotation of the stator of each alternator. A set of this nature would require to be manufactured specially and accordingly other methods must be sought. Electronic circuits could be used to obtain (by frequency division) the synchronised voltages required. These would then each require power amplifiers and phase shift circuits. While this method could be used, the large number of components required and the possibility of poor waveshape and inaccurate determination of phase change caused it to be put aside in favour of the following methods.

1. 50-c/s SUPPLY UNIT.

This was the basic frequency used for the excitation of the reactor cores and was obtained from the corporation 50-c/s supply.

To enable phase effects to be investigated, this supply was obtained through an 0.6kVA Zenith phase-shifting transformer capable of $\pm$ 180° rotation. The requirement of a high-impedance source was obtained by

connecting the 3-ph phase-shifting transformer in star-star and inserting a dummy load of 3 adjustable equal resistances in its secondary circuit. The circuit under test was connected in series with one of these resistances at the star-point, to prevent any large voltage to neutral developing in the metering and oscilloscope circuits. The complete circuit diagram of this supply unit is shown in Fig. 54.

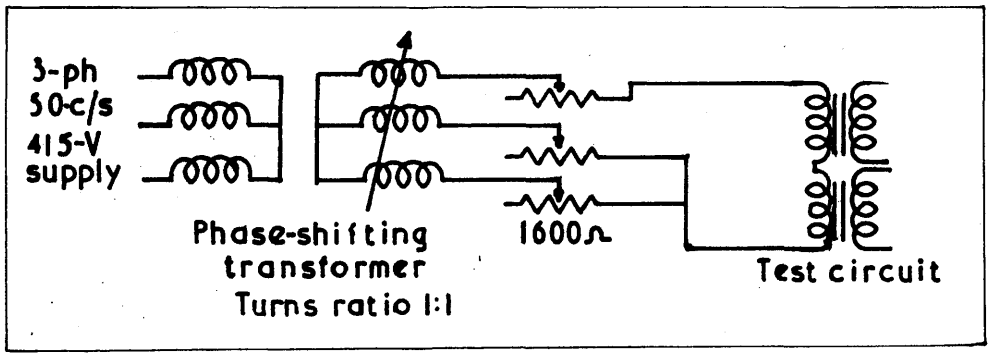

Fig. 54.
50-c/s Supply Circuit.

2. 100-c/s SUPPLY UNIT.

To obtain a high-impedance source at the above frequency, locked to the 50-c/s supply, a 1-ph alternator and a 3-ph synchronous motor coupled together were used.

Details of machines.

1) 2kVA, 220V, 1 ph, 50 c/s, 3000 r/m, Alternator (M68)

Stator resistance 250Ω

Rotor resistance 0.4Ω

2) 2 h.p., 380V, 5.3A, 3 ph, 50 c/s, 3000 r/m, Synchronous Motor (M69)

Stator resistance 3.6Ω/ph

Rotor resistance 260Ω

Theory of Operation.

The 3-ph synchronous motor is "run up" as an induction motor from the 50-c/s supply and then synchronized in the normal manner. The stator winding of the 1-ph alternator is energized from a d.c. source and the rotor 50-c/s output voltage observed. To enable the 1-ph machine to run as a synchronous motor, a supply voltage is selected to give zero phase difference between it and the rotor voltage. The numerical value of the rotor voltage is adjusted by variation of the excitation. When correct voltage conditions are obtained, the 1-ph machine can now run as a synchronous motor and the supply to the 3-ph synchronous motor can be disconnected. To provide a suitable synchronizing torque, an inductance should be inserted in series with the rotor of the 1-ph machine. If two of the supply leads to the stator of the 3-ph machine are interchanged and the supply reconnected, the resulting rotating m.m.f. will be in the reverse direction. The rotor winding of this machine, which is rotating at synchronous speed in the forward direction, will have a voltage induced at twice the supply frequency.

The number of turns on the rotor winding was large in comparison with the stator winding and consequently the induced voltage on open-circuit at 100 c/s tended to be dangerously high. To protect the insulation of the rotor windings, a non-linear resistor (Metrosil) was connected across the slip-rings of this machine.

The 100-c/s winding impedance obtained by this method was very high, which satisfied one of the requirements for the sine-current tests on the cores.

The circuit diagram of the machines and switching circuits are shown in Fig. 55.

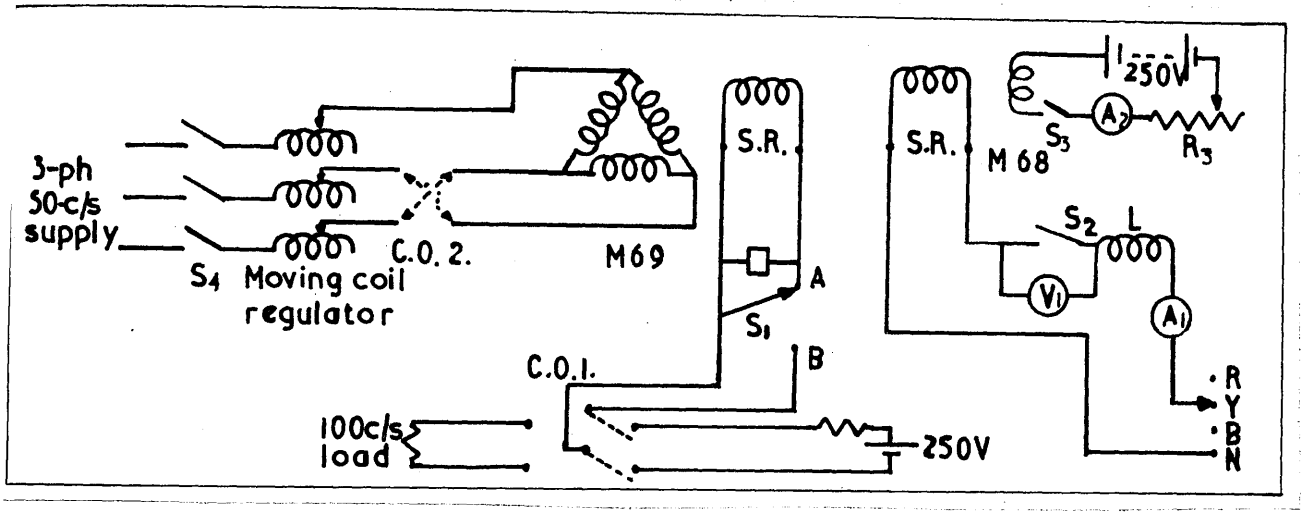

Fig. 55.
100-c/s supply circuit.

3. 150-c/s SUPPLY UNIT.

The non-linearity of the magnetization characteristic for core materials enables a 3-ph supply to be used to give a 1-ph output. The basic circuit[7 - 9] consists of a 3-ph transformer, whose star-connected primary winding is energized from a balanced 3-ph supply. The flux density in the core is higher than the normal value, with the result that a large third harmonic current will flow in the secondary winding which is in delta. If the delta is opened, the third harmonic current cannot flow and hence a third harmonic component of flux and phase voltage will result.* This voltage will appear across the open delta. When a load is connected across it, power will be supplied at the desired frequency.

---

* All triplen components will appear in the output wave, but the 9th and above are normally so small that they can be neglected.

To obtain suitable values of third harmonic voltage, three identical 1-ph transformer cores were used. Tapped primary windings were on the cores as obtained, and a common secondary winding linking all three was applied in the form of two 150 turn coils. A 3-ph core type transformer with 3-legged core is not suitable for this application, since the third harmonic fluxes which are in-phase in the 3 legs must find a return path through the air. This high reluctance path tends to suppress the 3rd harmonic fluxes.

The impedance of the source should be as high as possible to restrict the flow of harmonic currents from the circuit under test.

Due to slight magnetic differences in the three cores, a small voltage at fundamental frequency may appear across the secondary winding. To cancel out this small voltage, the primary turns may be adjusted by the various primary tappings as indicated in Fig. 56.

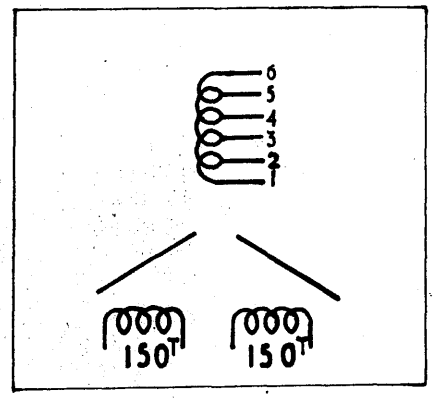

Primary phase winding
1 - 2 50% turns
2 - 3 25%
3 - 4 15%
4 - 5 8%
5 - 6 2%

Total primary turns/ph = 938
" " resistance/ph = 14.3Ω

Secondary 150T 22 SWG DSC 5.1Ω
150T 24 SWG DSC 8.5Ω

Fig. 56.
Details of primary phase winding.

Should the fundamental voltage component not be entirely suppressed by adjustment of the primary tappings; variable resistors were connected in series with each winding to give the final adjustments (Fig. 57). It must be realized that the resistance inserted was small, otherwise the primary voltage across the windings would be distorted. The 3-ph supply to the unit was obtained from a moving-coil regulator to enable the 150-c/s component to be easily varied.

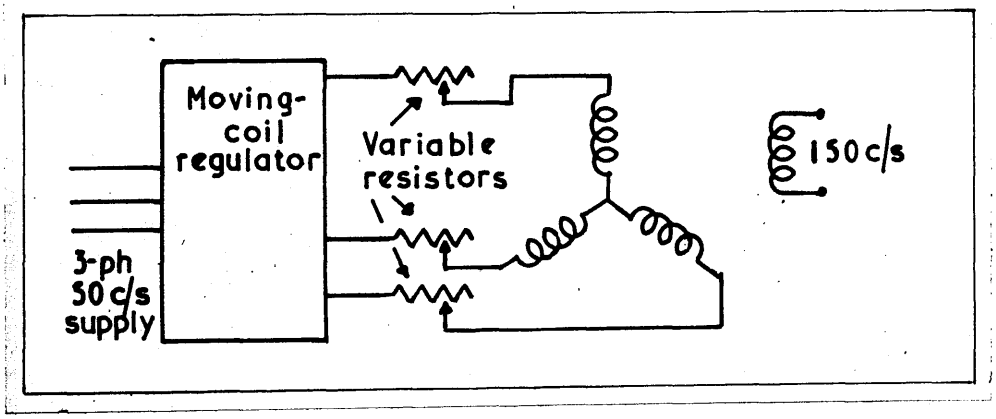

Fig. 57

Appendix (c)

1. Single Frequency Excitation.

To enable the results obtained under combined magnetization to be compared with the single frequency condition, separate tests were carried out for various values of simusoidal magnetizing force at 50, 100 and 150 c/s.

The circuit was connected as shown in Fig. 58. The windings, which were not energized, were open-circuited.

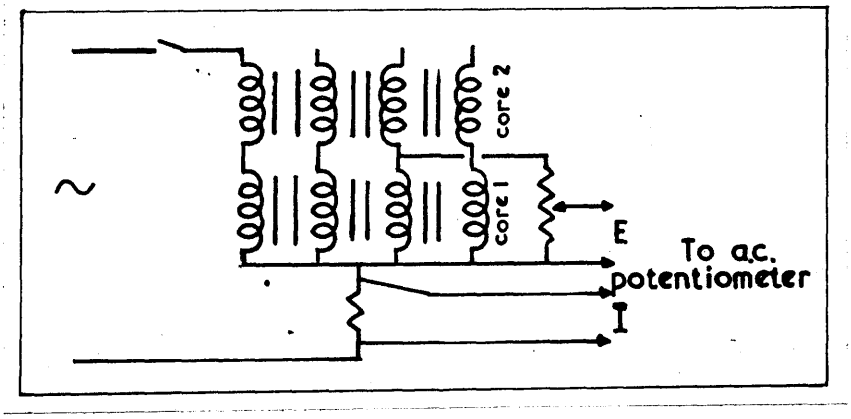

Fig. 58.

The variation of the individual core-loss values are shown graphically to a base of magnetizing force in Fig. 59. The variation of flux density components with magnetizing force is shown in Fig. 60. These values are used for comparison with conditions under combined magnetization in Chapter 4.

2. Calibration of valve voltmeter to read peak flux-density values.

Under conditions of combined magnetization, the induced voltage wave obtained across a secondary winding on the specimen can be re-entrant which prevents the use of the moving-coil rectifier voltmeter to obtain

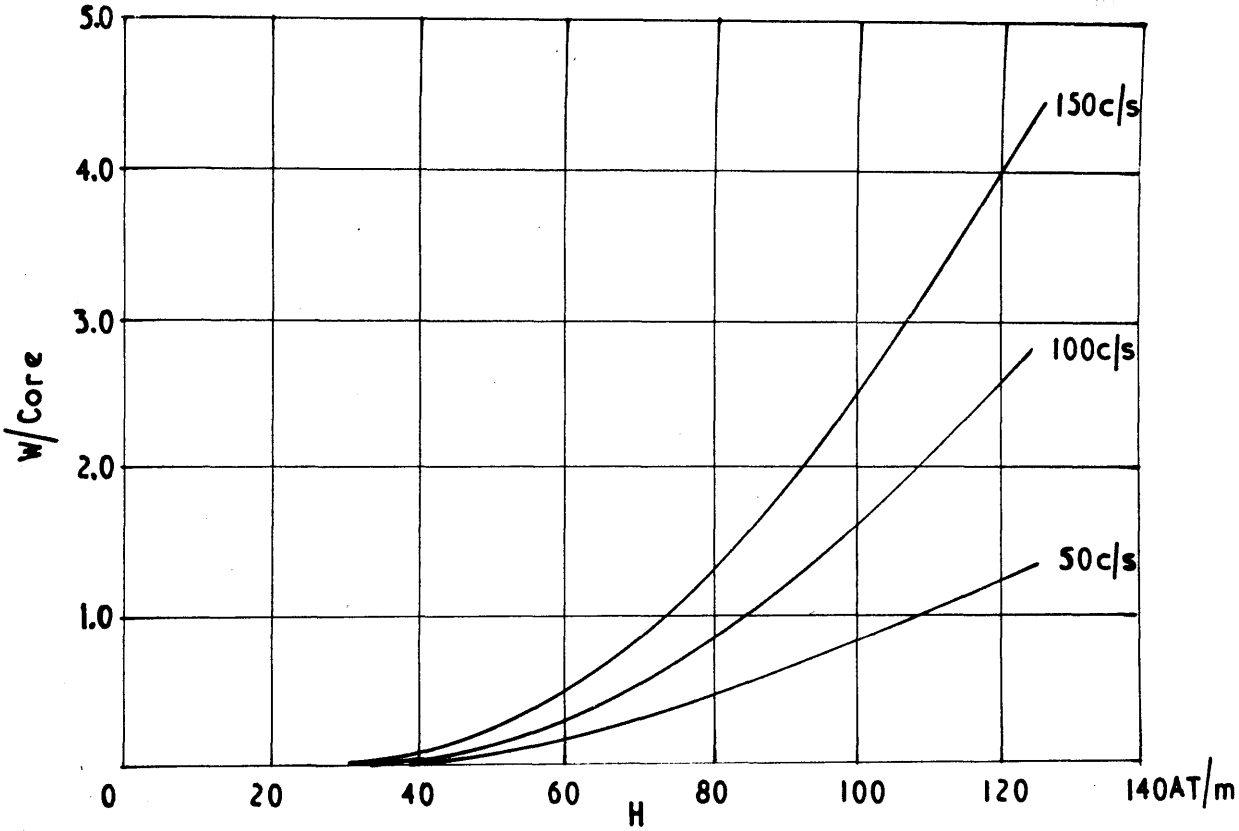

Fig. 59.
Variation of single frequency core loss

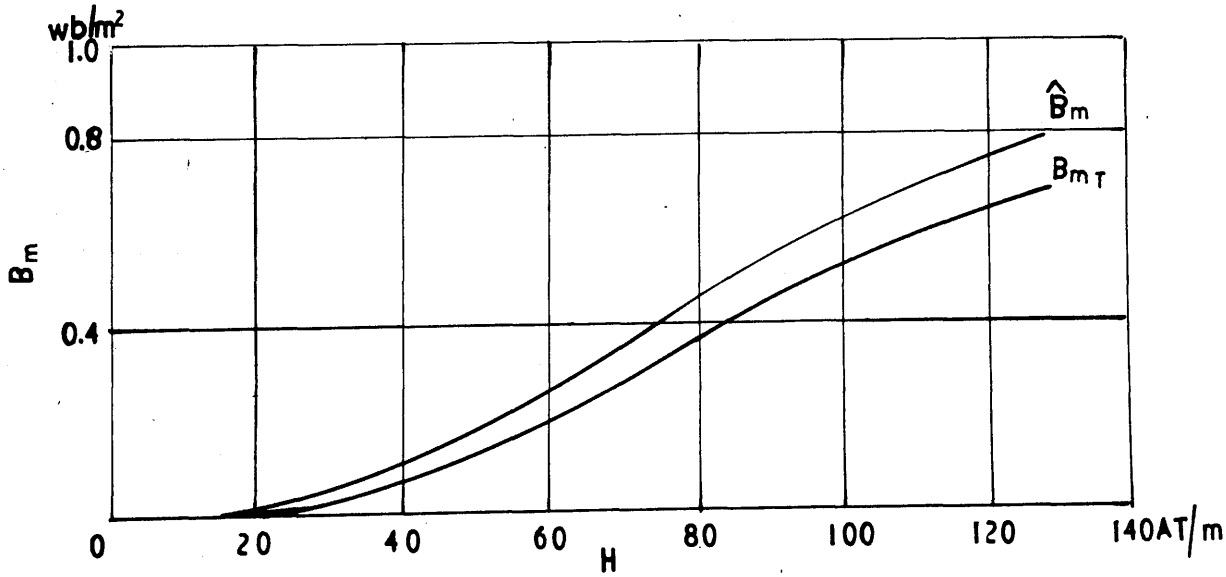

Fig. 60.
Variation of flux density components

the maximum flux density value.

Accordingly, the actual peak value of the flux wave was measured by means of a calibrated valve voltmeter. The flux wave was obtained from the standard R - C integrating circuit. With a perfect integrating circuit of this type the voltage across C would be zero, i.e. $R = \infty$. As this is an impractical case, it is usual to make R as large as possible and amplify the resulting voltage obtained.

In the circuit shown (Fig. 61) an amplifier with a gain of 100 was inserted between the integrating circuit and the valve voltmeter. The amplifier input impedance was approximately 2MΩ, so that the integrating circuit was not loaded by the measuring circuits.

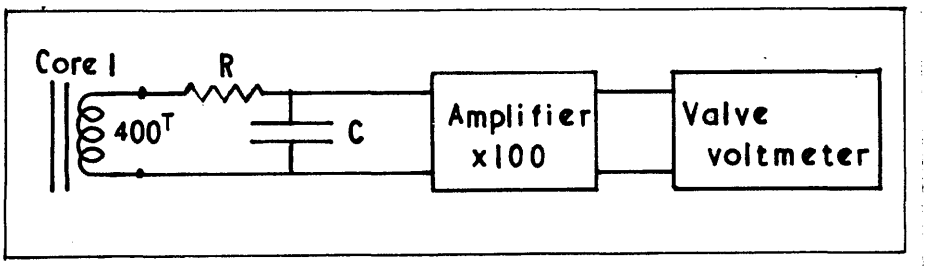

Fig. 61.

The valve voltmeter readings were calibrated against a moving-coil rectifer meter (V74, 0-50V) for single-frequency core magnetization.

$$B_m = 0.0738 \times V_{400T} \qquad (f = 50 \text{ c/s}).$$

Calibration.

V74	Valve Voltmeter	Factor
6.2	11.2	0.554
8.9	16.1	0.554
9.5	17.1	0.555

The valve voltmeter scale factor is taken as 0.555.

$$\therefore B_m = 0.0738 \times 0.555 \times V.V.$$

$$= 0.0408 \text{ V.V. weber/m}^2$$

3. Measurement of the r.m.s. voltage induced in the secondary windings of the cores.

When the cores are energized under sine-current conditions, the induced voltage waveform is non-sinusoidal and, hence, to obtain its r.m.s. value a thermal instrument was used. To prevent loading the secondary winding, a vacuo-junction was used with a unipivot micro-ammeter, which had a square-law scale, thereby enabling a direct reading to be obtained. Resistance was inserted in series with the heater circuit of the vacuo-junction. To obtain various voltage ranges this series resistance was altered as given below.

Details of Vacuo-Junction. (LV 8953/43).

5mA Heater resistance 93.1Ω

Cathode " 9Ω

Details of meter

Cambridge Unipivot

Resistance 10Ω at 20°C

Full Scale 120 divisions

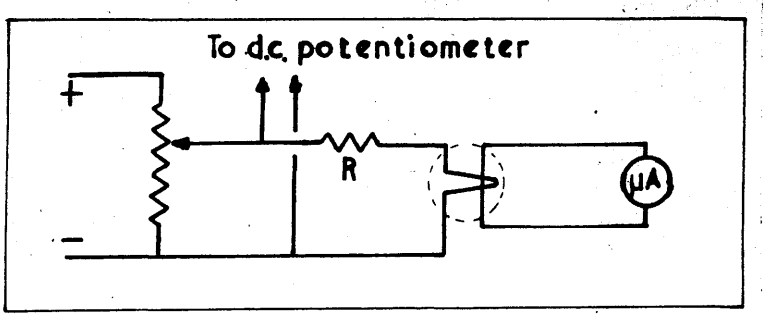

Fig. 62.

With the circuit connected as overleaf, the values of R were obtained for various voltage ranges from a d.c. calibration, using the d.c. potentiometer.

Meter full scale voltage	5	10	20	40	60	80	V
Additional Resistance.	2000	4090	8300	16900	25000	33900	Ω

4. Observation and recording of hysteresis loops.

To enable the loss loops obtained under conditions of combined magnetization to be inspected a cathode ray oscilloscope was used. The X-deflection was obtained proportional to the core magnetizing force and the Y-deflection proportional to flux. In this manner, the loss loop was obtained on the tube screen, which could be photographed.

Details of Oscilloscopes.

Cossor Double Beam Oscillograph, Model 339.

This unit was used to obtain the loop traces. The frequency response curve of the amplifier used to obtain the vertical deflection is shown in Fig. 63. It is seen that a flat response is obtained over the operating range 30 $\rightarrow 10^4$ c/s.

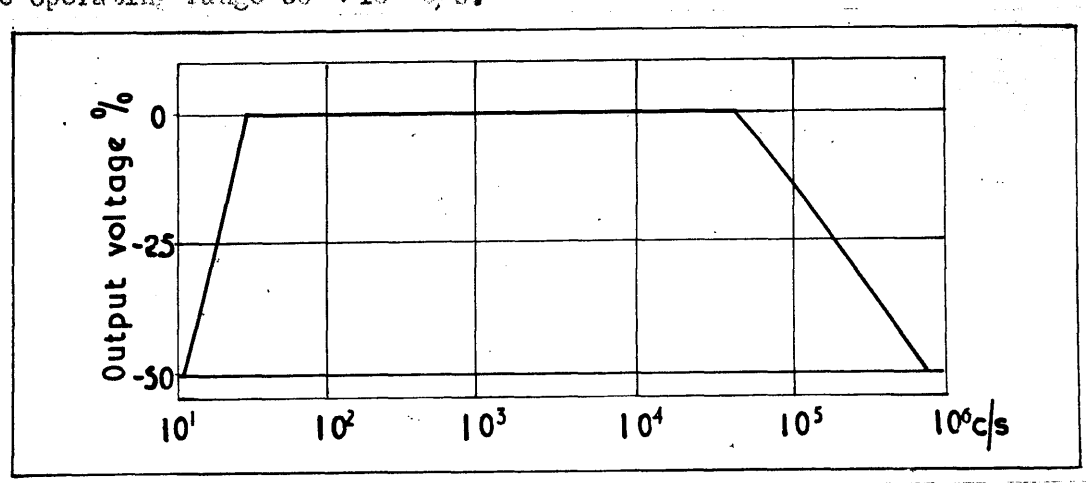

Fig. 63.
Amplifier response curve.

The flux density and magnetizing force waveforms were obtained using a Cossor Model 1035.

Magnetic Deflector Coils.

To obtain the horizontal or X deflections, pairs of magnetic deflector coils were fitted to the Model 339 oscilloscope. The following pairs of coils were wound to give suitable deflections for a wide range of current values: 60^T and 60^T, 40^T and 40^T, 15^T and 15^T, 10^T and 10^T. The eight coil leads were brought out to a terminal board on the side of the oscilloscope to enable them to be connected in series aiding or opposing depending upon the deflection required and the current available. This circuit could be inserted by an ammeter switch in series with either of the supplies to the test cores or the total current to them. In this way, horizontal deflections proportional to $\hat{h}_1$, $\hat{h}_n$ or $\hat{h}_{T_m}$ were obtained.

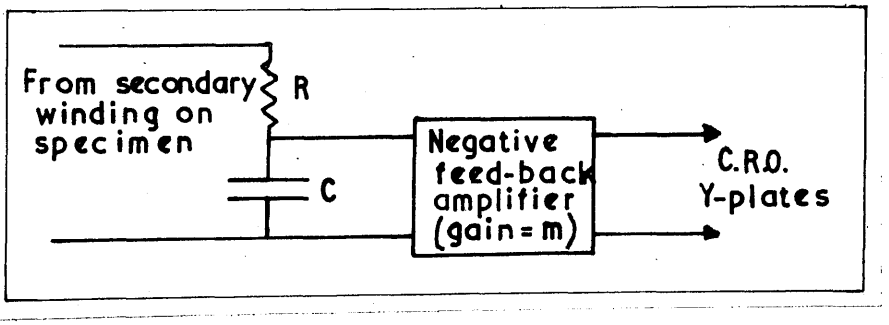

Fig. 64.

The standard R - C integrating circuit was used to obtain a voltage proportional to the core flux. The amplifier input impedance was approximately 2MΩ and hence its loading effect on the R - C circuit may be neglected.

$\therefore$ Instantaneous current in R-C Circuit = $\frac{v_r}{R}$

$\therefore$ Amplifier input voltage = $\frac{1}{RC}\int v_r\,dt \simeq \frac{1}{RC}\int v\,dt$

$\therefore$ Voltage applied to Y plates of oscilloscope

$$\simeq \frac{m}{RC}\int v\ dt$$

As the value of R is increased, for a given value of C, this circuit gives a closer approximation to $\int e dt$ but, simultaneously, the voltage across C decreases, requiring an amplifier with a larger gain. This is liable to introduce additional errors due to phase shift and it is usual to compromise between voltage across C and amplifier gain.

In the circuit used experimentally, R = 24kΩ, C = 4μF, and the amplifier gain, which was adjustable, approximately 100 → 200. This circuit gives the ratio $\frac{X_C}{R}$ = 3.3% at 50 c/s. Due to the relatively large inaccuracies (5%) introduced in the photography and developing of the loops, this integrating circuit is quite satisfactory.

Photographic Procedure.

The hysteresis loops were recorded using a Cossor Camera Model 427 and the flux density and magnetizing force waveforms on a Model 1428 camera. The 35 m.m. film used was Ilford 5B52 with an exposure time of 1 second. The developed film was enlarged and printed onto B.G.4 paper.

Appendix (d)

Derivation of eddy current loss under combined magnetization.

Assume a thin plate, of thickness t and width b, the thickness being small in comparison with the width. The plate carries a flux $B = B_{1_m} \sin \omega t + B_{3_m} \sin 3\omega t + \ldots B_{n_m} \sin n\omega t$. The flux density is assumed uniform over the cross section and the flux parallel to the axis of the plate. The reaction of the eddy currents on the inducing field is neglected since an approximate expression only is required.

Consider 1m axial length and 1m width of plate. For an elemental path with sides x m from the centre of the plate and depth dx, the flux enclosed in 1m width of path is

$$2x \times 1 \times B = 2x\,(B_{1_m} \sin \omega t + B_{3_m} \sin 3\omega t + \ldots .)$$

and the e.m.f. induced in this path is

$$e_x = 2x \frac{d}{dt} (B_{1_m} \sin \omega t + B_{3_m} \sin 3\omega t + \ldots)$$

$$= 2x\,\omega\,(B_{1_m} \cos \omega t + 3\,B_{3_m} \cos 3\omega t + \ldots)$$

The r.m.s. value is

$$E_x = \frac{4\pi f x}{\sqrt{2}} \sqrt{(\,B_{1_m}{}^2 + (3B_{3_m})^2 + \ldots)}$$

If the end portions of the path are neglected, then the eddy current is

$$i_x = \frac{E_x}{\frac{2\rho}{dx}} = \frac{\sqrt{2}\pi\, fx \sqrt{(B_{1_m}{}^2 + 9B_{3_m}{}^2 + \cdots)}\,dx}{\rho} \qquad (\rho \text{ measured in } \Omega\text{-m})$$

Hence eddy current loss in this path per metre length and breadth of the plate is

$$\omega_x = \frac{2\pi^2 f^2 x^2 (B1_m^2 + 9B3_m^2 \ldots\ldots) dx^2}{\ell^2} \times \frac{2\ell}{dx}$$

$$= \frac{4\pi^2 f^2 x^2 (B1_m^2 + 9B3_m^2 + \ldots) dx}{\ell}$$

$\therefore$ W = loss per metre length and breadth of plate

$$= \int_{x=0}^{x=\frac{t}{2}} \frac{4\pi^2 f^2 (B1_m^2 + 9B3_m^2 + \ldots) x^2 dx}{\ell}$$

$$= \frac{\pi^2 f^2 t^3 (B1_m^2 + 9B3_m^2 + \ldots)}{6\ell}$$

$\therefore$ Loss/cu.m. $= \frac{\pi^2 f^2 t^2 (B1_m^2 + 9B3_m^2 \ldots)}{6\ell}$ (A)

Now a voltmeter measuring r.m.s. quantities (see Appendix (d)) when connected across a winding of N turns on the core, area A, will read $E_{r.m.s.}$

Since $e = NA \frac{d}{dt} (B)$

$$= NA \frac{d}{dt} (B1_m \sin \omega t + B3_m \sin 3\omega t + \ldots)$$

$$= NA\omega (B1_m \cos \omega t + 3B3_m \cos 3\omega t + \ldots)$$

$\therefore$ $E_{r.m.s.} = \frac{NA\omega}{\sqrt{2}} \sqrt{B1_m^2 + 9B3_m^2 + \ldots}$

$\therefore$ $\sqrt{B1_m^2 + 9B3_m^2} = \frac{\sqrt{2}}{NA\omega} E_{r.m.s.}$

Eddy current loss/cu.m. from (A)

$$= \frac{2\pi^2 f^2 t^2 E_{r.m.s.}^2}{6\rho N^2 A^2 \omega^2}$$

$$= \frac{t^2}{12\rho N^2 A^2} E_{r.m.s.}^2$$

Hence the eddy current loss under conditions of combined magnetization can be obtained from core constants and the r.m.s. voltage. (In the above analysis, the flux density wave comprised only odd harmonics; while this is the more practical case the result is quite general and holds for even and odd harmonics.)

Eddy current loss for cores used in tests.

$$\text{Loss/cu.m.} = \frac{t^2 E_{r.m.s.}^2}{12 \rho N^2 A^2}$$

$$= \frac{(3.56 \times 10^{-4})^2}{12 \times 20 \times 10^{-6} \times 10^{-2} \times 16 \times 10^4 \times 1.495^2 \times 10^{-8}} E^2_{r.m.s.}$$

$$= 14.7E^2$$

$$\text{Loss/c.c.} = 1.47 \times 10^{-5} E^2$$

$$\text{Core volume:} = \frac{m}{D} = \frac{639}{7.8} = 82 \text{ c.c.}$$

$\therefore$ Eddy current loss/core = $121 \times 10^{-3} E^2_{r.m.s.}$ (400^T)